VOLUME XXXIX

GEMS & GEMOLOGY

SUMMER 2003

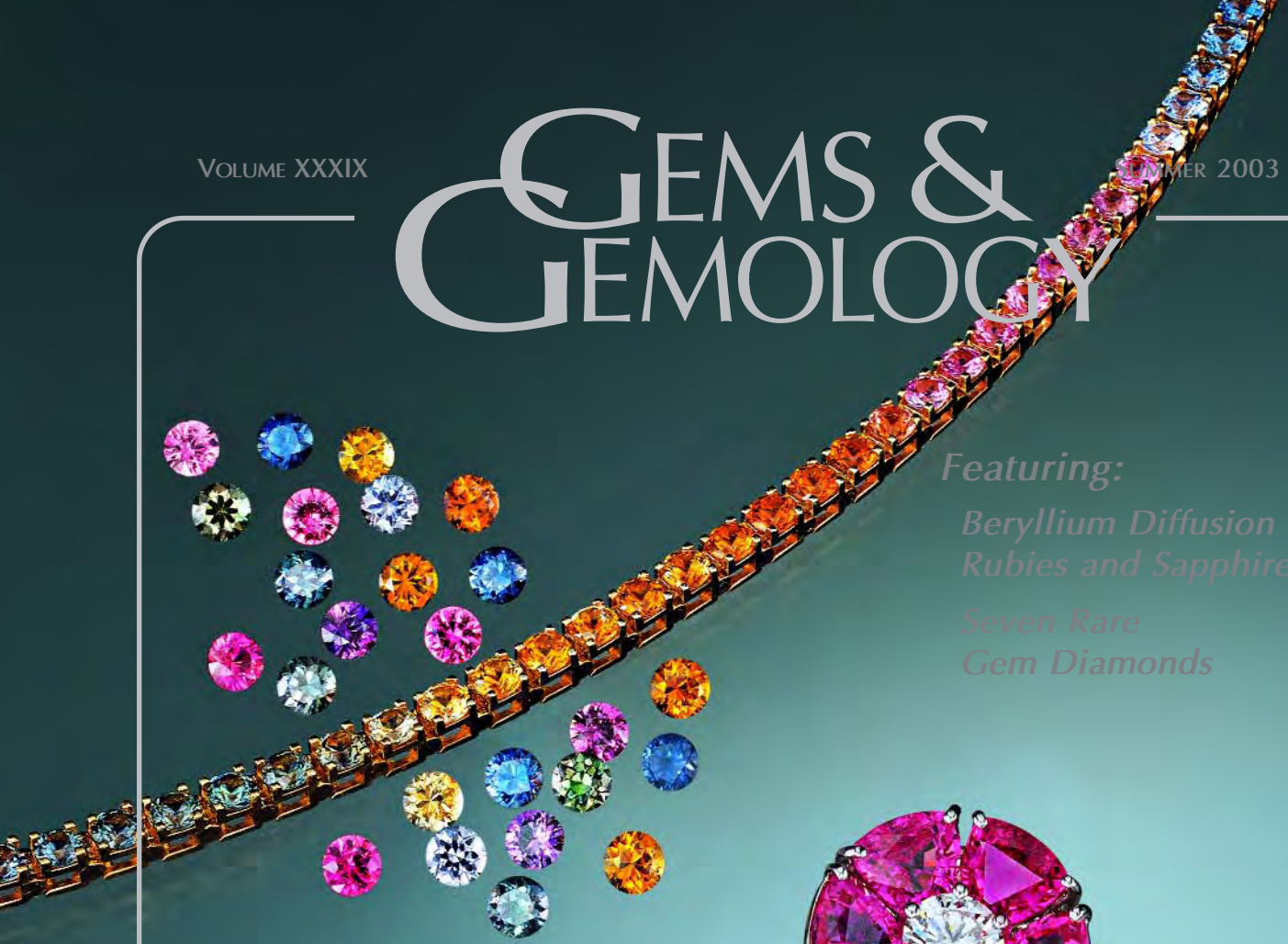

Featuring:

Beryllium Diffusion of Rubies and Sapphires

Seven Rare Gem Diamonds

THE QUARTERLY JOURNAL OF THE GEMOLOGICAL INSTITUTE OF AMERICA

GEMS & GEMOLOGY.
Summer 2003 VOLUME 39, NO. 2


pg. 130


pg. 137

EDITORIAL

FEATURE ARTICLE

An in-depth report on the process and characteristics of beryllium diffusion into corundum. Examination of hundreds of Be-diffused sapphires revealed that, in many instances, standard gemological tests can help identify these treated corundums.

NOTES AND NEW TECHNIQUES

A look at the background and some gemological observations of seven important diamonds on display at the Smithsonian Institution from June to September 2003, in an exhibit titled "The Splendor of Diamonds."

REGULAR FEATURES


pg. 157


pg. 161

BERYLLIUM DIFFUSION OF RUBY AND SAPPHIRE

John L. Emmett, Kenneth Scarratt, Shane F. McClure, Thomas Moses, Troy R. Douthit, Richard Hughes, Steven Novak, James E. Shigley, Wuyi Wang, Owen Bordelon, and Robert E. Kane

Over the past two years, the heat treatment of corundum involving lattice diffusion of beryllium (Be) at temperatures over 1800°C has become a major issue in the gem trade. Although initially only orange to orangy pink ("padparadscha"-like) sapphires were seen, it is now known that a full range of corundum colors, including yellow and blue as well as ruby, have been produced or altered by this treatment. An extension of the current understanding of the causes of color in corundum is presented to help explain the color modifications induced by Be diffusion. Empirical support is provided by Be-diffusion experiments conducted on corundum from various geographic sources. Examination of hundreds of rough and faceted Be-diffused sapphires revealed that standard gemological testing will identify many of these treated corundums, although in some instances costly chemical analysis by mass spectrometry is required. Potential new methods are being investigated to provide additional identification aids, as major laboratories develop special nomenclature for describing this treatment.

Early in 2002, it became apparent that corundum treated by a new technique in Thailand had been filtering into the marketplace unannounced, particularly in Japan. It was subsequently learned that these stones had been traded for at least six months prior to this discovery, perhaps longer. The first announcement of this situation—an alert issued by the American Gem Trade Association (AGTA) on January 8, 2002—prompted substantial activity in gemological laboratories worldwide. Quite rapidly it was demonstrated that this new process involved diffusion of the light element beryllium (Be) into a wide variety of corundum types to alter their color.

The diffusion of beryllium into corundum creates yellow, orange, or brown color components. The effectiveness of this process in turning pale-colored or nearly colorless corundum into vibrant yellows and oranges is dramatic. No less dramatic is the alteration of pink sapphire to a "padparadscha" appearance or a vivid orange, as well as the conversion of bluish rubies to a fine red color. It also can reduce the amount of blue in dark blue sapphires, rendering them a more attractive color (figure 1).

Our initial interpretation—that this color alteration was caused solely by the diffusion of beryllium into the stone in an oxidizing atmosphere—was denied by those involved with the treatment process, and was questioned by other gemologists. Their arguments hinged primarily on observations that apparently similar starting materials could emerge from this process as a variety of colors, or completely unchanged. We believe that those observations are correct, but their interpretation is not. To understand the unusual behavior of beryllium in this material, we will have to examine far more closely the origin of color in corundum.

In addition to their changes in color, these stones exhibit many other features—both internal and on the surface—that indicate very high-temperature heat treatment and/or long periods of treatment. Taken together, these features indicate that a new treatment regime has been introduced into the jewelry trade.

See end of article for About the Authors and Acknowledgments.
GEMS & GEMOLOGY, Vol. 39, No. 2, pp. 84–135.

Figure 1. The beryllium diffusion process can affect many colors of corundum, including ruby and blue sapphire. The Be-diffused stones shown here range from 0.40 to 5.05 ct. Photo by Harold & Erica Van Pelt.

We start this discourse with a short historical discussion of corundum heat treatment and the connection of this new treatment to previous processes. That is followed by a summary of recent progress on beryllium diffusion. Next we delve deeply into the causes of color in corundum, extending the current understanding, to elucidate how a minute amount of this light element can cause such a variety of dramatic color alterations. To this end, we performed a series of Be diffusion experiments in one of our laboratories. We also studied a large number of Be diffusion–treated sapphires (some, both before and after treatment), untreated sapphires, and sapphires treated only by heat, using a variety of gemological and analytical methods. On the basis of the examinations and testing conducted, we present criteria for determining if stones have been Be diffused—some are quite simple, and some require advanced analytical instrumentation.

Finally, we note that this new treatment process has caused gemological laboratories to re-evaluate their thinking about corundum treatments in general, and the manner in which the treated stones should be described on laboratory reports and other documents in particular. Current descriptive language used on reports issued by the AGTA Gemological Testing Center and the GIA Gem Laboratory is presented.

Before we proceed, let us take a moment to explain the nomenclature that we will use in this article. The original diffusion process in which titanium was diffused from the outside of a piece of corundum into the bulk of the stone, producing a blue layer under the surface, was called "surface diffusion" by some gemologists (see, e.g., Hughes, 1997, pp. 121–124). However, the term *surface diffusion* is used in many other disciplines to mean a process by which a material moves over a surface, rather than through the surface into the interior. As recommended by the International Union of Pure and Applied Chemistry (Kizilyalli et al., 1999), the scientifically correct term for the process by which a foreign material moves into and through a solid is *lattice diffusion*, previously referred to in the scientific literature as *bulk diffusion*. For the purposes of this article, we will use the term *lattice diffusion* or (in its shortened form) *diffusion* to describe this process.

BACKGROUND

Corundum has been heat treated with moderate color improvement since antiquity. However, today's modern heat-treatment techniques produce dramatic results when compared with the subtle changes of the past. The historic turning point was the discovery, apparently in the 1960s (see Crowningshield, 1966, 1970; Beesley, 1982), that the translucent milky white to yellow to brown and bluish white sapphire from Sri Lanka, known as geuda, could be transformed to a fine

transparent blue by atmosphere-controlled high-temperature heating. This discovery was made possible by the availability of simple furnaces capable of reaching temperatures in the ≥1500°C range. The striking color change in the geuda material was caused by the dissolution of rutile inclusions in the stone, and by the inward diffusion of hydrogen from the reducing atmosphere. The importance of hydrogen diffusion was not recognized until much later (Emmett and Douthit, 1993). Eventually, tons of previously worthless geuda corundum were converted to marketable transparent blue sapphire.

The benefits of this process with geuda sapphire led to successful experimentation with many types and colors of sapphire (e.g., Crowningshield and Nassau, 1981; Keller, 1982; Themelis, 1992; Emmett and Douthit, 1993) as well as off-color ruby. As a result, the vast majority of rubies and sapphires traded today have been heat treated.

Initially these gems entered the market without any form of disclosure. By the time buyers did learn they were treated, the stocks of gem merchants were full of stones with color created by a high-heat process. In the mid-1980s, international regulatory bodies such as CIBJO decided that, because the heat treatment of sapphire was a "traditional trade practice," such a treatment need not be declared in the course of trade. The concept that turning unattractive corundum into a gem by heating it in an atmosphere-controlled furnace should be regarded as "traditional" was questionable from the outset, but the situation had reached a stage where something had to be done to allow trading to continue. Thus, the heat-treated geuda sapphires were placed in the same category as the far milder historic corundum heat treatments.

Diffusion-treated corundum first appeared on the world market in the late 1970s (Crowningshield, 1979). This process marked a radical departure from all earlier corundum heat treatment in that it produced a thin outer layer of saturated blue coloration in otherwise colorless or pale-colored sapphire by diffusing titanium into the stone from the outside. As such, it represented the first successful attempt to add color to sapphire from an external source. The technology was developed by Union Carbide Corp. and then sold to Golay Buchel. Eventually, treaters in Thailand also used this process (Kane et al., 1990; Hughes, 1991a,b). Nearly all sapphires produced by this method were blue, but a few orange stones also were seen (Scarratt, 1983). In 1993, GIA researchers reported on the experimental production of red "diffusion-treated" corundum (McClure et al., 1993).

In October 2001, Australian gemologist Terry Coldham informed one of the authors that a treater in Chanthaburi, Thailand, had developed a new method to transform bluish red Songea (Tanzania) stones to a fine orange to red-orange (Coldham, 2002; Hughes, 2002). Shortly thereafter, several other sources confirmed this information. The stones were to be marketed under a variety of new color names, such as "Sunset Sapphire" ("Treated Songea sapphires . . . ," 2002).

During a visit to Bangkok in November/December 2001, another author saw the new treated orange sapphires in the gem market, as well as a large volume of orangy pink treated stones similar in color to traditional "padparadscha" sapphires. He later obtained samples for study. When staff members at the AGTA Gemological Testing Center (AGTA-GTC) examined these samples in New York, they found that all showed evidence of exposure to a high-temperature treatment (Scarratt, 2002a). When these stones were immersed in methylene iodide, many displayed unusual yellow-to-orange rims surrounding pink cores, which suggested that a yellow colorant was being diffused into pink sapphire.

On December 28, 2001, Ken Scarratt reported his observations to Richard Hughes, who then examined faceted sapphires just purchased in Bangkok by Pala International. He found yellow-to-orange rims on most pieces (see, e.g., figure 2). In early January 2002, AGTA and Pala International issued Internet warnings to their extensive mailing lists (Scarratt, 2002b).

Initially, the cause of these yellow-to-orange rims surrounding pink cores (with the overall color of the gems being orange to pinkish orange) was unknown. One of the authors (JLE) suggested in January that the features resulted from lattice diffusion of light elements, producing what are called "trapped-hole color centers" in the crystal lattice of the corundum. While the color produced and the elements added were different, the process was essentially identical to that used more than a decade earlier to produce a blue rim on sapphire by the diffusion of titanium. However, gemologists at Bangkok's Gem Research Swisslab (GRS) and the Gem and Jewelry Institute of Thailand (GIT) suggested that the color enhancement in this orange to orangy pink corundum was due to a

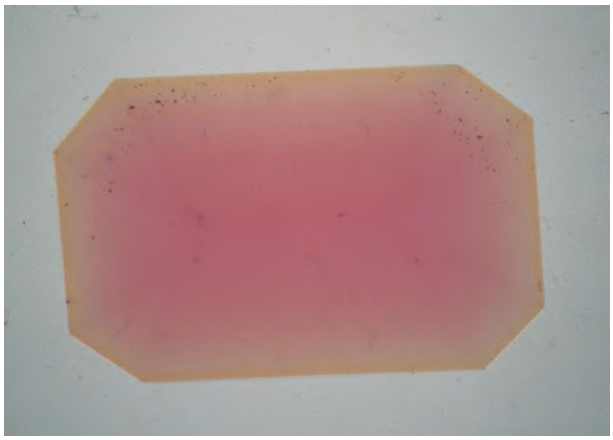

Figure 2. Most of the Be-diffused stones seen early on, particularly in the pink-orange color range, showed distinct yellow-to-orange surface-conformal layers when viewed in immersion. Photomicrograph by Shane F. McClure; magnified 10×.

change in the oxidation state of iron brought about by simple heat treatment (GIT, 2002; Proust, 2002; Weldon, 2002).

At the same time the orange color rims were observed, other unusual features were seen in these stones. Significant overgrowths of synthetic corundum were noted on rough stones (Scarratt, 2002b). In addition, remnants of these synthetic overgrowths were seen in stones re-cut and polished, raising the issue of what portion of the faceted stone was natural (McClure, 2002a). These features, plus unusual inclusion damage, suggested that an entirely new form of heat treatment had been initiated in Thailand.

Toward the end of January 2002, the GIA Gem Laboratory engaged one of the authors (SN) to analyze the treated stones using secondary ion mass spectrometry (SIMS, see Box A). During the AGTA-sponsored Gemstone Industry and Laboratory Conference held in Tucson in early February 2002, another of the authors presented the SIMS data, which showed that not only did these stones contain beryllium, but there also was a direct correlation between the depth of color penetration and the depth of Be penetration (McClure et al., 2002). At the time, no standards for chemically analyzing the amount of beryllium in sapphire were available, and thus the absolute magnitude of the Be concentration was incorrect in these data (Wang and Green, 2002a); however, the relationship between beryllium content and the color-altered zone was very clear. Specifically, the concentration of Be decreased from the edge toward the center of suspected treated orangy pink sapphires, and the highest Be concentrations occurred in the yellow-to-orange surface-related color zones. These results, combined with the surface-conformal nature of the rims, proved that beryllium had been diffused into the stones from an external source for the purpose of creating the observed color.

Following the discovery that Be was the element being diffused into the sapphires, two of the authors began a series of experiments designed to replicate the treatment being used in Thailand (see "Beryllium Diffusion into Corundum: Process and Results" section below). They guessed that the Thai treaters would use chrysoberyl, since it was commonly recovered with pink sapphire in Madagascar. Therefore, they heated Madagascar sapphires in the presence of crushed chrysoberyl ($BeAl_2O_4$) to provide the beryllium, and found they could produce all the color modifications seen with the Thai treatment (Emmett and Douthit, 2002a). Simultaneously, scientists at D. Swarovski in Wattens, Austria, were carrying out similar experiments (McClure, 2002b). By May 2002, both the Swarovski and Emmett/Douthit teams had independently reproduced the results of the Thai process.

After the 2002 Tucson Show, many gemologists began studying this material, which was available in abundance. On May 4, 2002, a meeting was held in Carlsbad, attended by several of the present authors, Dr. George Rossman of the California Institute of Technology, and representatives of the SSEF Swiss Gemmological Institute and the Gemological Institute of Thailand. At this meeting, the results of GIA and AGTA studies and those of Emmett and Douthit were presented and debated. Subsequently, many contributions to the understanding of these stones have appeared in the literature (Coldham, 2002; Hänni, 2002; Hänni and Pettke, 2002; Pisutha-Arnond et al., 2002; Qi et al., 2002; Peretti and Günther, 2002; Fritsch et al., 2003).

On February 7, 2003, at the Tucson Show, AGTA held a panel discussion on this new process; presentations were given by several of the present authors and others (Shor, 2003). While Thai processors and dealers were still denying that the sapphires were being treated by Be diffusion ("Thailand . . . ," 2002), the information presented by this panel was indisputable. Don Kogen, president of Thaigem.com, attended this and other Tucson meetings on Be diffusion as the representative of the Chanthaburi Gem and Jewelry Association (CGA). He vowed to return to his CGA colleagues with this information to help resolve the situation.

BOX A: SIMS ANALYSIS

SIMS (secondary ion mass spectrometry) allows us to measure the trace-element concentrations in gems down to ppm (parts per million), a capability never before needed by gemologists. SIMS is one of two commercially available techniques that can measure a wide range of elements down to ppm levels or below—the other is LA-ICP-MS (laser ablation–inductively coupled plasma–mass spectrometry)—without requiring special preparation or significant damage to the gem. It is the remarkable color alteration produced by as little as 10 ppma of beryllium in ruby and sapphire that has forced us to embrace such sophisticated analytical instrumentation. Embracing it has not been easy, as SIMS instruments cost $750,000–$2,000,000 each and LA-ICP-MS is more than $400,000, well beyond the financial capability of most gemological laboratories. Thus, gem labs typically send samples to major analytical laboratories, recognizing that the cost of a single SIMS analysis can be several hundred dollars.

The first commercial SIMS instrument was developed to analyze the moon rocks brought back by the Apollo astronauts in 1969, and the technique has been used by mineralogists and petrologists ever since. Today SIMS is also indispensable to the semiconductor industry for analysis of semiconductor wafers. SIMS operates by focusing a beam of oxygen ions onto the sample in a vacuum chamber. Ions of the sample material are knocked off the surface of the sample by the oxygen ion beam and drawn into a mass spectrometer, which then sorts the ions according to their atomic weight and charge. Once sorted, the ions are counted, and the counts are converted into a quantitative analysis of the sample (for more information, see Hervig, 2002). Figure A-1 shows a SIMS instrument in operation.

As material (ions) must be removed from the stone, an important question is how much damage is done to the gem during this kind of analysis. The oxygen ion beam itself is very small, and is scanned over a square 150 by 150 µm in area, with material removed to a depth of about 200 nm. This shallow depression on a polished gemstone is nearly impossible to see with the unaided eye, but can be observed with a gemological microscope if light is reflected off the surface at certain angles (figure A-2). Although generally unnecessary, a light polishing can remove this very small depression.

Figure A-1. Shown here is a SIMS instrument in use at Evans East. This PHI 6600, manufactured by Physical Electronics, employs a quadrupole mass spectrometer to detect and sort ions from the corundum sample.

As with all sophisticated analytical instruments, achieving accurate calibration is a primary issue for SIMS. Having a calibration standard made out of the same type of material as the one being analyzed is by far the best method. (Standards made from other materials can, at best, provide relative concentrations.) One of the authors (SN) has prepared synthetic sapphire standards for the analyses reported in this article, by ion implantation. Widely used in the semiconductor industry, this technique can place a broad variety of elements into sapphire with a concentration accuracy of a few percent or better (Leta and Morrison, 1980). Thus, we can achieve an overall measurement accuracy of better than 25%—an impressive level when one considers that we are trying to measure only 5 to 50 atoms out of a million.

LA-ICP-MS has also been used successfully for this purpose by other researchers. SIMS was chosen for our research because several authors had experience with this instrument in detecting light elements in corundum.

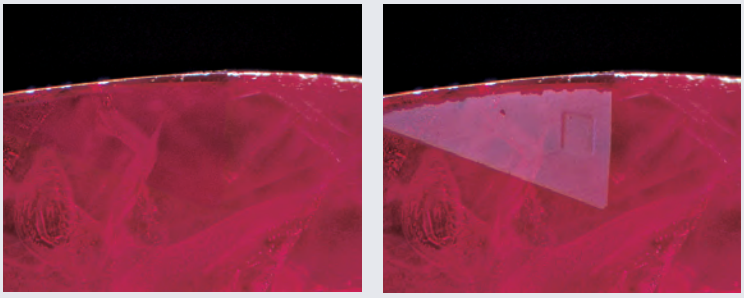

Figure A-2. The ruby in these images was tested with SIMS and then examined at 25× magnification. In standard darkfield illumination, no mark is visible (left). With reflected light, however, the mark left behind by the SIMS instrument can be seen (right). The mark is only visible with careful illumination. It would be extremely difficult to find with a hand loupe. Photomicrographs by Shane F. McClure.

Shortly thereafter, on February 20, 2003, the Chanthaburi Gem and Jewelry Association issued a press release (CGA, 2003) in which they reported that their members had been introducing beryllium into corundum by adding chrysoberyl to the crucibles in which the stones were heated. They further stated that these Be-diffused stones would now be sold separately from other heat-treated corundum.

The Be-diffusion process is, without question, the most broadly applicable artificial coloration of natural corundum ever achieved (see figures 1 and 3). Analyses have indicated that the beryllium concentration in the diffused region is only about 10 to 35 parts per million atomic (ppma[1]) or 4.4 to 15.5 ppmw (see table 1 for a comparison of ppma to ppmw for selected elements). That such minute concentrations of a foreign element could result in such a wide variety of colors and color modifications in corundum is truly unique. To understand how this occurs, we need to examine the causes of color in corundum much more closely than gemologists have done in the past. Much of the information in the following section has appeared in the scientific literature over the past 40 years, or is the result of studies by one of the authors (JLE) over the past 15 years.

COLOR IN CORUNDUM

The range of color in natural corundum is very extensive, with nearly all colors being represented (figure 4). Pure corundum is comprised only of aluminum and oxygen, and is colorless. Moreover, its spectrum exhibits no absorption (i.e., the material is transparent) from 160 nm in the ultraviolet to 5000 nm in the infrared. Gem corundum owes its many colors to impurities (typically trace elements) that have replaced aluminum in the crystal lattice. These impurities can be the direct cause of color, or they can chemically interact with one another to cause color, or to modify the strength (saturation) of a color. For the purpose of this section, we will limit the discussion to colorants of natural corundum and will ignore the additional colorants used in the production of synthetic corundum.

Figure 3. The Be-diffusion process is capable of causing dramatic changes in the color of corundum, such as altering pink sapphire (left, before treatment) to pink-orange (right, after treatment). The samples weigh approximately 1 ct each; photo by Sriurai Scarratt.

The causes of color in corundum are manifold and have been addressed in many publications. A good general review is provided by Fritsch and Rossman (1987, 1988); Häger (2001) recently reviewed the colors of corundum extensively in the context of heat treatment. The basic causes of color (also referred to as chromophores) are well known: Cr^{3+} produces pale pink through deep red as concentrations increase, Fe^{3+} produces a pale yellow, Fe^{2+}-Ti^{4+} pairs produce blue, and less well recognized Mg^{2+}-trapped-hole pairs are responsible for yellow to

TABLE 1. Comparison of ppma and ppmw for selected elements.[a]

Element	ppma	ppmw
Beryllium	1.000	0.442
Sodium	1.000	1.128
Magnesium	1.000	1.192
Silicon	1.000	1.378
Potassium	1.000	1.919
Calcium	1.000	1.996
Titanium	1.000	2.349
Chromium	1.000	2.550
Iron	1.000	2.739
Gallium	1.000	3.420

[a]*Calculated as:*

$$ppma = \frac{(\text{molecular weight of } Al_2O_3)/5}{(\text{atomic weight of the element})} \bullet ppmw$$

[1] The more commonly used units for trace-element analyses are ppmw (parts per million by weight), usually written as *ppm*. One ppm means that there is one microgram of impurity in one gram of crystal. In this article we choose to use the units *ppma* (parts per million atomic) to state trace-element concentrations. One ppma means that there is one trace-element atom for each million atoms (for corundum, i.e., 400,000 Al atoms + 600,000 O atoms). These units are chosen because it is the *concentration* of trace elements that determines how they chemically interact, not their relative weights.

Figure 4. Non-diffused corundum (here, approximately 0.40 ct each), whether natural or heat treated, comes in a wide variety of colors. Courtesy of Fine Gems International; photo by Harold and Erica Van Pelt.

orangy yellow (Kvapil et al., 1973; Schmetzer, 1981; Schmetzer et al., 1983; Boiko et al., 1987; Emmett and Douthit, 1993; Häger, 1993). A much wider range of colors is produced by combinations of these primary chromophores. For example, green is caused by Fe^{3+} yellow plus Fe^{2+}-Ti^{4+} blue. Purple or violet is a combination of Cr^{3+} red with Fe^{2+}-Ti^{4+} blue, and orange can be a combination of the Mg^{2+}-trapped-hole yellow plus the Cr^{3+} pink.

While these causes of color are understood in very general terms, a more detailed understanding is required to determine the impact of adding beryllium to the already complex set of natural trace elements in corundum. In addition, we must understand the chemical interactions that occur among the various trace elements within the corundum crystal lattice. Although most of us are more familiar with chemical interactions in liquids than in solids, the latter nonetheless occur during the growth of the corundum crystal in nature and during its heat treatment at high temperatures.

First, we must note that there are two general classes of impurities in the corundum lattice: (1) those such as Cr^{3+} that have the same chemical valence (i.e., a positive charge of three) as Al^{3+} and are termed *isovalent*; and (2) those such as Mg^{2+} or Ti^{4+} with a valence different from that of the Al^{3+} they replace—termed *aliovalent*. The most common impurities in corundum are (by valence):

+1—Hydrogen (H)
+2—Magnesium (Mg)
+2—Iron (Fe)
+3—Iron (Fe)
+3—Chromium (Cr)
+4—Titanium (Ti)
+4—Silicon (Si)

Unfortunately, we know of no complete trace-element analyses (that is, down to the parts per million atomic—ppma—level) in the literature for any natural corundum sample. Yet, as we shall see, as little as 5 to 10 ppma of an impurity can have a substantial impact on the color of corundum.

Isovalent Ions. Cr^{3+} by itself in corundum produces a red coloration—from pale pink through deep red, depending on its concentration (McClure, 1962; figure 5). The quantitative relationship between the strength of the optical absorption and the concentration of chromium is well known, primarily because it has been carefully studied for ruby laser design (Dodd et al., 1964; Nelson and Sturge, 1965).

Fe^{3+} in corundum at high concentration (≥ 2,500 ppma) produces a weak yellow coloration (McClure, 1962; Eigenmann et al., 1972; figure 6). The relationship between the strength of the absorption and the Fe^{3+} concentration is not nearly as well understood as that of Cr^{3+}. The weak broad bands at 540, 700, and 1050 nm, and the narrow peak at 388 nm, have been assigned to single Fe^{3+} ions, while the narrow peaks at 377 and 450 nm have been tentatively assigned to Fe^{3+}-Fe^{3+} pairs on the nearest-neighbor lattice sites (Ferguson and Fielding, 1971, 1972; Krebs and Maisch, 1971). However, this does not preclude the existence of a higher-order cluster with additional ions or other point defects. A quantitative relationship between the strength of each of these iron-absorption features and iron concentration has not been completely established.

Charge Compensation. The field known as *defect chemistry* provides a very useful framework for studying charge-compensation mechanisms at trace-element concentrations and the chemical interactions among trace elements (Kröger, 1974; Kingery et al., 1976; Chiang et al., 1997; Smyth, 2000). In this context a "defect" refers to any deviation from a perfect lattice. Thus impurities, ion vacancies, interstitial ions, and free electrons or (electron) holes are defects. To help explain the impact of diffusion treatment, we will review here a few principles of defect chemistry as it relates to corundum.

In discussing corundum coloration, it simplifies matters somewhat if we think about the charge of an ion relative to the charge of a perfect lattice. In defect chemistry, ions with excess positive charge (e.g., Ti^{4+} in Al_2O_3) are termed *donors*, because they must "give up" an extra electron to enter the corundum lattice. Similarly, ions with a relative charge of –1 are termed *acceptors*, because they must "accept" an electron from some other ion in the lattice. Ti^{4+} (for example) has one extra positive charge than the Al^{3+} ion it can replace in corundum, so we say that its relative charge is +1. Mg^{2+} has one less positive charge than the Al^{3+} it can replace, so we say that its relative charge is –1. If both magnesium (relative charge –1) and titanium (+1) are incorporated together, they will tend to attract each other and co-locate at adjacent or nearby sites in the atomic lattice, thereby balancing their charges. Acceptor or donor properties can also be ascribed to other point defects in the corundum lattice. Thus, oxygen vacancies (relative charge +2) and aluminum interstitials (+3) are donors, while oxygen interstitials (–2) and aluminum vacancies (–3) are acceptors.

A crystal must be electrically neutral, which means that the sum of all the relative positive charges and electron holes equals the sum of the relative negative charges and free electrons. Consequently, when an ion with a valence of more or less than +3 replaces Al, the excess or deficiency of electrical charge must be compensated in some way so that the average positive charge still is +3. There are several ways *charge compensation* can occur. During growth of corundum at low temperature, pairs of ions, one with a valence of +4 and one with a valence of +2, could be incorporated near each other in a crystal. The total charge of the pair, +6, is the same as the two Al ions they would replace. Thus the crystal remains electrically neutral. Vacancies (atoms missing from lattice sites) and interstitial ions (atoms located between lattice sites) can also charge compensate trace elements.

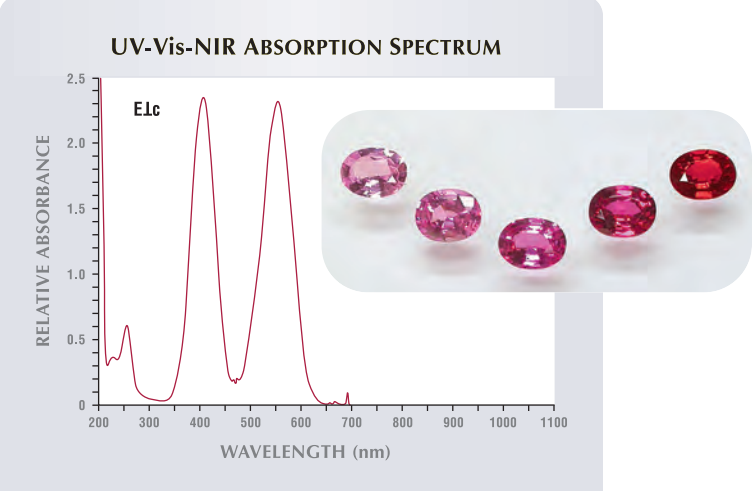

Figure 5. These synthetic rubies and sapphires are colored only by chromium. As the concentration of chromium increases (left to right), so does the saturation of the red. The spectrum shows chromium absorption in corundum. The samples weigh approximately 2.5 ct each; photo by Sriurai Scarratt.

Figure 6. The 1.10 ct Australian sapphire on the left is unusual in that its color results only from a high concentration of iron. The 1.40 ct heat-treated Sri Lankan sapphire on the right is colored by Mg^{2+}-trapped-hole centers. Iron causes pale yellow in sapphire primarily by absorption of Fe^{3+}-Fe^{3+} pairs as shown in this spectrum. The narrow peak at 388 nm and the broad bands at 540, 700, and 1050 nm are attributed to Fe^{3+}, while the narrow peaks at 377 and 450 nm are attributed to Fe^{3+}-Fe^{3+} pairs. Photo by Maha Tannous.

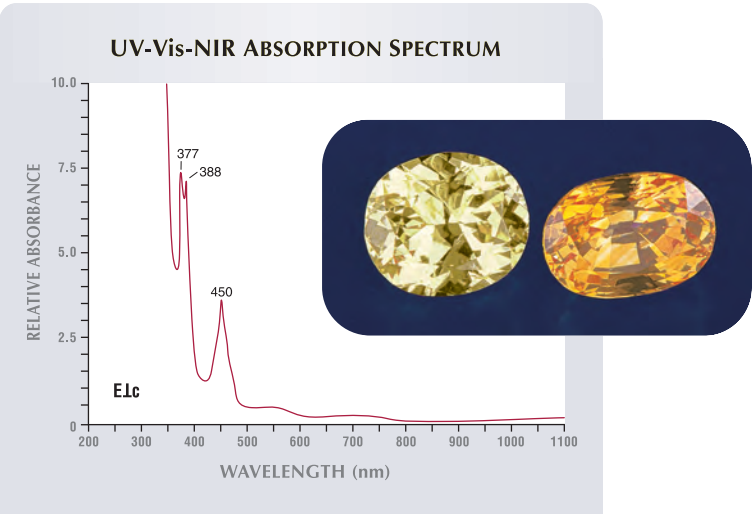

For example, an oxygen vacancy can charge compensate two divalent (+2) ions, and an oxygen interstitial can charge compensate two tetravalent (+4) ions. Likewise, an aluminum (Al^{3+}) vacancy can charge compensate three tetravalent ions, and an aluminum interstitial ion can charge compensate three divalent ions. In special cases, a free electron (relative charge –1) can charge compensate a tetravalent ion; or an electron hole (relative charge +1, hereafter simply called a *hole*) can compensate a divalent ion. (A hole in corundum can be viewed as an oxygen ion carrying a charge of –1 rather than –2.)

The way aliovalent ions are charge compensated can be a large factor in determining the color of corundum. As noted above, when an aliovalent ion such as Ti^{4+} is incorporated into a corundum crystal during growth, it can (in principle) be charge compensated by a divalent ion such as Mg^{2+}, or by an aluminum vacancy, or by an oxygen interstitial ion. However, it takes far less thermal energy to incorporate a divalent ion than to produce an aluminum vacancy or an oxygen interstitial ion. Corundum growth in nature takes place at temperatures from 250°C to 1400°C, depending on the growth environment (G. Rossman, pers. comm., 2003). At these temperatures, it is far more likely that Ti will be charge compensated by a divalent ion (e.g., Mg^{2+} or Fe^{2+}), assuming one is available in the growth medium, than by a vacancy or an interstitial ion. However, when corundum is grown in the laboratory at temperatures near its melting point (~2045°C), or is heat treated at high temperatures, charge compensation by vacancies, interstitial ions, holes, or electrons becomes more probable.

Aliovalent Ions. Fe^{2+} in corundum is an acceptor (Dutt and Kröger, 1975; Koripella and Kröger, 1986). When not associated with other impurity ions, it produces little or no coloration. Its major absorption bands are expected to be located in the near-infrared portion of the spectrum but have not been observed. In corundum with a relatively high iron concentration, Fe^{2+} often is found paired with Fe^{3+}, leading to the creation of an *intervalence charge-transfer* (IVCT) absorption (Burns, 1981; Nassau, 1983; Fritsch and Rossman, 1987) centered at 875 nm (Krebs and Maisch, 1971; Smith and Strens, 1976). This band is very broad, with the short-wavelength edge extending into the red region of the spectrum, thereby producing a weak gray-blue coloration. Because this absorption feature is rarely seen in crystals that do not contain titanium, it is sometimes difficult to evaluate how much of the blue coloration is contributed by this band (as opposed to that contributed by the Fe^{2+}-Ti^{4+} pairs). Fe^{2+} also can be charge compensated by tetravalent donor ions (e.g., Si^{4+} or Ti^{4+}) forming donor-acceptor pairs; by hydrogen, which is also a donor; or, in the absence of either of these options, by an oxygen vacancy or an aluminum interstitial ion.

Mg^{2+} in corundum is also an acceptor (Mohapatra and Kröger, 1977; Wang et al., 1983). It can be charge compensated by tetravalent donor impurities (e.g., Si^{4+} or Ti^{4+}) or, in their absence, by an oxygen vacancy or a hole. Charge compensation by an oxygen vacancy can occur when the crystal grows in reducing conditions, or is heat treated in a reducing atmosphere (Emmett and Douthit, 1993). When corundum is grown or heat treated in oxidizing conditions, charge compensation of Mg^{2+} appears to be by holes. The Mg^{2+}-induced trapped hole (an O^{1-} ion in the lattice) absorbs light very strongly in the blue region of the spectrum (figure 7), which leads to a yellow to orangy yellow color in natural sapphire. In high-purity synthetic sapphire containing only Mg^{2+}, the color is a violet-brown. The difference between these two colors is caused by the location of the trapped hole in the lattice. In the latter case, the hole is trapped close to the Mg^{2+} ion. However, in natural sapphires, which contain

Figure 7. The absorption spectrum of the Mg^{2+} trapped hole, as seen here in synthetic corundum, produces the strong yellow to orangy yellow color in some natural sapphires that are heat treated without beryllium.

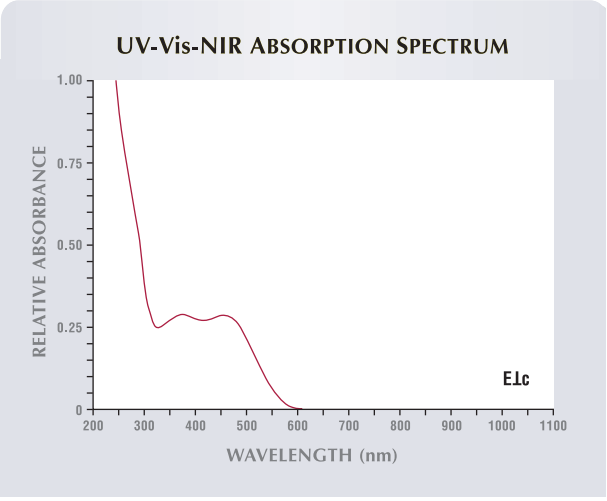

a variety of other impurities, the hole would preferentially associate with Cr^{3+} if available, or with Fe^{3+} in the absence of Cr^{3+}, leading to an altered absorption spectrum. As we shall see, in corundum Be^{2+} behaves much like Mg^{2+}. The heat-treated yellow sapphires of Sri Lanka and the natural-color or heat-treated yellow portions of the sapphires from Rock Creek, Montana, are both colored by the Mg^{2+}-trapped-hole mechanism. As shown in figure 6, the weak yellow produced by Fe^{3+} and the orangy yellow of the Mg^{2+}-induced trapped hole differ greatly in appearance. At this point we should note that the Mg^{2+}-related absorption center may be more complex than a simple Mg^{2+}-induced trapped hole. Häger (1996) has shown that the addition of iron increases the absorption strength of the trapped hole in synthetic sapphire. The details of this interaction remain to be elucidated.

One of the unusual properties of the Mg^{2+}-trapped-hole coloration in corundum is its sensitivity to oxygen partial pressure (oxygen concentration in the furnace atmosphere; Mohapatra and Kröger, 1977; Wang et al., 1983; Emmett and Douthit, 1993). If corundum containing Mg^{2+} is heat treated in pure oxygen, the color saturation is maximized. If that stone is then re-heated at an oxygen partial pressure of 10^{-3} atmospheres (atm), the color saturation is greatly reduced. This very strong relationship between color saturation and oxygen partial pressure is not observed with other chromophores in corundum, such as Cr^{3+}, Fe^{3+}, and Fe^{2+}-Ti^{4+}.

Silicon, a common trace element and (as Si^{4+}) a donor in corundum (Lee and Kröger, 1985), produces no coloration but poses some unique issues. All of the other impurities discussed so far normally occupy octahedral sites (i.e., a site surrounded by six oxygen atoms) in corundum and in many other minerals. Si almost always occurs in a tetrahedral site (surrounded by four oxygen atoms) in minerals, although there are no tetrahedral cation sites in the corundum lattice. So far, we do not know whether Si occupies an octahedral site in natural corundum, or forms as micro- or nano-sized crystals of some simple aluminosilicate mineral embedded in the corundum crystal. We do know, however, that in Si-containing synthetic corundum that has been heated to high temperature and cooled rapidly (that is, compared to geologic cool-down times), at least a portion of the silicon is located on octahedral aluminum sites (Lee and Kröger, 1985). If Si actually occupies an aluminum site, it will be "active"; that is, it will take part in the charge-compensation process as a donor. If it is part of a nano-crystal of another mineral phase, it will not. Since we are primarily concerned here with corundum that has been heat treated for tens to hundreds of hours at a very high temperature during the Be-diffusion process, we will make the assumption that low concentrations of naturally occurring silicon (i.e., ≤100 ppma) are in solution on Al^{3+} sites. Proving this conjecture will require additional studies. We may eventually find that only a portion of the silicon is active.

Figure 8. These magnificent blue sapphires (weighing approximately 2–4 ct) owe their color primarily to Fe^{2+}-Ti^{4+} pairs. Courtesy of Gordon Bleck; photo by Maha Tannous.

Fe^{2+}-Ti^{4+} acceptor-donor pairs, located on nearest-neighbor Al sites in corundum, produce the strong blue color that we normally associate with sapphire (figure 8), resulting from strong absorptions at 580 and 700 nm. Figure 9 shows the Fe^{2+}-Ti^{4+} absorption spectrum of a synthetic sapphire sample containing only Fe and Ti impurities at color-significant concentrations. This IVCT absorption feature in corundum was first explained by Townsend (1968). More recent studies indicate that the actual defect cluster may contain other ions and point defects in addition to single iron and titanium ions (Moon and Phillips, 1994).

The relative effectiveness of each of these trace elements, or trace-element pairs, in coloring corundum varies widely. Considering the color saturation in a 2 ct stone, in the course of earlier research we observed the following: 2,500 ppma Fe^{3+} will produce a weak yellow color; 1,000 ppma Cr^{3+} will produce a strong pink-red; 50 ppma of Fe^{2+}-Ti^{4+} pairs will produce a very deep blue; and, finally, 15 ppma of Mg^{2+}-hole pairs will produce a strong

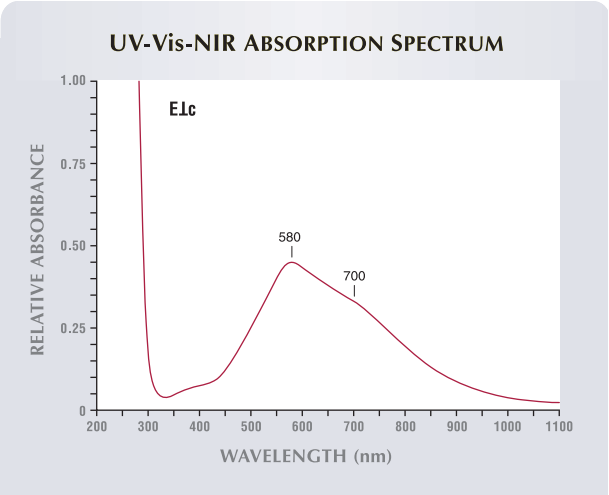

Figure 9. This is the absorption spectrum of Fe^{2+}-Ti^{4+} pairs in synthetic sapphire containing only iron and titanium.

orangy yellow (figure 10). Thus, to understand the color of corundum, we must be able to analyze for these elements, and those that interact with them, down to the level of a few ppma, which is usually not possible, particularly for lighter elements, with energy-dispersive X-ray fluorescence (EDXRF) spectroscopy or electron microprobe analysis. To measure both light and heavy elements in corundum at such low levels, we have found it necessary to use SIMS or LA-ICP-MS (again, see Box A).

Figure 10. The effectiveness of trace elements in coloring corundum varies widely. These samples illustrate the effects of ~3,000 ppma Fe^{3+} (1.10 ct natural yellow sapphire in center), ~1,000 ppma Cr^{3+} (193.58 ct synthetic ruby rod at top), ~50 ppma Fe^{2+}-Ti^{4+} pairs (2.54 ct blue synthetic sapphire wafer in center), ~20 ppma Mg^{2+} (40.04 ct purplish brown synthetic sapphire disc in lower left), and ~25 ppma Cr^{3+} with ~25 ppma Mg^{2+} (large orange boule on right). Photo by Maha Tannous.

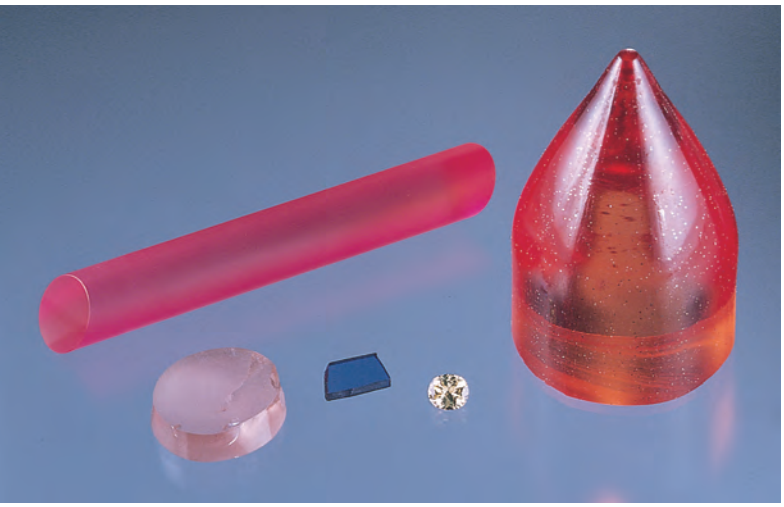

Interactions Among Elements. Natural corundum typically contains most of the elements listed above at some concentration levels, and most of these impurities will interact with each other to affect the color. Because of the higher energy required to incorporate aliovalent ions into the crystal lattice, the isovalent ions of Fe^{3+} and/or Cr^{3+} usually are incorporated at much higher concentrations (when they are available in the growth environment). Thus, for most corundum, the Fe concentration usually exceeds, by at least one order of magnitude, the concentrations of Ti, Si, or Mg (as well as other trace elements of less significance).

It is well known that, in the case of natural sapphire, there is little or no correlation between the concentrations of iron and titanium and the saturation of blue coloration. This is perhaps the most obvious indication that the interaction among impurities is as important as the presence of the impurities themselves in determining corundum color (Häger, 1992, 1993, 2001; Emmett and Douthit, 1993). With defect chemistry, we can describe chemical reactions in solids in a way that is directly analogous to what is done for chemical reactions in liquids or gases (Pauling, 1956). Thus, once we know the relative positions of the donor and acceptor energy levels for corundum (see Box B), we can predict how the impurities will chemically interact (Smyth, 2000). For many of the impurities in corundum with which we are concerned, the relevant energy levels have been determined by F. A. Kröger and his co-workers; an extensive compilation is contained in Kröger (1984) and its references.

From the defect chemical reactions and energy-level positions, we can formulate a series of rules about impurity interactions. These rules will not be valid for all concentration levels or all temperatures. They become less valid as concentrations of key elements (such as Mg and Ti) exceed ~100 ppma or at temperatures substantially above room temperature. A correct formulation requires solving the equilibrium chemical defect reactions for all of the impurities simultaneously, which is beyond the scope of this article. However, the following rules are useful for a wide variety of situations and, more importantly, will serve to illustrate the types of chemical reactions that occur among impurities in corundum:

- When Fe, Ti, and Mg are present, Ti will charge compensate Mg before Fe.
- When Fe, Si, and Mg are present, Si will charge compensate Mg before Fe.
- When both Ti and Si are present with Fe and Mg, Ti will charge compensate both Mg and Fe before Si will charge compensate Mg and Fe.
- When the concentration of Mg exceeds the sum of the concentrations of Si and Ti, Mg will be charge compensated by oxygen vacancies if the corundum formed or later was heat treated at low oxygen partial pressures. If it was formed or heat treated at high oxygen partial pressures, the Mg will be charge compensated by a trapped hole.

A simple example excluding silicon (Häger, 2001) will illustrate how these rules can be applied. In all of the examples given here, we assume an Fe concentration substantially greater than the concentration of Ti, Si, Mg, and Be, as this is typical of natural sapphire. Suppose we have an iron-containing sapphire with 60 ppma Ti^{4+}. If this stone grew or was heat treated in a reducing environment, all 60 ppma Ti^{4+} would form Fe^{2+}-Ti^{4+} pairs, so the stone would be deep blue. Another stone with exactly the same iron and titanium content but also with 40 ppma Mg^{2+} would be a lighter blue, since 40 ppma of the Ti^{4+} charge compensates the Mg^{2+} leaving only 20 ppma of Ti^{4+} to form Fe^{2+}-Ti^{4+} pairs.

Now consider that the magnesium concentration of our stone is 60 ppma. All 60 ppma of the Ti^{4+} must charge compensate the 60 ppma Mg^{2+}, leaving none to form Fe^{2+}-Ti^{4+} pairs. Thus, if the stone has only a few hundred ppma of iron, it is nearly colorless; with more iron, it would be pale yellow or greenish yellow.

To push our example one step further, suppose that the magnesium content is even higher, at 75 ppma. Now there is 15 ppma excess Mg^{2+} that is not charge compensated by Ti^{4+}. If this stone formed or was treated at low oxygen partial pressures, it will be nearly colorless or pale yellow, depending on its iron concentration (as for the 60 ppma Mg^{2+} case). This is because at low oxygen partial pressures, the charge compensation is by oxygen vacancies. However, high oxygen partial pressure would result in a strong orangy yellow color (figure 11), due to charge compensation of the 15 ppma excess Mg^{2+} by holes forming the trapped-hole color center.

Using square brackets (such as [Mg]) to denote concentrations, we have summarized these interactions for iron-containing sapphire in table 2.

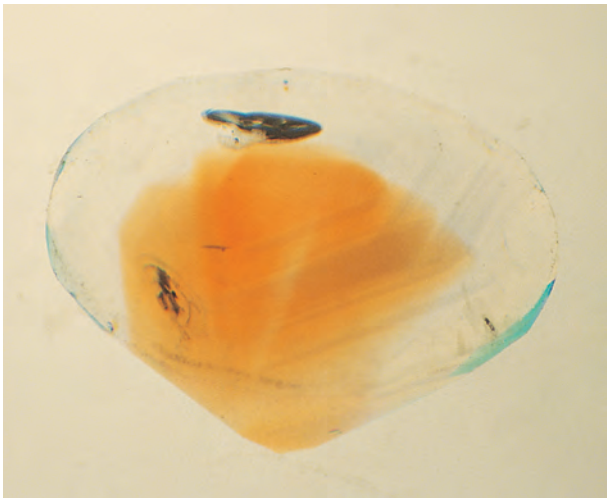

Figure 11. This strong orangy yellow color zone in a heat-treated Montana sapphire is caused by the presence of Mg^{2+} trapped-hole centers. Photomicrograph by Shane F. McClure; immersion, magnified 10×.

Aspects of this relationship between Fe, Ti, and Mg have been discussed previously (Häger, 1992, 2001; Emmett and Douthit, 1993). Häger (1993, 2001) represented the charge compensation of titanium by magnesium as $MgTiO_3$ (that is, Ti and Mg form a cluster occupying two nearest neighbor Al sites). While this is certainly possible, it is not at all necessary. The charge compensation of these two ions only requires that they be in the same general region of the lattice.

The Mg, Fe, Ti relationship described (Häger, 1992, 1993, 2001; Emmett and Douthit, 1993) is unfortunately an oversimplified model for natural corundum. The actual trace-element chemistry of natural corundum is often far more complex. For

TABLE 2. Relative trace-element concentrations and color in iron-bearing corundum.

Composition[a]	Color
$[Ti^{4+}] >> [Mg^{2+}]$	Very dark blue under reducing conditions
$[Ti^{4+}] > [Mg^{2+}]$	Blue under reducing conditions
$[Ti^{4+}] \approx [Mg^{2+}]$	Nearly colorless or iron colored (pale yellow to greenish yellow) under oxidizing or reducing conditions
$[Mg^{2+}] > [Ti^{4+}]$	Nearly colorless or iron colored (pale yellow to greenish yellow) under reducing conditions; strong yellow to orangy yellow under oxidizing conditions

[a] *Key to symbols:*
> "greater than" (approximately 5–25 ppma excess)
>> "much greater than" (approximately 25–100 ppma excess)
≈ nearly equal to

BOX B: UNDERSTANDING TRACE-ELEMENT INTERACTIONS IN CORUNDUM

There are several different ways to picture interactions (chemical reactions) among ions in solids. One of these, known as the *band model* (Bube, 1992; Smyth, 2000), has been exceedingly effective in describing semiconductors. Surprisingly, it has also proved very effective in describing materials like corundum, where all constituents other than aluminum and oxygen are at a concentration of 1% or far less. Figure B-1 shows a band-model energy-level diagram of corundum and some of its trace elements. In this model, the energy of an electron (in electron volts) is plotted on the vertical axis. The extent of the horizontal axis is meant to imply only that the corundum energy levels are the same everywhere in the crystal. The lowest energy level on this plot is known as the *valence band*, because it contains all the valence electrons of corundum. The uppermost energy level is called the *conduction band*, because if it contained a lot of electrons, the solid would conduct electricity. In corundum, the conduction band is empty at room temperature, which is why pure corundum is an excellent electrical insulator. The region between the valence band and the conduction band is called the *band gap* or *forbidden band*, which has a width of approximately 9 electron volts in corundum. In pure corundum, the energy-level diagram consists of only the valence band and the conduction band.

When trace elements (impurities) are added to corundum, they can form discrete energy levels that are often in the band gap. These energy levels are shown here as short lines to indicate they are localized around the impurity ion. To understand how these ions interact with one another, we need to know their positions relative to each other; their absolute positions in the band gap are of somewhat lesser importance. There is an agreed-upon convention by which the ions are labeled: Donor ions, such as titanium (see "Color in Corundum" section), are labeled with their charge *before* donating their electron, while acceptors are labeled with their charge *after* accepting the electron.

If we place magnesium into the corundum lattice on an aluminum site replacing an aluminum ion, it must have an overall charge of +3 (like Al^{3+}) for the crystal to remain electrically neutral. But we know that the charge on Mg is +2. One method to accommodate this discrepancy is to create a hole (a missing electron) in the valence band near the Mg^{2+} ion. This type of charge compensation only occurs in highly oxidizing environments. Since the relative charge of a hole is +1, the hole plus the Mg^{2+} ion makes a total charge of +3 to satisfy the Al^{3+} site requirement. It is this Mg^{2+}-hole pair that absorbs light, giving rise to the yellow and brown hues in Mg-containing corundum. Physically, the hole corresponds to one of the oxygen ions near the magnesium having a charge of –1 rather than the normal charge –2. A more structural way of looking at this situation is to observe that an Al^{3+}-O^{2-} group has been replaced by an Mg^{2+}-O^{1-} group having the same total charge of +1.

If titanium, a donor, were introduced into otherwise high-purity corundum, its preferred valence would be +3, and thus it would meet the charge requirements of the Al^{3+} site. What happens if both Ti and Mg are in a corundum crystal in the same amounts? The Ti^{3+} electron donor level is far above the Mg acceptor level, so an electron is transferred from Ti^{3+} (which becomes Ti^{4+}) to the Mg^{2+}-hole pair (which becomes just Mg^{2+}). The electron and the hole combine, or annihilate each other, to refill the valence band or, physically, the O^{1-} near the Mg^{2+} becomes O^{2-} as is normal. In this energy-level diagram, electrons move (fall) down to positions of lower energy. This interaction can also be pictured from the point of view of the hole rather than the electron. In that perspective, the hole is transferred from the Mg^{2+}-hole pair to the Ti^{3+}, resulting in Mg^{2+} and Ti^{4+} exactly as before. Also in this energy-level diagram, holes fall up. It doesn't matter which view is used since they are both the same, but usually we use the electron point of view if there are excess donors and the hole point of view if there are excess acceptors.

We now see a little more clearly what charge compensation is, and how it takes place. By this mechanism of donor-acceptor electron (or hole) transfer, the two ions charge compensate each other as +2 and +4, adding to +6, which is the charge of the two Al^{3+} ions they replace. This electron transfer only occurs because the Ti donor level is far above the Mg acceptor level and electrons always move down to the lowest available energy level. If the acceptor level was above the donor level, it would not occur. The Mg^{2+}-Ti^{4+} pair does not absorb light in the visible region of the spectrum, so its formation does not produce color in corundum. However, other pairs absorb light strongly and lead to strong coloration. Figure B-2*A* shows the formation of a pair between the Ti^{3+} donor and the Fe^{2+}-hole acceptor, where the Ti^{3+} becomes Ti^{4+} and the Fe^{2+}-hole pair becomes just Fe^{2+}. This donor-acceptor transfer creates the Fe^{2+}-Ti^{4+} pair responsible for the blue coloration in sapphire.

The Ti^{3+} donor level lies far above all acceptor levels in corundum, and thus will always transfer its electron (becoming Ti^{4+}) to some acceptor impurity if one is available. This is one of the reasons why the Ti^{3+} absorption spectrum is never

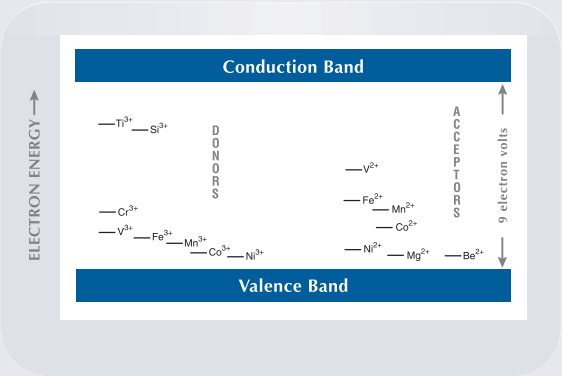

Figure B-1. In this energy-level diagram of impurities in corundum, trivalent donor ions are shown on the left, with divalent acceptor ions on the right. A charge-compensating donor-acceptor pair can form when the donor level is above the acceptor level. There is no significance to the lateral positions of the energy levels; the vertical positions are absolute, measured from the top of the valence band. Data from Kröger (1984) and references therein.

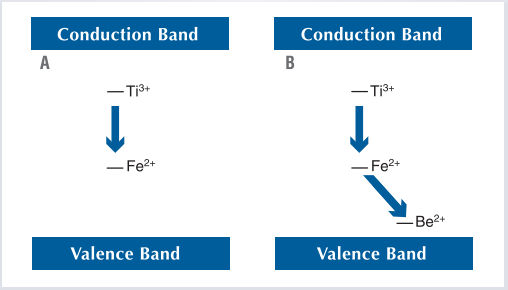

Figure B-2. In A, *the Ti^{3+} donor exchanges an electron with the Fe^{2+}-hole acceptor, thus producing the Fe^{2+}-Ti^{4+} pair responsible for blue in sapphire. In* B, *when beryllium is diffused into* A, *the Be^{2+}-hole acceptor presents a more attractive site (lower energy) for the Ti^{3+} donor electron than Fe^{2+}, causing the electron to be transferred to the Be^{2+}-hole acceptor (or the Be-induced hole is transferred to the Fe^{2+}). The transfer results in Fe^{2+} becoming Fe^{3+}, eliminating the Fe^{2+}-Ti^{4+} pair and the blue color. The Be^{2+}-Ti^{4+} pair formed does not absorb light in the visible region of the spectrum and thus does not contribute color to the sapphire.*

observed in natural corundum.

Now if there are two donors at different levels and a single acceptor, the highest donor will preferentially charge compensate the acceptor. If the two donor energy levels are close together, they will both take part in charge compensation of the acceptor. The same situation occurs in reverse if there are two acceptors and a single donor. That is, the lowest acceptor preferentially charge compensates the donor unless they are both close together (see figure B-2).

Silicon in corundum is a little more complex (see discussion in "Color in Corundum" section). In natural unheated corundum, silicon probably exists as broadly distributed nano- or micro-crystals of a silicate mineral. However, when the host corundum crystal is heat treated at a high temperature for a long time, all or part of the silicon will enter the corundum lattice in solution, replacing aluminum and producing the donor states shown in figure B-1 (Lee and Kröger, 1985). Si^{4+}-Mg^{2+} pairs do not add color. Si^{4+}-transition metal pairs in corundum have not been studied.

There are no published data on the position of the Be acceptor level. However, because the oxygen partial pressure dependence on the strength of the Be^{2+}-hole pair absorption is very similar to that of the Mg^{2+}-hole pair, as is the absorption spectrum itself, the energy levels must be fairly close to each other. For the examples in this article, we have assumed they are at the same level.

Now we can see the origin of the rules we have stated in the "Color in Corundum" section. If $[Ti^{4+} + Si^{4+}] > [Mg^{2+} + Be^{2+}]$, there are more than enough donor electrons to annihilate all trapped holes associated with Be^{2+} and Mg^{2+}, and thus the yellow coloration cannot form. Likewise, if $[Mg^{2+} + Be^{2+}] > [Ti^{4+} + Si^{4+}]$ there are excess Mg^{2+} or Be^{2+} trapped-hole pairs to cause the yellow coloration.

We can also see why the absorption spectrum of Be in high-purity corundum is different from that in Cr-containing corundum. In pure synthetic corundum, the Be-induced trapped hole is near the Be^{2+} ion, producing an orangy brown. However, if Cr^{3+} (a donor) is also present, the Be-induced hole is transferred to the Cr^{3+} (holes fall up), producing a Cr^{3+} trapped-hole pair and, thus, the characteristic orangy yellow coloration. (The Cr^{3+} trapped-hole pair could combine to form Cr^{4+}, but much more work is needed to determine if it does.) The Fe^{3+} donor state is below that of the Cr^{3+} donor state, so if both ions are present the Be-induced hole again pairs with Cr^{3+}, producing orangy yellow. In corundum without Cr^{3+} (or where Cr^{3+} is less than the excess holes available), holes would pair with the Fe^{3+} to produce an Fe^{3+} trapped-hole pair (or perhaps Fe^{4+}). The Fe^{3+} trapped-hole pair may be responsible for the unusual "Post-it" yellow color observed in some Be-diffused sapphire. Additional research involving Be diffusion into sapphire with only iron as an impurity will be required to elucidate this matter. By examining the relative energy-level positions of other donor and acceptor ions, however, we can deduce how they will interact.

example, adding silicon, a common trace element in corundum assuming that it is fully active, the condition for the formation of the trapped-hole color center changes from $[Mg^{2+}] > [Ti^{4+}]$ to $[Mg^{2+}] > [Ti^{4+} + Si^{4+}]$, so more magnesium is needed to observe the yellow trapped-hole color. Zr^{4+} (zirconium) can be expected to react chemically in ways similar to Ti^{4+} and Si^{4+}. Likewise, Ca^{2+} (calcium) and Ba^{2+} (barium) will react similarly to Mg^{2+}. The problem becomes substantially more complex when we consider the possible roles of other transition metal impurities such as vanadium (V), manganese (Mn), cobalt (Co), and nickel (Ni), each of which can potentially exist in multiple valence states. V and Mn could exist in corundum in 2+, 3+, or 4+ valence states; thus, they could be either donors or acceptors, or both. As donors, they could suppress the formation of trapped-hole color centers by forming donor-acceptor pairs with excess divalent ions. As acceptors, they would enhance the formation of trapped-hole color centers by forming donor-acceptor pairs with excess tetravalent ions. Ni and Co could act as acceptors, enhancing the probability of trapped-hole color center formation. Enhancing trapped-hole formation increases the yellow color component, while reducing trapped hole formation reduces the yellow component.

Vanadium is commonly observed in Cr-containing corundum (Hänni and Pettke, 2002; Peretti and Günther, 2002), and Mn is often seen in trace-element analyses of corundum. There appears to be no information in the literature on Ni and Co concentrations in natural corundum. It is important to note that, in discussing these additional trace elements, we are not referring to concentrations high enough to contribute color on their own part. We are referring to concentrations in the range of 1 to 30 ppma, where they might play a significant role in the charge-compensation relationships among ions. Table 3 lists additional trace elements that could potentially impact the color of corundum if they were in solid solution, whether naturally occurring or from a diffusion process. Several appear in two or three columns, because they can potentially assume two or three valences. Thus, a quantitatively accurate analysis of the color of a ruby or sapphire would, in principle, require a complete trace-element analysis down to a level of a few ppma. Much additional trace-element data on a wide variety of natural corundum, as well as additional diffusion experiments, will be needed before we fully understand which of these ions may be important. Inasmuch as most natural corundum exhibits color zoning (figure 12), and thus zoning of trace-element concentrations, such an analysis would indeed be time consuming. Fortunately, we can understand the main features of how the addition of beryllium alters the color of most types of corundum by considering only the short list of trace elements presented earlier: Fe, Cr, Ti, Si, Mg, and perhaps V.

TABLE 3. Trace elements other than Fe, Mg, Ti, and Cr that could impact the color of corundum.

Valence			
+1	+2	+3	+4
Hydrogen	Beryllium	Vanadium	Carbon
Lithium	Calcium	Manganese	Silicon
Sodium	Vanadium	Cobalt	Manganese
Copper	Manganese	Nickel	Germanium
Silver	Cobalt		Zirconium
	Nickel		Tin
	Copper		Lead
	Zinc		Vanadium
	Cadmium		
	Tin		
	Barium		
	Lead		

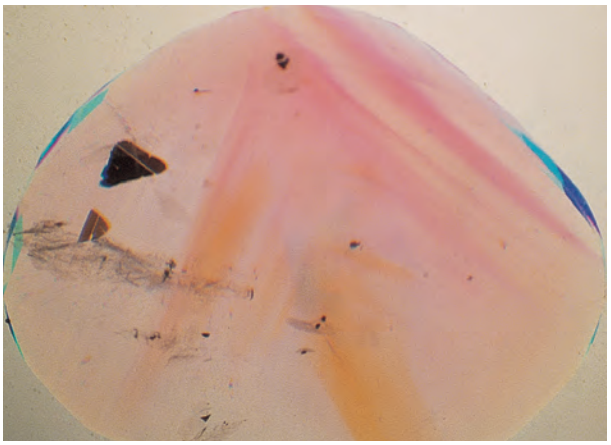

Figure 12. Variations in trace-element concentrations create the color zoning typically seen in many natural sapphires, such as the orange and pink zones shown here, which makes accurate chemical analysis very laborious. Photomicrograph by Shane F. McClure; immersion, magnified 10×.

Color Modifications Associated with Beryllium Diffusion. Now that we have an idea of how different elements interact in corundum, we can turn to

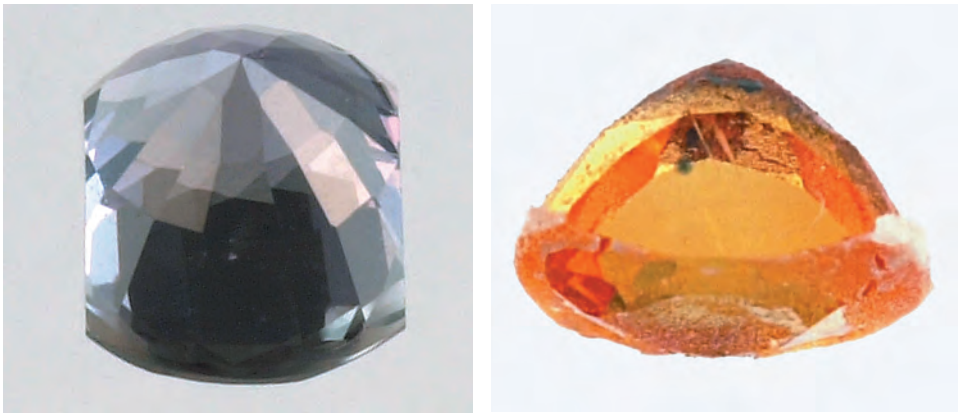

Figure 13. Many of the off-color sapphires from Songea that do not improve with standard heat treatment (left) will turn a strong orangy yellow after Be diffusion (right). This stone weighs 0.50 ct; photos by Elizabeth Schrader.

the specific case of beryllium and the color modifications caused by the diffusion of beryllium into natural corundum. As noted earlier, the presence of Be has been established in the color-altered layer of sapphires heat treated in Thailand by the "new" method (McClure et al., 2002; Wang and Green, 2002a,b), at concentrations well above those measured in unaltered regions. When beryllium is added to corundum by diffusion, there is another layer of complexity in color determination, because the beryllium concentration is not always spatially uniform throughout the stone (see Appendix). The final color may be some combination of the remaining core of original color plus the Be-altered outer color. We will return to this point later, and for the present consider only Be-induced color modifications resulting from a uniform beryllium concentration.

Drawing on our earlier studies (Emmett and Douthit, 1993) of Mg-induced trapped holes in corundum and subsequent research, our working hypothesis was that Be^{2+} would position itself in the corundum lattice by replacing an aluminum ion, thus becoming an acceptor (again, see Box B). As such, it would act much like Mg^{2+}, trapping holes and producing a strong yellow coloration under exactly the same conditions. However, given the very small size of Be^{2+}, we thought that its solubility in corundum would be lower than that of Mg. From experimental measurements on Be-diffused corundum (Hänni and Pettke, 2002; McClure et al., 2002; Peretti and Günther, 2002; Wang and Green, 2002a,b; see also the "Beryllium Diffusion into Corundum: Process and Results" section below), it appears that concentrations of diffused beryllium range from about 10 to 30 ppma, and that 10 to 15 ppma can produce a strong yellow coloration. In many ways, then, the effect of diffusing beryllium into corundum is similar to that of increasing the magnesium concentration. Thus, we can add the following to our list of rules:

- Ti^{4+} will preferentially charge compensate Be^{2+} before Fe^{2+}.
- The condition for the formation of a yellow trapped-hole color center in an oxidizing atmosphere becomes $[Mg^{2+} + Be^{2+}] > [Ti^{4+} + Si^{4+}]$.

With these simplified rules, we can predict most of the color modifications that will result from beryllium diffusion. First, let us examine the light green and light blue sapphires typical of Songea (Tanzania), the Montana alluvial deposits, and the pale-colored or colorless sapphire that results from heat treating some Sri Lankan geuda. In such stones, we have the condition that $[Ti^{4+} + Si^{4+}] \geq [Mg^{2+}]$ (that is, donor impurities are slightly greater than or about equal to acceptor impurities). The addition of beryllium as an acceptor changes the concentration relationship to $[Mg^{2+} + Be^{2+}] > [Ti^{4+} + Si^{4+}]$—so there is an excess of acceptor impurities. In a reducing atmosphere, the excess acceptor impurities (Mg^{2+}, Be^{2+}) will be charge compensated by oxygen vacancies and thus produce no color. However, in an oxygen atmosphere, excess Mg^{2+} and Be^{2+} will trap holes, producing a strong yellow to orangy yellow coloration (figure 13). This is the reason that beryllium diffusion of corundum must always be carried out in a highly oxidizing atmosphere. In the cases of Montana alluvial sapphire, Sri Lankan sapphire, and Sri Lankan geuda, there are many stones with $[Mg^{2+}] > [Ti^{4+} + Si^{4+}]$ that are nearly colorless or pale yellow as a result of slightly reducing conditions during formation. When these stones are heat treated in an oxidizing atmosphere, strong yellow colors will be produced. When beryllium is diffused into these stones so that $[Mg^{2+} + Be^{2+}] >> [Ti^{4+} + Si^{4+}]$, a very saturated orange will result.

Some of the first Be-diffused stones studied in the U.S. were pink/orange combinations, the result of processing pink sapphires from Madagascar. Pink Madagascar sapphire contains Cr^{3+} far in excess of

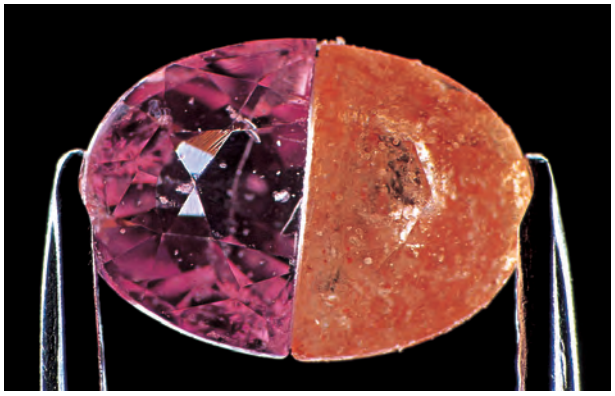

Figure 14. When Be-induced yellow color is added to the natural pink color of some Madagascar sapphires, a bright orange is produced, as can be seen in this 0.51 ct pink sapphire that was cut in half with one half then being Be diffused. Photomicrograph by Shane F. McClure; magnified 10×.

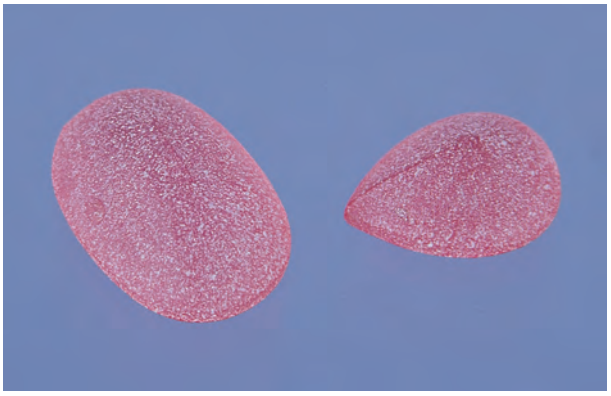

Figure 15. These two pink preforms (the larger weighs 0.77 ct) were reportedly subjected to the Be-diffusion process 10 times in Thailand, yet they did not change color. Photo by Maha Tannous.

the added beryllium concentrations, so the Cr^{3+} concentration is largely unaffected by heat treatment. Thus, we can apply our previous rules for Fe-containing corundum to corundum that also contains Cr, taking into consideration the original Cr-pink body color. For example, when Be is diffused in an oxidizing atmosphere into a pink Madagascar sapphire where $[Ti^{4+} + Si^{4+}] \geq [Mg^{2+}]$, the chemistry changes to $[Mg^{2+} + Be^{2+}] > [Ti^{4+} + Si^{4+}]$, which shifts the stone from donor- to acceptor-dominated; the resulting trapped holes produce a yellow coloration. When this yellow coloration permeates most or all of the original pink sapphire, an orange stone results (figure 14).

Some of the pink stones do not change color with Be diffusion. In that case, we have $[Ti^{4+} + Si^{4+}] >> [Mg^{2+}]$, which becomes $[Ti^{4+} + Si^{4+}] > [Mg^{2+} + Be^{2+}]$ from the Be diffusion; the material remains donor-dominated, does not trap holes, and does not become orange (figure 15). Earlier it was discussed that other transition elements may also play a role as donors or acceptors. As previously noted, the pink Madagascar sapphires contain 5 to 20 ppma of vanadium. If V acts as a donor in these stones, which we would expect, it could also play a role in suppressing the formation of trapped-hole color centers. Substantial additional analytical work and careful optical spectroscopy will be required to resolve these issues.

We also need to understand the impact of Be diffusion into blue sapphire. As noted previously, dark blue natural sapphire results from the condition $[Ti^{4+}] >> [Mg^{2+}]$. (Note again that we are assuming an iron concentration far in excess of the Ti^{4+} concentration.) If Be is diffused into such stones, the condition becomes $[Ti^{4+}] > [Mg^{2+} + Be^{2+}]$, and the stone is still blue but much reduced in color saturation. Thus, it is possible to render unacceptably dark blue sapphire into marketable blue colors.

It is interesting to note that the earlier diffusion process—of titanium into otherwise colorless or pale-colored sapphire (see, e.g., Kane et al., 1990)—is just the reverse of the process previously described. The sapphire typically used in the blue diffusion process is the very pale yellow, pale blue, pale pink, or completely colorless material that results from the unsuccessful heat treatment of some Sri Lankan geuda. For this material, we can presume the condition $[Mg^{2+}] \sim [Ti^{4+} + Si^{4+}]$, since it did not turn blue or yellow from the initial heat-treatment process. Note that it also contains iron. When titanium is diffused into the stone, the condition in the diffusion layer shifts to

Figure 16. A dark blue color layer is formed near the surface when Ti is diffused into sapphire. This 1.3-mm-thick section was sawn from a 1.45 ct stone, and shows a Ti diffusion–induced layer of blue color that is 0.4 mm deep. Photo by Shane F. McClure; immersion.

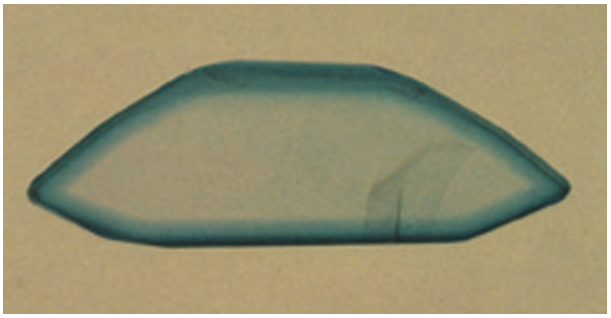

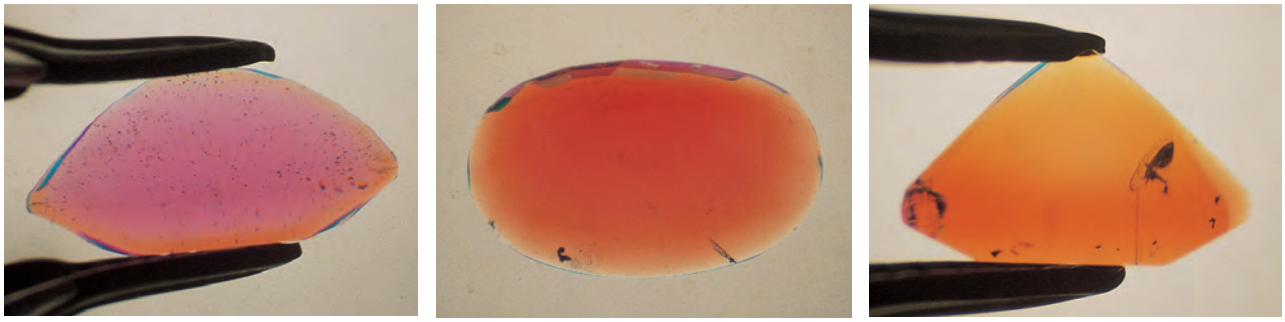

Figure 17. Depending on the duration of the Be-diffusion process, the induced color layer can penetrate to any depth, including throughout the stone. This figure shows examples of shallow (left), moderate (center), and deep (right) penetration. Photomicrographs by Shane F. McClure; immersion, magnified 10×.

$[Ti^{4+} + Si^{4+}] >>> [Mg^{2+}]$; that is, it becomes donor dominated, and a very dark blue layer is formed (figure 16). Since titanium has a much greater solubility in corundum than does beryllium, the final condition is $[Ti^{4+} + Si^{4+}] >>> [Mg^{2+}]$, rather than $[Ti^{4+} + Si^{4+}] > [Mg^{2+}]$. Nevertheless, it becomes clear that the mechanisms behind the Ti blue-diffusion process and the Be-diffusion process are essentially the same.

The foregoing discussion addressed the color modifications in various types of corundum assuming that the added Be is essentially uniformly diffused throughout the stone. We now need to consider the effect of non-uniform diffusion of beryllium into a natural-color stone that has essentially uniform natural coloration, such as the orangy pink (padparadscha-like) sapphires in which the final color appearance is produced by diffusing a layer of yellow into an originally pink stone. Depending on the duration of the diffusion process, the depth of penetration can vary from a few tenths of a millimeter to the full thickness of the stone (see the Appendix and figure 17).

As a hypothetical example, suppose we start with a 2 ct pink Madagascar sapphire, and examine how the color could alter with diffusion time. It can be assumed that we are dealing with a stone where $[Be^{2+} + Mg^{2+}] > [Ti^{4+} + Si^{4+}]$, and thus the Be-diffused areas will exhibit added yellow coloration from the trapped-hole color centers that form during the diffusion process. From our experiments (see the Appendix), we know that the diffusion depth for this type of material is about 2 mm in 40 hours at 1800°C. If the diffusion is conducted for one hour, the penetration depth will be roughly 0.35 mm; the pink overall color of the stone will be slightly modified in the direction of a padparadscha color. In 10 hours, the penetration will be about 1 mm and the stone will be the orangy pink of a good padparadscha. Further increasing the diffusion time, and thus the depth to which the Be penetrates, will successively yield pinkish orange, orange, and finally a very saturated deep orange coloration as the beryllium penetrates the entire stone (figure 18).

Ruby is another important example of color modification with diffusion depth. Many of the rubies from Songea and Madagascar contain substantial iron and titanium, and thus have a strong blue hue component as a result of Fe^{2+}-Ti^{4+} pairs. As discussed previously, Be diffusion in an oxidizing atmosphere shifts the equilibrium from $[Ti^{4+} + Si^{4+}] > [Mg^{2+}]$ to $[Mg^{2+} + Be^{2+}] > [Ti^{4+} + Si^{4+}]$, so the blue component becomes yellow. If these stones are Be diffused all the way through, the entire blue component is replaced with yellow, and the stone becomes a very strong orange. However, if the Be diffusion only penetrates into the stone a relatively short distance, the yellow surface layer will visually cancel out or offset the bluish core. Thus, the

Figure 18. The depth of the Be-diffusion layer directly affects face-up color. The stone on the far left has a very shallow diffusion layer. Moving right, each stone has a progressively deeper layer, making each more orange than the last. These stones weigh 0.80–1.89 ct; photo by Maha Tannous.

Figure 19. Be diffusion can produce good ruby colors (center, 5.05 ct) from strongly purplish or brownish red stones from some localities that typically do not respond to standard heat treatment, such as the small stones from Songea in this image. Photo by Maha Tannous.

appearance will be a good ruby red. In this way, many attractive red rubies can be produced from stones with a strong purple component (figure 19).

In principle, these stones can be detected easily by observing the yellow rim in immersion. However, it is conceptually possible to create the same visual effect without producing a yellow surface-conformal layer. After processing such rubies with full Be penetration, so they turn orange, we can reduce saturation of the yellow trapped-hole color component by heating the stones at a lower oxygen partial pressure. Reducing the oxygen partial pressure will reduce the yellow coloration. Thus, by "tuning" the oxygen partial pressure in a heat-treatment process that takes place after the Be-diffusion process, an optimal ruby color may be achieved. This full-depth diffusion followed by an oxygen partial pressure post-process could also be used with our pink sapphire above to achieve padparadscha coloration without a visible diffusion layer. Unfortunately, rubies and padparadscha-colored sapphires produced by this two-step method will be more difficult to detect.

It is also useful to consider the color modifications resulting from partial Be diffusion into a blue sapphire where $[Ti^{4+}] > [Mg^{2+}]$. As we have already discussed, uniform Be diffusion into such stones converts them from blue to yellow. However, a green overall color appearance results when the inward diffusion of beryllium converts only the outermost layer from blue to yellow. If this green stone were to be heat treated subsequently in a reducing atmosphere, it would be blue with a colorless outer layer (figure 20).

BERYLLIUM DIFFUSION INTO CORUNDUM: PROCESS AND RESULTS

Over the course of the last year and a half, the authors have conducted numerous experiments into both the Be-diffusion treatment of corundum and the characteristics of rubies and sapphires that have been treated by this method. This first section describes those experiments conducted primarily to explain the nature of beryllium diffusion and how it affects corundum. The following section reports on the examination of known Be-diffused corundum samples, as well as natural-color and heat-treated stones, to establish criteria by which rubies and sapphires treated by this new diffusion process can be identified.

The extensive set of experiments in this first section were initiated to understand and then replicate Thai results, to study the diffusion rates, and to determine just how broadly applicable this new process was to a wide variety of different types of corundum. By conducting these experiments in the laboratory, we could fully control all aspects of the process and not have to guess the treatment conditions (which has been the case with stones processed in Thailand).

Materials and Methods

Corundum Samples. For the Be-diffusion experiments, we selected samples from large lots of

Figure 20. Partial Be diffusion of a blue sapphire followed by heating in a reducing atmosphere can create a colorless layer around the outside of an otherwise blue stone, in effect lightening the overall color. Photomicrograph by Shane F. McClure; immersion, magnified 27×.

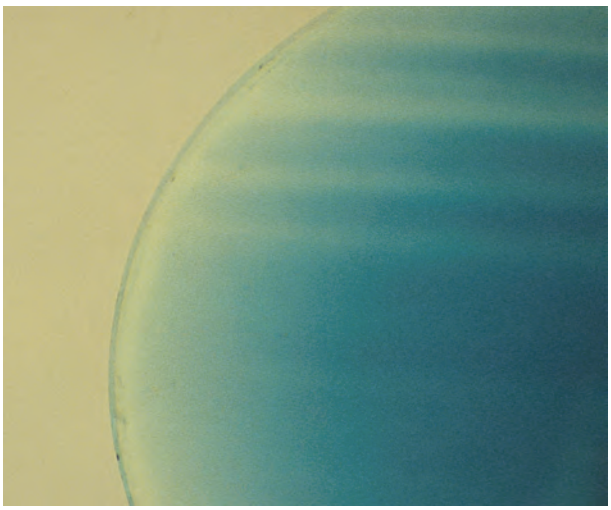

rough sapphire that were mined from several different localities, including Australia, Madagascar, Tanzania, and Montana, as detailed in table 4. In general, we preferred to use small pieces (≤ 0.5 ct) to assure that we could diffuse beryllium completely through the samples in 50 hours or less; however, we also conducted experiments on larger individual pieces to measure diffusion depths. Many of the samples listed in table 4 are from large, carefully collected mine-run parcels from the deposits indicated, and thus they contain a wide range of stone sizes. From these lots we selected samples primarily on the basis of size, while endeavoring to maintain representative color and clarity.

For spectroscopic experiments on Be-diffused Thai-processed sapphire, we obtained a variety of samples (15 pieces) in Bangkok that ranged from 0.25 ct to 2.1 ct. According to the treaters, they were comprised of both Songea pale green and blue sapphire that had been processed to a vivid yellow, and Madagascar pink sapphire processed to padparadscha and saturated orange colors. As much as possible, samples were chosen with the c-axis perpendicular to the table facet to facilitate obtaining absorption spectra that included the ordinary ray (o-ray) optical direction. On these 15 samples, the culet was ground off parallel to the table and polished to produce wafers from 0.5 to 1.8 mm thick. Samples with similar geometry were also prepared from rough material produced in our diffusion experiments, or from rough pieces prior to diffusion treatment. Samples polished before diffusion treatment required repolishing after diffusion treatment. In total, about 30 samples were prepared and studied.

In addition to the natural sapphire samples described in table 4, four types of high-purity synthetic corundum were also used for the Be-diffusion experiments and spectroscopic testing (see table 5). These samples were prepared as polished wafers prior to Be diffusion, and repolished afterward. In all cases the c-axis was perpendicular to the polished face. We have not tested low-purity gem-grade Verneuil-grown sapphire.

Applying Beryllium Compounds. To apply beryllium to the surfaces of the corundum samples for diffusion, we used both molten fluxes (Emmett, 1999) and dry powders as carriers for Be-containing compounds. (A *flux* in this context is a high-temperature solvent for inorganic compounds.) While it is common knowledge that Thai heat treaters employ fluxes in many processes, the actual formu-

TABLE 4. Rough corundum samples used for Be-diffusion treatment experiments.

Origin	Color	Lot size	Avg. stone size	Source
King's Plain, New South Wales, Australia	Basaltic dark blue, transparent to opaque	10 kg	0.3–0.5 ct	Great Northern Mining
Subera Area C, Queensland, Australia	Basaltic dark blue, transparent to opaque	10 kg	0.3–0.5 ct	Great Northern Mining
	Yellowish green		0.3–0.8 ct	
Wutu Township, Shandong Province, China	Basaltic dark blue	1 kg	~0.3 ct (large crystals sliced for wafers)	Diversified Mineral Resources
Antsiranana, Madagascar	Basaltic dark blue, dark green	250 g	0.3–0.6 ct	Budsol Co., Hargem Ltd.
Ilakaka, Madagascar	"Pink" sapphire[a]	350 g	0.4–1.0 ct	Wobito Brothers, Allerton Cushman & Co., Paul Wild
Dana Bar, Missouri River, Montana	Pale green, pale blue	1 kg	1.5 ct	American Gem Corp.
Dry Cottonwood Creek, Montana	Very pale green, very pale yellowish green	10 kg	0.7 ct	American Gem Corp.
Rock Creek, Montana	Pale blue, pale yellowish green	10 kg	0.7 ct	American Gem Corp.
Yogo Gulch, Montana	Medium blue, violet	200 g	0.2 ct	American Gem Corp.
Sri Lanka	"Colorless" heat-treated geuda[b]	100 g	0.3–1.0 ct	Paul Wild
Songea, Tanzania	Pale blue, pale yellowish green	600 g	0.3–1.2 ct	American Gem Corp.
	Ruby, ranging from bluish red to brownish red			
Umba, Tanzania	A wide variety	600 g	3 ct	Nafco Gems, Paul Wild

[a]*This parcel of "pink" sapphires showed a range of pink color saturation, and also included some violetish pink, pale yellow, pale blue, and colorless pieces.*
[b]*The sapphires in this parcel ranged from colorless to very pale blue, pink, or yellow, after heat treatment in an oxidizing or reducing atmosphere.*

lations are closely guarded trade secrets. Rather than attempt to find out actual Thai formulas, we chose to formulate our own from calcium borate, calcium phosphate, sodium phosphate, or a sodium feldspar (a silicate mineral). To each main flux component we added small amounts of Al_2O_3 and ZrO_2 to raise the flux viscosity at high temperatures. To these fluxes we then added ~4% natural chrysoberyl that had been finely powdered. Chrysoberyl, $BeAl_2O_4$, is 7.1% Be or 19.7% by weight BeO.

These flux mixtures were blended with water or alcohol containing a binder until they reached the consistency of a heavy paint. For water mixtures, Varethane™ or methocel was used as a binder. (Methocel is a modified cellulose ether used as a binder in many industrial applications.) For alcohol mixtures, orange shellac was used as a binder. Little consistent difference was noted among the binders. The rough stones were dipped into the flux paint mixture and then allowed to dry. Polished corundum wafers were hand painted on both sides with the mixtures.

Dry powders, that is, mixtures of a carrier and a beryllium compound, do not melt and flow like a flux. The dry powders used were very high purity Al_2O_3 containing either 4% powdered chrysoberyl or 0.8% very high purity BeO. We also used a mixture containing 2.65% BeO. Two application methods were employed. First, we completely buried the corundum samples in the powder mixture, in an alumina crucible. This is the original technique developed by Union Carbide Corp. (Carr and Nisevich, 1975, 1976, 1977). It works very well from the point of view of diffusion uniformity, but sintering of the powder to a fairly solid mass made sample recovery laborious. In the second method, the powder was mixed to the consistency of a paint, just as was done for the fluxes, and applied to rough stones and polished wafers as previously described. This latter process makes sample recovery very easy but does not always result in completely uniform diffusion.

Heat Treatment. Heat-treatment experiments were conducted with an electrically heated furnace manufactured by Thermal Technology of Santa Rosa, California (figure 21). The modified type-1000A furnace uses a graphite heating element and graphite insulation, and is capable of operation at 2500°C (which far exceeds the 2045°C melting point of corundum). For controlled atmosphere operation, the furnace separates the heating element from the sapphires with a muffle tube made from Coors 99.8% Al_2O_3 ceramic. This ceramic muffle tube becomes very soft at temperatures over 1800°C, and it can collapse if it becomes too hot. This limits the temperature for the long runs typical of beryllium diffusion to 1800 to 1850°C. The sapphires are placed inside the muffle tube where any type of process gas can flow over them. A more detailed description of this equipment and how it is used can be found in Emmett and Douthit (1993).

For the heat-treatment experiments described below, the process gas used was pure oxygen. This choice was made because, as discussed earlier, the trapped-hole coloration is sensitive to oxygen partial pressure, and is maximized in 100% oxygen.

TABLE 5. SIMS analyses of synthetic corundum showing the low levels of Fe, Ti, and Cr (non-ruby) in ppma.[a]

Samples[b]	Na	K	Be	Mg	Ca	Cr	Fe	Ga	Ti
SS1, SG Czochralski-grown synthetic sapphire	0.48	0.07	1.46	0.16	0.02	0.8	0.04	3.1	1.27
SS8, CSI Hemlite grade heat exchanger method–grown synthetic sapphire	0.39	0.14	13.4	0.83	0.04	0.25	0.03	0.94	1.98
SS3, SG Czochralski-grown light red synthetic ruby	0.18	0.02	1.57	0.05	0.02	316	0.04	1.8	2.14
SS18, SG Czochralski-grown dark red synthetic ruby	0.23	0.04	1.57	1.27	0.04	2580	0.13	7.5	2.00

[a] *Data taken before Be diffusion except sample SS8 which was measured after.*

[b] *SG: Saint-Gobain Crystals and Detectors, 750 S. 32nd St., Washougal, WA 98671. CSI: Crystal Systems Inc., 27 Congress St., Salem, MA, 01970.*

The coated sapphires were placed in shallow alumina crucibles made from Coors 99.8% Al_2O_3 ceramic. When the stones were embedded in a dry powder, deeper Coors crucibles were used. Depending on the number of stones in a sample lot, up to 12 separate experiments could be run in the furnace at the same time. For these experiments, temperatures of 1780°C or 1800°C were chosen. Run times from 25 to 100 hours at temperature were chosen, with 33 hours being typical.

Spectroscopy. The ultraviolet-visible and near-infrared (UV-Vis-NIR) spectra were recorded for the range 200–1100 nm at room temperature using a Hitachi U-2000 spectrophotometer. More than 60 spectra were collected on natural and synthetic Be-diffused sapphire wafers. For those natural sapphire samples where the color was not spatially uniform, reproducible spectra were assured by the method described by Emmett and Douthit (1993). Spectra were recorded only for the o-ray (E⊥c).

There are three feasible methods for determining trapped-hole spectra. In all cases we refer to these methods as producing *differential spectra*. First, the spectra can be taken in the Be-diffused layer and in the center of the stone where beryllium has not penetrated. If the spectrum from the unaltered portion of the sample is subtracted from that from the Be-diffused region, the trapped-hole spectrum will result. This method works well with synthetic sapphire and ruby, where dopant concentrations are spatially uniform, but it leads to inaccurate results on natural corundum samples, which are rarely uniform in chemistry.

The second method is to take one spectrum before Be diffusion and another after. If the before spectrum is subtracted from the after spectrum, an accurate trapped-hole spectrum results. This technique works very well on uniform synthetic corundum samples, and on natural samples if great care is taken to assure both measurements are taken through exactly the same place in the sample (Emmett and Douthit, 1993).

The third method, for use on a sample already diffused, is to take two spectra on the sample equilibrated at two different oxygen partial pressures. As noted previously, the strength of the trapped-hole absorption spectrum is very sensitive to oxygen partial pressure. From a practical point of view, the spectrum is taken on the Be-diffused sample as received. Then the sample is heated to 1650°C for a few hours in an oxygen partial pressure of 10^{-3} atm, cooled, and the spectrum is taken again. If the after spectrum is subtracted from the as-received spectrum, the spectrum of the trapped-hole center results. This works well on synthetic corundum samples, and on natural corundum samples if great care is taken to position the sample as described above. Heating for a few hours at 1650°C has little impact on a sample that has been heated for a few tens to hundreds of hours at temperatures of 1800°C or above. For the work described here, the second or third method was used on all samples, as the first method proved to be too inaccurate.

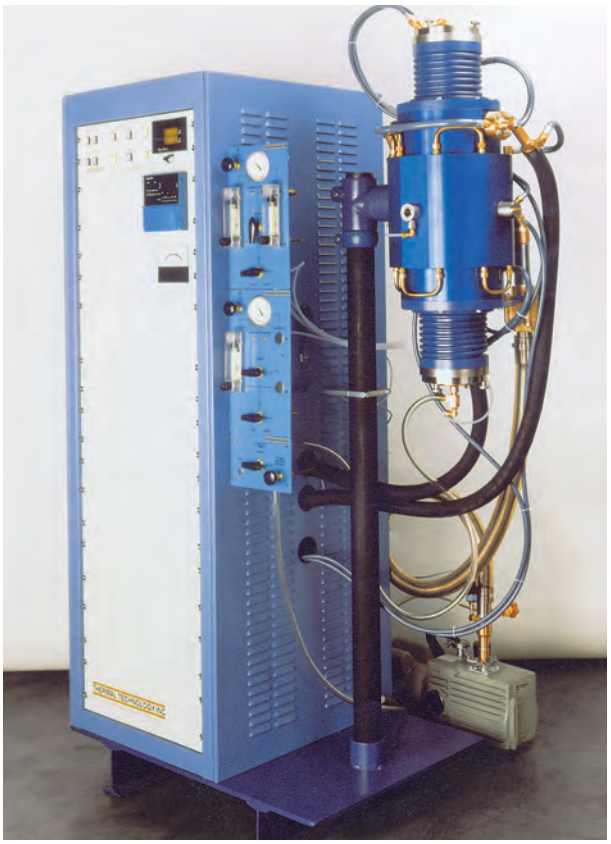

Figure 21. Most of the Be-diffusion experiments described in this article were conducted using an electrically heated furnace. Photo courtesy of Thermal Technology Inc.

Chemistry. Secondary ion mass spectrometry with element-in-sapphire standards (again, see SIMS Box A) was used at Evans East to determine Be and other trace-element concentrations in some of the natural Be-diffused wafer samples used for absorption spectroscopy, and in some of the synthetic samples before and/or after Be-diffusion treatment.

Results and Discussion

Identification of the Be-Induced Trapped Hole. In April 2002, we initiated a set of experiments to determine the origin of the color induced by Be diffusion. We believed that we were observing trapped-hole-center absorption, similar to that observed much earlier in both natural and synthetic corundum (Mohapatra and Kröger, 1977; Wang et al., 1983; Emmett and Douthit, 1993; Häger, 1993). Because holes only form in corundum under highly oxidizing conditions, the concentrations of Mg- or Be-hole pairs are very sensitive to the oxygen partial pressure at which they are equilibrated in the furnace. An orange sapphire Be-diffused in Thailand from pink Madagascar starting material was chosen for the first experiment. Figure 22 shows the results. At an oxygen partial pressure of 10^{-2} atm (1% oxygen, 1 atm total pressure), the Be-induced coloration has been reduced by about one half. This extreme sensitivity is not typical of the spectra of single ions in corundum.

From this experiment, we can also determine the absorption spectrum of this Be-induced coloration. By taking the differential spectrum of the figure 22 spectra, we obtain the result in figure 23, which is the absorption spectrum of the Be-induced coloration in this sapphire. Note that it is quite similar to the Mg^{2+}- trapped hole pair spectrum presented in figure 7. These two pieces of data, taken together and compared with the well-studied example of the Mg^{2+}-trapped hole pair, form the basis of our identification of the Be-induced coloration as arising from Be-induced trapped-hole formation. These spectral changes are reversible. When the sample was then equilibrated at an oxygen partial pressure of 1 atm, the original absorption spectrum was restored. Subsequently, we tested a wide variety of sapphire samples from different locations over a wider range of oxygen partial pressures and temperatures with very similar results. In each case, the predominant 460 nm absorption band appeared and showed the same oxygen partial pressure dependence (see "Absorption Spectra" section below). Additional confirmatory evidence of the induced trapped hole nature of these spectra would be the change of the spectra with temperature. It is known that such spectra broaden to the low-energy side when the stones are heated several hundred degrees above room temperature. Data that tend to confirm this are shown in the "Gemological Testing and Identification" section, but additional studies would be useful.

Be-Diffusion Experiments. The next task was to diffuse beryllium into sapphire under controlled conditions to study the effects. Since the inception of this project, we have conducted 17 furnace runs devoted to beryllium-diffusion experiments, using different samples, carriers, and application methods, at tem-

Figure 22. These absorption spectra were taken of a pink sapphire that was Be diffused, both as received and after a portion of the Be-induced coloration was removed by equilibrating the stone at a lower (10^{-2} atm) oxygen partial pressure.

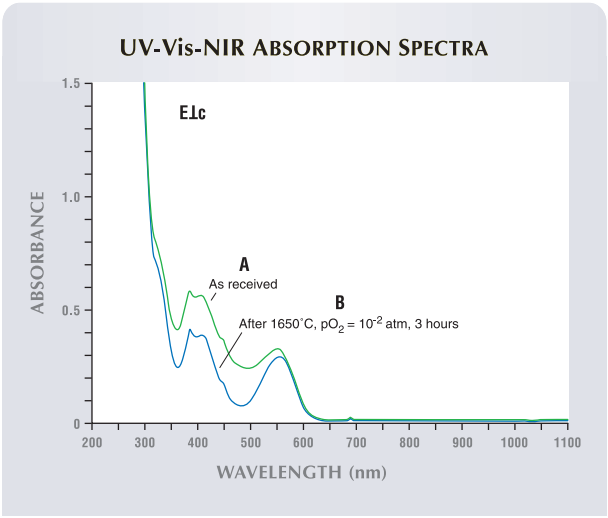

Figure 23. The absorption shown here represents the difference (B–A) of the two spectra shown in figure 22. Because the chromium spectrum is unchanged by re-equilibration of the stone at a lower oxygen partial pressure, this differential spectrum shows the absorption associated with the beryllium-induced coloration.

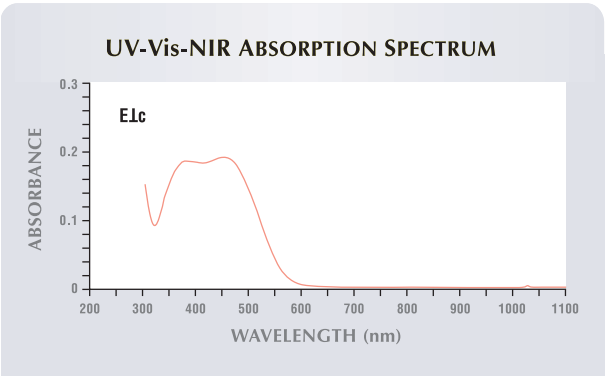

TABLE 6. Selected beryllium-diffused corundum experiments.

Experiment	Samples	No. of pieces	Carrier	Application method	Temp. (°C)	Time (hrs)
1	Madagascar pink	7	Calcium phosphate flux + 4% chrysoberyl	Paint	1800	25
	Sri Lanka near colorless heat-treated geuda	8				
2	Madagascar pink	6	Calcium borate flux + 4% chrysoberyl	Paint	1800	25
	Sri Lanka colorless heat-treated geuda	9				
3	Madagascar pink	8	Sodium phosphate flux + 4% chrysoberyl	Paint	1800	25
	Sri Lanka colorless heat-treated geuda	7				
4	Madagascar pink	6	Na-feldspar flux + 4% chrysoberyl	Paint	1800	25
	Sri Lanka colorless heat-treated geuda	4				
5	Madagascar pink	10	Al_2O_3 + 4% chrysoberyl powder	Embedded in powder	1780	100
	Sri Lanka colorless heat-treated geuda	10				
6	Madagascar pink	3	Al_2O_3 + 0.8% BeO powder	Embedded in powder	1780	33
	King's Plain blue	3				
	Dry Cottonwood Creek	3				
	Subera	3				
	Rock Creek	3				
	Songea ruby	3				
	Songea blue-green	3				
	Sri Lanka colorless heat-treated geuda	3				
	SS8 synthetic sapphire	1				
7	SS1 synthetic sapphire	1	Al_2O_3 + 2% MgO powder	Embedded in powder	1780	100
	Madagascar pink	5				
	Sri Lanka colorless heat-treated geuda	6				
	Rock Creek	5				
8	Madagascar pink	3	Al_2O_3 powder	Embedded in powder	1780	33
	King's Plain blue	3				
	Dry Cottonwood Creek	3				
	Subera	3				
	Rock Creek	3				
	Songea ruby	3				
	Songea blue-green	3				
	Sri Lanka colorless heat-treated geuda	3				
	SS8 synthetic sapphire	1				
9	Songea blues, greens, and ruby	311	Al_2O_3 + 2.65% BeO powder	Paint	1800	33
10	King's Plain	363	Al_2O_3 + 2.65% BeO powder	Paint	1800	33
11	Rock Creek	146	Al_2O_3 + 2.65% BeO	Paint	1800	33
12	Ilakaka, Madagascar	150	Al_2O_3 + 2.65% BeO powder	Paint	1800	33
13	Shandong, China—very dark blue wafer	1	Al_2O_3 + 2.65% BeO powder	Paint	1800	33
14	Synthetic ruby wafer	2	Al_2O_3 + 2.65% BeO powder	Paint	1800	33

peratures from 1780°C to 1800°C and treatment times of 25, 33, and (in two cases where the samples were embedded in powder) 100 hours. In each of the 17 runs, from 1 to 14 separate experiments were conducted for a total of 105 individual experiments. A subset of the 105 experiments is presented in table 6. In addition, another 21 furnace runs, for a total of 53 individual experiments, were conducted

Figure 24. Experiments 1–4 in this study were able to reproduce every color and color layer that we had observed in the Be-diffused samples processed in Thailand. Some of those colors are shown by these corundum samples (0.4–2.1 ct). Photo by Maha Tannous.

to produce differential spectra, and to study oxygen partial pressure dependence of the trapped-hole absorption spectra. As first reported in Emmett and Douthit (2002a), experiments 1 through 4 reproduced the full range of colors and diffusion-layer phenomenology that we had observed in the Thai-processed stones (see, e.g., figure 24). The stones showing color modification exhibited the typical surface-conformal color layer with a thickness of roughly 1.4 mm. A few of the pink Madagascar stones did not change color. As discussed previously, this lack of color modification can be attributed to the chemistry of the specific sapphire, where $[Ti^{4+} + Si^{4+}] > [Mg^{2+} + Be^{2+}]$ or, more completely, [the total of all donors] > $[Mg^{2+} + Be^{2+}]$. With the exception of the silicate (sodium-feldspar) flux, there were few or no discernable differences in the apparent effectiveness of the fluxes. The corundum samples in the silicate flux showed little or no color modification, and thus silicate fluxes were not pursued further.

During this same time period, there was a large amount of disinformation coming from Thailand to the effect that neither beryllium nor chrysoberyl was involved in the new treatment process, and that these dramatic color modifications were the result of naturally occurring impurities. As a direct consequence, a more extensive set of experiments was undertaken to significantly narrow the possibilities (Emmett and Douthit, 2002b).

The next experiment (No. 5) was designed to eliminate any possible effect from the flux itself. To accomplish this, ground natural chrysoberyl was mixed with high-purity reagent-grade Al_2O_3 powder. Another set of stones was packed in this powder mixture in high-purity alumina crucibles and heat-treated. The longer time for this experiment (100 hours vs. 25 hours for experiments 1–4) was chosen to assure that we could diffuse completely through some of the smaller stones. The results of this experiment, in terms of induced coloration, were just like the flux diffusion experiments, with the additional fact that the smaller stones were diffused, and thus colored, completely through. Again, a few of the pink Madagascar sapphires did not show any color alteration.

Natural chrysoberyl is not a high-purity material containing just BeO and Al_2O_3. It can contain significant quantities of iron, chromium, and/or a variety of other elements. Since we had no low-level trace-element analyses on natural chrysoberyl, it was at least conceptually feasible that trace-element impurities in the chrysoberyl could be responsible for the induced coloration in corundum. To address that possibility, high-purity reagent-grade BeO powder was procured, and mixtures were made with the high-purity Al_2O_3 powder and used in experiment 6. A wide variety of representative sapphires were then heated for 33 hours at 1780°C. The results of these experiments were the same as the earlier experiments using chrysoberyl (that is, all the orangy pink, orange, orangy yellow, and yellow colors were produced). Again, some of the pink Madagascar sapphires remained unchanged in color.

We also wished to evaluate the possible role of magnesium. As discussed earlier, if $[Mg^{2+}] > [Ti^{4+} + Si^{4+}]$, the trapped-hole yellow coloration will form when corundum is heat treated in an oxygen atmosphere. It is at least possible that Thai fluxes could contain some Mg compounds, which might diffuse into the corundum causing the yellow trapped-hole coloration. To determine if magnesium diffusion could be a factor in the Thai process, we added 2% MgO into the high-purity Al_2O_3 powder in experiment 7. Even after heating for 100 hours, there was no induced coloration in the stones. This result was consistent with what we would expect, since the diffusion rate of magnesium into sapphire is very low, and an $MgAl_2O_4$ (spinel) layer forms rapidly at the interface between the sapphire and the powder.

As a final check, we conducted a "null" experiment (No. 8). We embedded a group of test sam-

ples from several different localities in high-purity Al_2O_3 powder with no other additives, and replaced the entire inside ceramic surface of the furnace to assure no beryllium contamination from previous experiments. These samples were again heat treated for 33 hours at 1780°C. In this case, there were no substantive color modifications at all.

To determine the diffusion rate of beryllium, we sectioned several of the larger stones from the various experiments described above, so we could measure the thickness of the diffusion layer. From these measurements, the chemical diffusion coefficient was determined to be roughly 10^{-7} cm^2/sec (see Appendix). While this is a rather crude measurement, we note that this diffusion coefficient is about 1/100 that of hydrogen in corundum (El-Aiat and Kröger, 1982), and about 100 times that of titanium (our measurements) in corundum, at the same temperature. Also noted were minor variations in diffusion depth for different stones processed for the same duration at the same temperature. The variation of diffusion rate with impurity concentration is well known for diffusion measurements in solids.

To further understand the role of Be^{2+} in corundum, we diffused Be into colorless, very high-purity synthetic sapphire and high-purity synthetic ruby, with Fe contents on the order of 0.1 ppma or less and titanium contents of only about 2 ppma. Table 5 shows the low concentrations of Fe, Ti, and for the sapphire samples, Cr. These high-purity materials were chosen in an attempt to ensure that existing impurities in these materials could not cause any significant coloration. Beryllium diffusion into these types of materials resulted in concentrations ranging from 13 to 35 ppma. Figure 25 shows samples of both the Czochralski-grown and heat exchanger method (HEM)-grown synthetic sapphire after beryllium diffusion (for information on HEM, see Khattak and Schmid, 1984; Khattak et al., 1986). Both samples exhibit a strong orangy brown diffusion layer. Clearly, 10 to 30 ppma beryllium is a very strong chromophore in both natural and synthetic corundum, and there is no question that beryllium diffused into corundum in an oxygen atmosphere is the single causative agent of these color modifications.

Figure 25. These two high-purity synthetic sapphire samples were Be diffused in the experiments described in the text. The cube was Czochralski grown by Union Carbide Corp., while the cylinder (14 mm in diameter) was grown by Crystal Systems Inc. using the heat exchanger method. The concentration of beryllium in these samples is approximately 14 ppma, which illustrates that beryllium is a very strong colorant in sapphire. Photo by Maha Tannous.

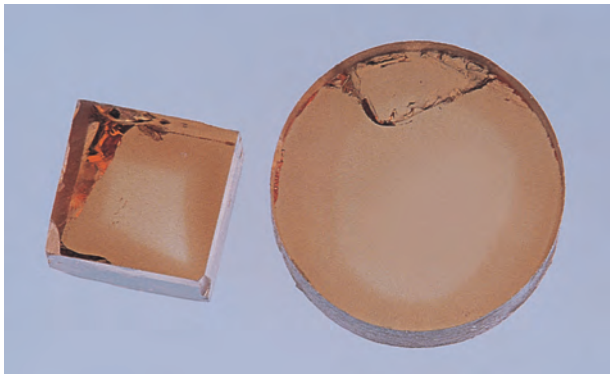

After completing the experiments above, we were curious as to just how universal this Be-induced color modification might be. Using a combination of aluminum oxide and 2.65% BeO powder mixed as a paint, we performed Be-diffusion experiments on a wide variety of natural corundum samples (again, see table 4). All of these experiments were run at 1800°C for 33 hours. The color alteration produced is evident in these before-and-after pictures of mine-run sapphire and ruby from Songea, Tanzania (experiment 9, figure 26); Rock Creek, Montana (experiment 11, figure 27); King's Plain, Australia (experiment 10, figure 28); and Ilakaka, Madagascar (experiment 12, figure 29). Using the same procedure as for experiments 9 through 12, we obtained similar results with sapphire from Dry Cottonwood Creek and Eldorado Bar, Montana; Subera, Australia; Shandong, China; and Umba, Tanzania. While this list is not exhaustive of sapphire deposits by any means, it does imply broad applicability of the Be-diffusion process. Many additional photographs of the colors produced by Be diffusion into corundum are shown in Themelis (2003).

The reason that beryllium diffusion modifies the color of most corundum can be easily understood. Gem corundum usually is not strongly colored, which means that the net concentration of either Fe^{2+}-Ti^{4+} pairs or Mg^{2+}-hole pairs is not large. Consequently, reducing the effective concentration of Fe^{2+}-Ti^{4+} pairs or increasing the effective concentration of Mg^{2+} by diffusing in 10 to 30 ppma beryllium, has a strong impact on color.

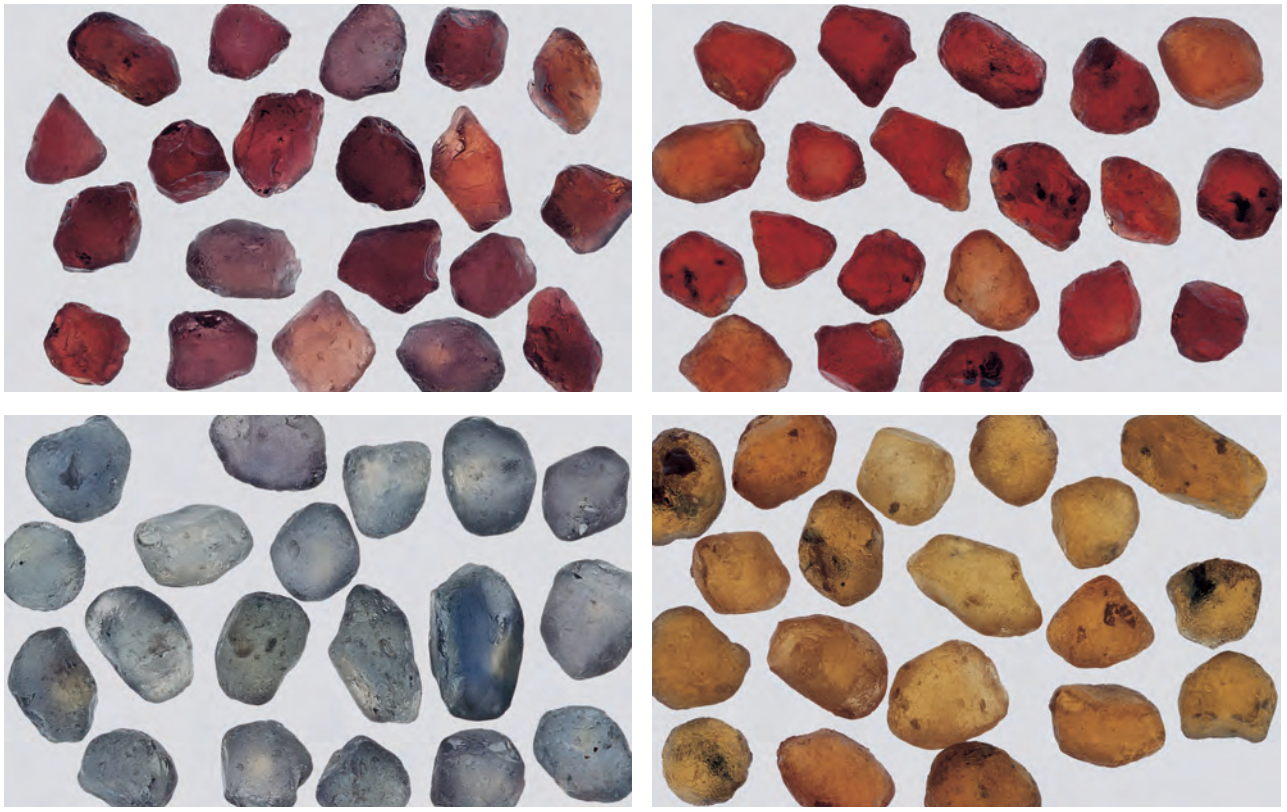

Figure 26. These two groups of different colors of sapphire rough (top, 0.5–1.2 ct; and bottom, 0.8–2.5 ct), from Songea, Tanzania, are shown before (left) and after (right) Be diffusion by the authors. Photos by J. Emmett.

Experiments on Blue Sapphire. From our analysis of the impact of beryllium diffusion on very dark blue sapphires where $[Ti^{4+}] >> [Mg^{2+}]$, we find that beryllium diffusion should produce the condition $[Ti^{4+}] > [Mg^{2+} + Be^{2+}]$, substantially reducing the blue color saturation. To test this point (experiment 13), we cut a very thin (0.9 mm) wafer of extremely dark blue sapphire from a Shandong crystal (figure 30A). Figure 30B shows the same wafer after Be diffusion in an oxygen atmosphere. The lighter blue areas have been rendered either colorless or pale yellow by the mechanisms previously discussed, and the remaining blue areas are much less saturated. After subsequent normal heat treatment in a reducing atmosphere (figure 30C), the yellow areas have been rendered essentially colorless, while the previously colorless or pale blue areas in figure 30B are a more saturated blue.

Figure 27. Rough sapphire from Rock Creek, Montana, also responded well to Be diffusion, as seen in these images before (left) and after (right) Be-diffusion treatment. These samples weigh 0.4–1.4 ct. Photos by J. Emmett.

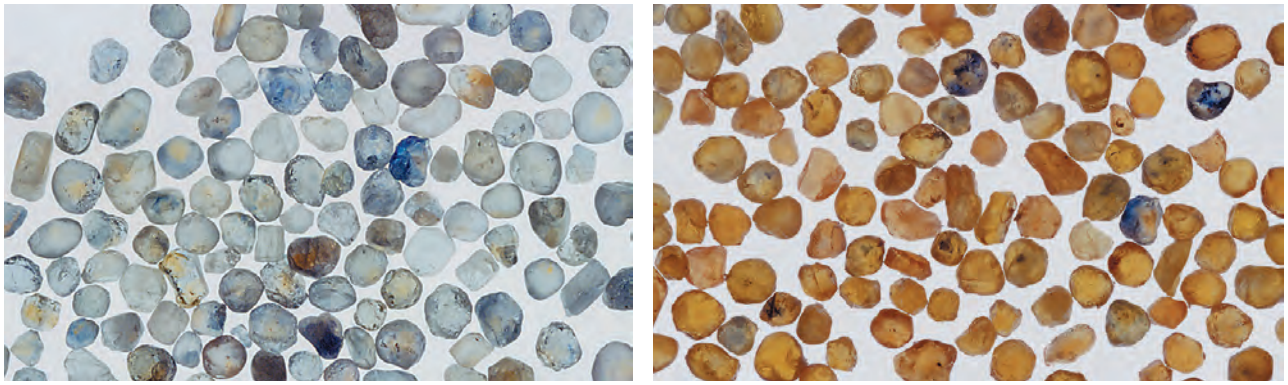

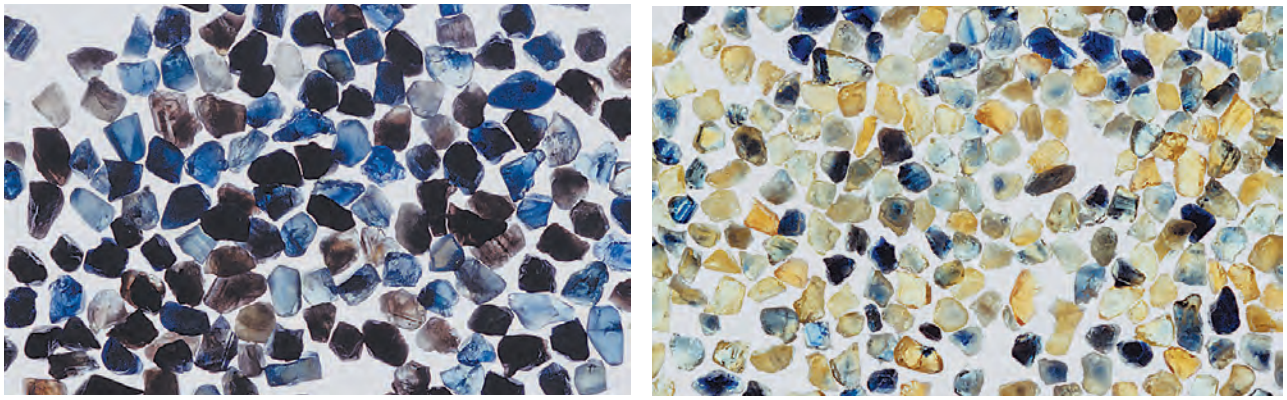

Figure 28. Significant color alteration was also seen in this parcel of rough sapphire from King's Plain, NSW, Australia (average 0.3–0.5 ct), shown here before (left) and after (right) Be-diffusion treatment. Photos by J. Emmett.

Overall the blue areas are now far less saturated than in the wafer before treatment. Thus, a simple process for turning some types of very dark-blue sapphire into a much lighter blue is to diffuse beryllium into the crystal, followed by a standard reduction heat-treatment process. This process can be conducted in 30 to 60 hours on pieces of rough sapphire sufficient to cut 2 ct faceted stones. Given the efficacy of this two-step processing, it is recommended that high-value blue sapphires also be tested for Be-diffusion treatment.

Absorption Spectra. Figure 31 shows the differential absorption spectrum of a Be-diffused high-purity synthetic sapphire (sample SS8 in table 5) and a similar spectrum of an orange Madagascar sapphire that was Be diffused in Thailand from originally pink material (sample TD-1). While these two spectra both show strong absorption in the blue region, there are significant differences. The absorption peak of the SS8 synthetic sapphire is centered at 420 nm, while that of the natural sapphire is at 460 nm. In addition, the SS8 material exhibits a weak broad band centered at about 700 nm. To gain some insight into these differences, we diffused beryllium into two synthetic rubies (SS3 and SS18) that contained different levels of chromium but otherwise were of very high purity. The differential absorption spectra of both were essentially the same (see, e.g., figure 31).

Comparing the Be-diffused SS3 differential spectrum with that of the Be-diffused natural sapphire (TD-1), we note that both show peaks at 380 nm and 460 nm, and neither shows the 700 nm peak. The 460 nm peaks are essentially identical, while the 380 peaks exhibit different amplitudes. It thus appears that the spectral differences between the SS8 synthetic sapphire and the sample TD-1 natural sapphire are associated with the presence of chromium. In high-purity Be-containing synthetic sapphire, the trapped hole is associated with the beryllium ion. However, in sapphire containing chromium in addition to beryllium, the Be-induced trapped hole will preferentially

Figure 29. Rough sapphire from Ilakaka, Madagascar (average 0.4–1.0 ct), also showed dramatic color differences, as evident in this material before (left) and after (right) Be-diffusion treatment. Photos by J. Emmett.

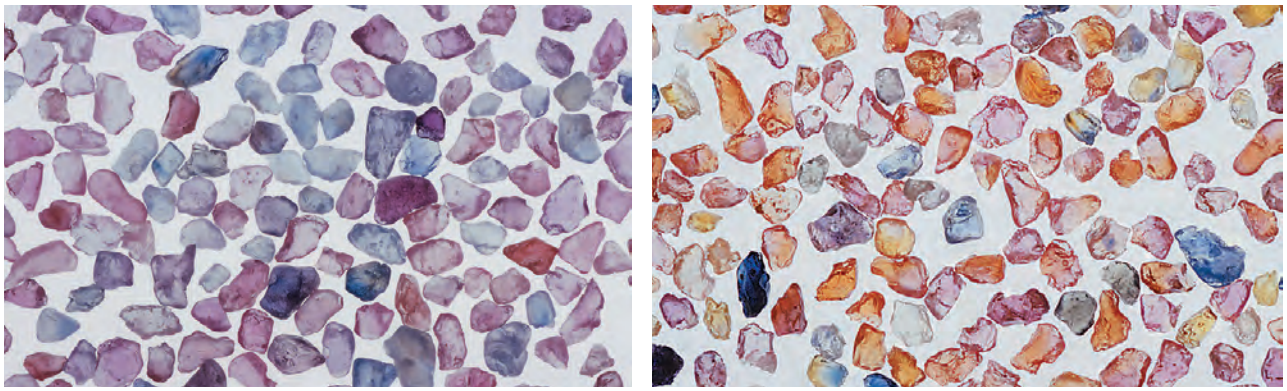

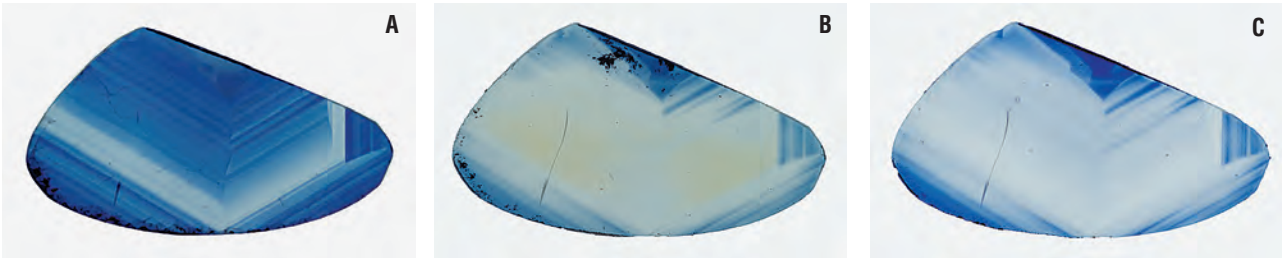

*Figure 30. This thin wafer (0.9 × 16 mm) was cut from an extremely dark blue sapphire crystal from Shandong, China. It is illuminated from below so that the color is apparent. The wafer in its untreated state is on the far left (*A*). After Be diffusion in an oxygen atmosphere (*B*), most of the blue color has been removed or greatly lightened and a small amount of yellow color has appeared. Subsequent standard reduction heat treatment removed the yellow color and slightly increased the saturation of the blue (*C*). The blue color has now effectively been lightened by this process. Photos by J. Emmett.*

associate with the Cr^{3+} ion (again, see Box B). Thus, the differential absorption spectrum in this case is that of a trapped hole near a Cr^{3+} ion, not that of a trapped hole near an Mg^{2+} ion, a result we anticipated in the "Color in Corundum" section. There are two possibilities for the origin of this spectrum. First, we could be observing the spectrum of a Cr^{3+}-trapped hole pair. Second, we could be observing the spectrum of Cr^{4+} resulting from combining the hole and the Cr^{3+} ion. Determining which of these possibilities is correct will require significant additional research.

In sapphire that does not contain chromium, but does contain Fe^{3+}, beryllium-induced trapped holes will preferentially associate with Fe^{3+} rather than Be^{2+}. The resulting absorption spectrum again can be a Fe^{3+}-trapped hole pair, or the spectrum of Fe^{4+}. We would expect the absorption spectrum from the hole association with Cr^{3+} to differ somewhat from the spectrum of the association with Fe^{3+}. However, all the natural sapphires for which we have both SIMS data and careful differential spectroscopy contain chromium at ≥ 10 ppma. Thus it is understandable why all exhibit the 460 nm absorption if it is indeed associated with a Cr^{3+}-hole pair. To test this hypothesis, we need to diffuse Be into sapphire containing iron, but not containing chromium at more than a few ppma. There are two possibilities for obtaining such material. First, it may be possible to find such stones among the "colorless" heat-treated Sri Lanka geuda. Second, a high-purity iron-doped synthetic sapphire could be grown. We are working with a number of colleagues to pursue both approaches. Be diffusing such material should allow us to unambiguously observe the Fe^{3+}-hole pair spectrum, and thus resolve remaining color issues.

Figure 31. This figure shows the beryllium-induced absorption from sample TD-1 (a Thai Be-diffused pink Madagascar sapphire), sample SS3 (a Be-diffused synthetic ruby), and sample SS8 (a high-purity synthetic sapphire grown by the heat-exchanger method). The absorption spectrum of the Cr-containing samples differs significantly from that of SS8, because the beryllium-induced trapped hole interacts with the chromium.

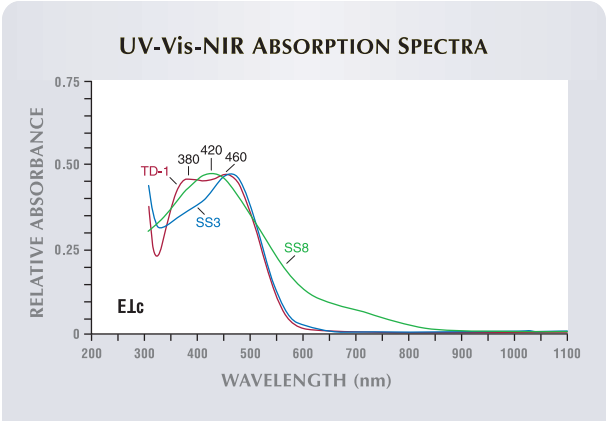

GEMOLOGICAL TESTING AND IDENTIFICATION

It is essential that the role of the diffused Be in corundum be understood before any identification techniques, whether simple or complex, are proposed. The foregoing provides that foundation. The experiments described below were conducted to characterize Be diffusion–treated ruby and sapphire, and to provide possible identification criteria.

Materials and Methods

Samples. The number of samples (898) examined for the gemological identification portion of this study is necessarily quite large, to examine as many of the effects of the Be-diffusion process as

possible, and yet there are stones from some geographic areas, and in some color combinations, that remain to be studied.

From the 898 samples, 285 were known to be beryllium diffused, 178 were used for before-and-after experiments, and 435 were not diffused. Approximately half were faceted. The known-diffused samples were either acquired as such directly from treaters or dealers in Thailand, were proved to be Be diffused through chemical analysis or characteristic color zoning, or were treated by us. These samples were yellow, pink to orange to red, blue, purple, green, and colorless; they came from Madagascar (Ilakaka and unspecified deposits), Montana, Tanzania (Songea and Umba), and unknown localities.

The samples that were obtained for the before-and-after experiments were either colorless or showed the following colors before treatment: light yellow, yellowish orange, pink, brownish red, blue, purple, green, brown, and gray, with some multicolored. These samples were sourced from Australia (Lava Plains), Laos, Montana, Madagascar (Ilakaka, northern, and unspecified deposits), Sri Lanka, Tanzania (Songea and Umba), Thailand (Kanchanaburi and unspecified deposits), Vietnam (Lam Dong, Quy Chau, and unspecified deposits), and unknown localities.

The samples that were not Be diffused were colorless to yellow to orange, pink to purple to red, blue to green, brown, gray, and mixed pale colors; both natural-color and standard heat-treated stones were represented. Specific information on the sample population and the tests to which they were subjected can be found in the Be-diffusion samples table in the *G&G* Data Depository (http://www.gia.edu/gemsandgemology, click on "*G&G* Data Depository").

Standard Gemological Testing. Routine gem testing was performed on a portion of the samples examined for this study, although not all samples were studied by all methods (again, see the Be-diffusion samples table in the *G&G* Data Depository). The tests included determination of refractive index, specific gravity by the hydrostatic method, and pleochroism, as well as observing absorption spectra from desk-model spectroscopes and the reaction to ultraviolet radiation.

Since color distribution was anticipated to be the most important identification criterion, we examined virtually all samples with a gemological microscope, using various types of lighting and immersion techniques.

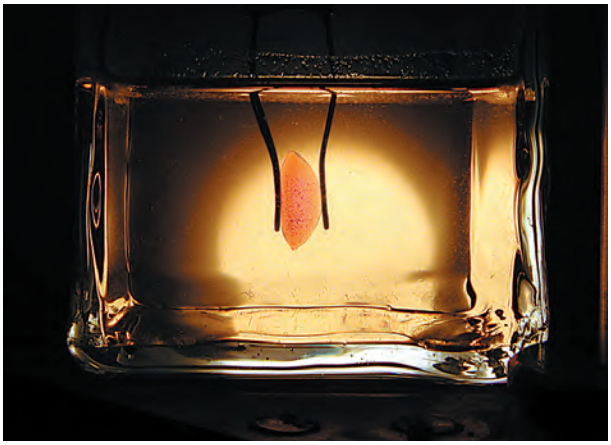

Figure 32. This Be-diffused sapphire is shown in an immersion cell filled with methylene iodide; a diffuser plate was placed between the light source and the cell. In conjunction with a horizontal microscope, this was one of the methods used to examine the stones in this study. Photo by Ken Scarratt.

Our equipment included a horizontal binocular microscope configured with an immersion cell (figure 32), and upright microscopes with both a standard immersion cell and specially prepared, grooved, translucent white plastic trays. In all cases, the samples were immersed in methylene iodide (di-iodomethane, R.I.=1.74). (Other immersion fluids, such as water or baby oil, may be used, but their lower refractive indices render them less effective.) Illumination of the sample with diffused white light greatly facilitated the observation of color gradients. Low magnification (10×) was used to search for surface-conformal color zoning, whereas higher magnification (up to 63×) was used to examine internal and surface features.

UV-Vis-NIR Spectroscopy. The UV-Vis-NIR spectra at room and liquid-nitrogen temperatures were recorded for the range 190–900 nm using Unicam UV500 and Hitachi U-2000 instruments. Spectra for natural, heated, and Be diffusion–treated stones—both faceted and in the form of polished wafers—were recorded in the direction of the o-ray (E⊥c).

Infrared Spectroscopy. The infrared spectra of selected samples (including natural, heated, and Be-diffusion treated of various colors) were recorded in the range of 6000–400 cm^{-1} using Fourier-transform infrared (FTIR) spectrometers (Nicolet 560 and 760, Nexus 670, and Avitar) and various accessories (beam condenser, diffuse reflectance

Figure 33. Not all sapphires treated with beryllium have an intense color, as this 14.38 ct Be-diffused sapphire illustrates. It has a medium tone very similar to that of some natural-color sapphires. It is interesting to note that the thin orange layer present in this stone is visible even without immersion, which is not usually the case. Photo by Maha Tannous.

[DRIFTS], and attenuated total reflectance [ATR]). We employed an MCT-B detector and a KBr beam splitter, using various resolutions (from 0.5 to 4.0 cm^{-1}), to observe the O-H region and other spectral areas of interest.

Raman Spectroscopy. Raman spectra were gathered using a laser Raman microspectrometer (Renishaw 1000 system) at both room and liquid nitrogen temperatures, with an argon-ion laser providing excitation at 514.5 nm. We used this technique to determine whether any Raman peaks were induced or changed as a result of Be diffusion, as well as to identify surface-reaching fluxes, synthetic overgrowths, and crystal inclusions.

Chemistry. Chemical analysis by energy-dispersive X-ray fluorescence (EDXRF) was performed on an EDAX DX 95 and a Spectrace QuanX. The full range of elements within the detection limits of these instruments was surveyed (from sodium through the heavier elements). This technique was primarily used early in the study of these new diffused materials to see if there were any elements peculiar to this treatment that were detectable by these instruments (see, e.g., McClure et al., 2002). This did not prove to be the case, showing that this testing technique is not useful for this purpose.

To search for light elements in the diffused layer, we also used SIMS analysis at Evans East (again, see Box A). Since February 2002, we have submitted 62 rubies and sapphires to SIMS analysis with 153 separate analyses. Samples were selected from stones known to have been treated in Thailand by beryllium diffusion; stones treated to specific parameters by two of the authors; stones that were known to be untreated; and stones that were submitted by clients for examination and laboratory reports.

Results and Discussion

Visual Appearance. We observed that many of the colors produced by Be-diffusion treatment are very saturated, particularly those in the pink-orange, yellow, and orange ranges (again, see figure 1). These colors have never been common in natural corundum, even among typical heat-treated sapphires. The availability of large quantities of such colors in one place, as several of the authors have seen in Thailand, would immediately suggest that they have been treated by this new technique. When a single stone is examined, however, color alone is not diagnostic, as natural and heat-treated sapphires and rubies exist in all the colors seen in Be-diffused corundum (see Box C and chart figure C-31). Note, too, that not all sapphires treated with Be diffusion produce such

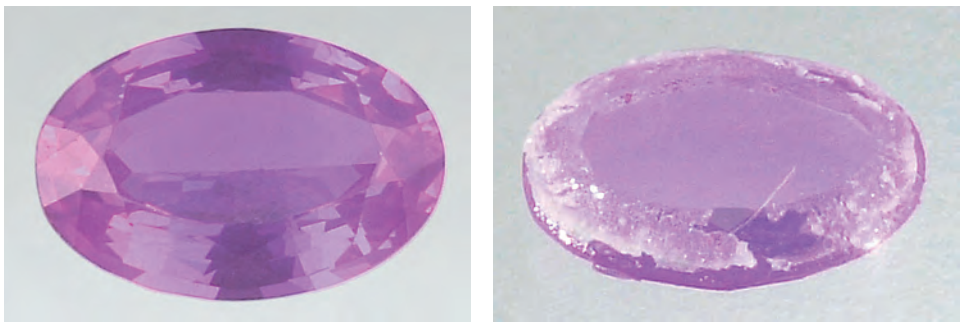

Figure 34. A wafer cut from this 0.83 ct Vietnamese pink sapphire (before treatment, left) was Be diffused for this study (right). There was no observable change in color (the white material is residual flux). Photos by Elizabeth Schrader.

vibrant, saturated colors (figure 33). In fact, as discussed in the "Color in Corundum" section, some stones do not change color at all, even though SIMS analysis shows that beryllium has penetrated them (figure 34). In addition, as described earlier, this new treatment can lessen the intensity of color in some dark blue sapphires.

Optical and Physical Properties. The refractive index, birefringence, pleochroism, and specific gravity of our samples did not vary significantly from those properties recorded for other types of natural or treated corundum. This is consistent with the very low concentration of beryllium that has been detected in the diffused stones (see table 7). The Be diffusion–treated stones had a broad range of reactions to UV radiation, from inert to strong, and the fluorescence colors varied from orange to reddish orange. This probably is due to the wide variety of corundum being subjected to this treatment. However, we did notice a somewhat higher-than-expected occurrence of moderate-to-strong orange fluorescence to long-wave UV in the pink-orange stones. This reaction was by no means consistent, and in our experience it is not uncommon in non-diffused stones of the same color. Consequently, it cannot be considered a useful identification clue.

Most of the diffused stones we tested, particularly those in the yellow-to-orange range, showed weak-to-strong 450 nm iron-related absorption in the desk-model spectroscope. All the samples with a pink or red component, as well as some orange stones, also showed Cr absorption in the red region of the spectrum (692 and 694 nm). The Fe-related absorption was stronger than expected for some of

TABLE 7. Representative trace-element compositions of corundum by SIMS (ppma).[a]

Sample no.	Color	Notes	Be	Na[b]	Mg	Si	K[b]	Ti	Cr	Fe	Ga	Geographic source
Untreated												
48718	Red		1.15	2.04	45.2	38.4	0.63	334	4300	6.55	62.9	Mong Hsu, Myanmar
49081	Green		1.46	0.12	80.3	17.8	0.03	63.2	90.1	1461	16.1	Montana, U.S.
49081	Orange		1.46	0.20	76.1	16.1	0.04	63.0	80.7	1358	13.0	Montana, U.S.
49089	Yellow		1.48	3.96	35.8	17.7	0.17	29.1	4.61	2646	39.7	Unknown
49089	Blue		1.52	0.16	9.20	18.2	0.03	120	2.57	1998	29.6	Unknown
49102	Pink		1.42	0.10	28.5	40.3	0.07	742	1061	8.91	18.4	Vietnam
Before / after Be-diffusion treatment												
49106	Yellowish brown	Before	1.24	0.07	56.8	22.1	0.04	40.1	237	2496	20.7	Songea, Tanzania
49106T	Orange	After	17.4	0.54	43.9	15.4	0.41	28.6	222	1610	28.8	Songea, Tanzania
45031	Pink	Before	1.20	0.04	105	na	0.02	na	292	153	22.7	Unknown
45002	Pinkish orange	After	13.2	0.13	109	na	0.09	na	322	145	25.4	Unknown
45494	Pink	Before	1.44	0.62	167	na	0.12	121	928	158	51.1	Unknown
45493	Pinkish orange	After	18.0	2.20	134	na	0.67	89.9	781	115	33.6	Unknown
Be diffusion–treated samples												
45033	Orangy red	Center	16.4	0.28	76.5	na	0.18	na	712	1056	19.0	Unknown
45033	Orangy red	Edge	19.2	0.21	78.5	na	0.14	na	707	1083	19.5	Unknown
45490	Yellow	Center	3.14	0.03	11.8	na	0.01	15.8	3.93	1509	46.9	Unknown
45490	Yellow	Edge	24.5	0.04	5.20	na	0.01	20.0	3.91	1490	33.8	Unknown
48415	Red		25.1	0.43	64.0	na	0.24	47.4	4118	2441	53.8	Unknown

[a] *na = not analyzed. Accuracy of Be and Fe is ±10–20%; Ga, Mg, Si, Ti, Cr, Na, and K is about ±30%. A complete listing of the analyses performed for this study can be found in the G&G Data Depository (www.gia.edu/GemsandGemology, click on "G&G Data Depository").*

[b] *High concentrations of Na and K in some analyses could be due to surface contamination.*

Figure 35. A wide variation in the penetration depths of surface-conformal color layers can be seen in this group of faceted Be-diffused sapphires (0.51–1.92 ct), immersed in methylene iodide. Photo by Maha Tannous.

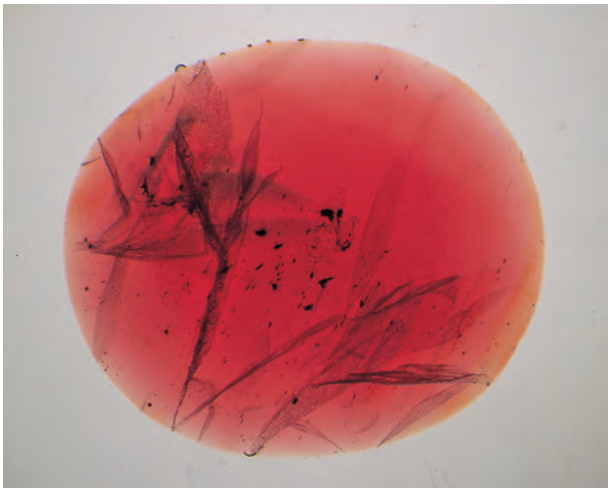

Figure 36. The vast majority of predominantly red Be-diffused samples we examined showed a relatively thin, surface-conformal layer of orange color. The layer in this 5.05 ct stone is somewhat uneven, which suggests that it was recut after treatment. Photomicrograph by Shane F. McClure; immersion, magnified 10×.

the colors tested. We believe this absorption is related to the starting material used for Be diffusion, rather than to the treatment itself. It must be emphasized, however, that this observation is in no way diagnostic of Be diffusion, as many natural yellow or orange sapphires show similar absorption.

Color Distribution. Beryllium diffusion came to the attention of gemologists and the trade after yellow-to-orange three-dimensional surface-conformal layers were seen on faceted orangy pink padparadscha-like sapphires (McClure et al., 2002; Scarratt 2002a,b). We have never observed—either in the course of this study or in our many years of experience—such a three-dimensional layer of color paralleling the surface of a natural-color polished gemstone. To the best of our knowledge, it can only be caused by a diffusion treatment.

Therefore, careful observation of color distribution became critical to this investigation. Exami-

Figure 37. Many different combinations of Be-diffused colors are possible. Some, as in this 1.51 ct purple and orange briolette with an orange surface-conformal layer, are very unusual. Photomicrograph by Shane F. McClure; immersion, magnified 10×.

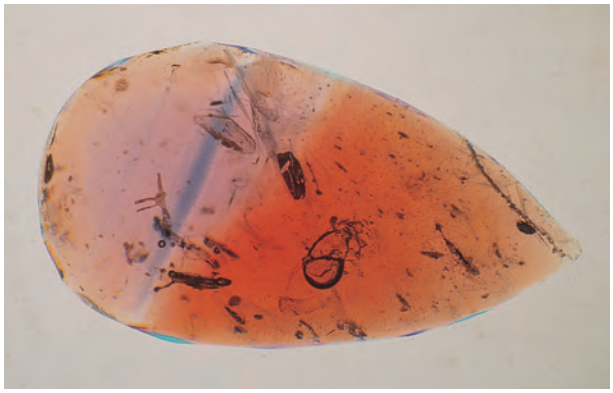

Figure 38. Natural color zoning in corundum does not conform to the faceted shape of the stone. Instead, it follows the structure of the corundum crystal, creating angular zones and parallel bands, as can be seen in this group of non-diffused rubies and sapphires (0.14–1.29 ct). Photo by Maha Tannous; in immersion.

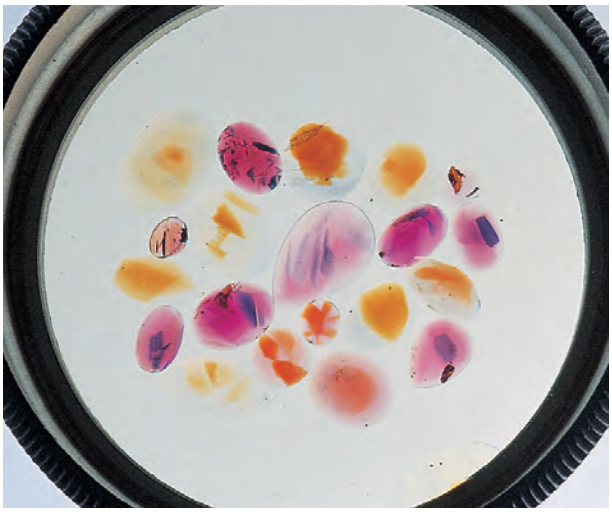

Figure 39. A Be-diffused stone will not always have a complete surface-conformal layer of color, which could cause confusion with natural color zoning. We had the diffused piece of rough on the left cut into the 1.74 ct stone in the center. As can be seen with immersion on the right, the orange diffusion layer was evident only as concentrations just under the surface along the edges of the table and one side of the pavilion, and not all the way around the stone. Left and center photos by Maha Tannous; photomicrograph on the right by Shane F. McClure, magnified 10×.

nation of the Be-diffused samples in our study with magnification and immersion revealed that *all* of the fashioned orangy pink and pinkish orange samples showed color zones that related directly to the faceted shape of the stone (see, e.g., figure 35). In some, this zone penetrated as much as 80% of the stone (again, see figure 17 right and chart figure C-1); those stones with the deepest penetration appeared most orange. The vast majority of the predominantly red faceted samples also showed orange surface-conformal color zones (figure 36). The few blue Be-diffused sapphires we have examined all showed a thin, colorless surface-conformal layer overlaying typical blue hexagonal zoning.

However, most of the Be-diffused yellow and orange samples were colored throughout, with less than 10% showing a layer of surface-conformal color. Sapphires of other colors, such as green and purple, typically revealed orange or yellow surface-conformal layers overlying purple, green, or blue central colors (figure 37).

Figure 40. Occasionally Be-diffused corundum shows both surface-conformal color layers and natural color zones that correspond to the crystal structure, as seen in this 1.29 ct briolette. Photomicrograph by Shane F. McClure; immersion, magnified 10×.

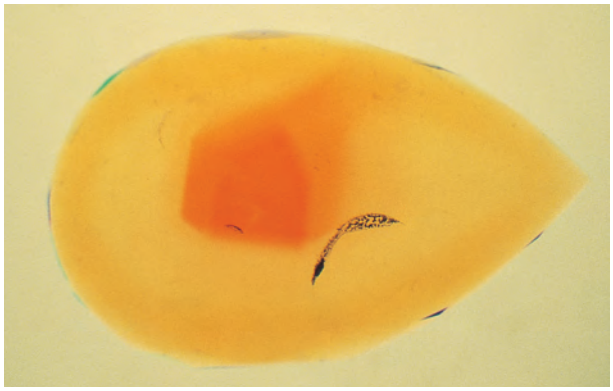

The color distribution in an untreated sapphire, or even in a sapphire that has been heated by standard methods, generally will follow the trigonal crystal structure of corundum. Stones cut from such crystals may show angular or straight color banding that conforms to the corundum's crystal morphology and related trace-element distribution, rather than to the shape of the faceted stone (figure 38). In addition, some natural-color stones are faceted to use isolated zones of color in a way that results in an unusual color distribution (e.g., a dark blue zone located in the culet of an otherwise colorless stone or, in the case of a padparadscha sapphire, an orange zone retained along one edge to produce the optimum color). Although we have never observed a natural color zone that conformed to the faceted surface of the polished stone, a Be-diffused piece of pink or red rough also might be cut in such a way that the orange color component does not conform to the facets of the finished stone, but rather merely forms a concentration of orange, for example, along one or several edges (figure 39). The gemologist must develop a keen sense for color distributions that are not completely surface conformal, which will indicate that further testing (such as SIMS) is needed. Therefore, *any* near-surface concentration of yellow or orange color should be viewed with suspicion.

In several of our samples, the surface-conformal color layer was present in conjunction with natural angular or banded color zones; these even overlapped one another in some cases. In such instances, the two types of zoning were easily distinguished and the relationship of color to faceted

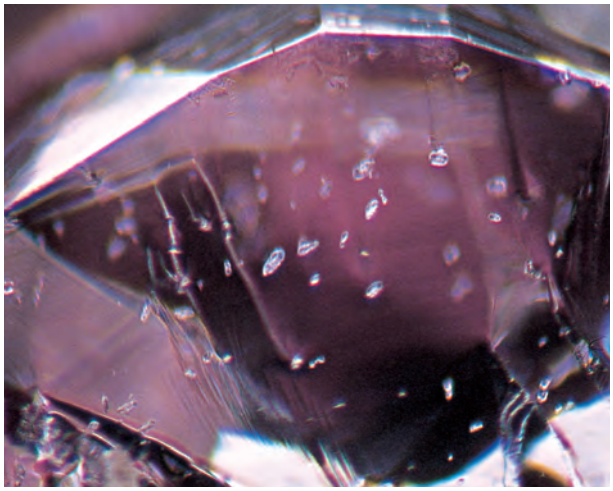

Figure 41. Undamaged zircon inclusions in Madagascar sapphires typically appear as small transparent subhedral (rounded) crystal grains. Photomicrograph by Shane F. McClure; magnified 40×.

shape proved that a color-causing element had been diffused into the stone from an external source (figure 40 and chart figure C-4).

Magnification. Inasmuch as standard gemological tests, other than the observation of a surface-conformal color layer, have not provided proof of Be diffusion, we believed that other evidence obtained from microscopic examination could be critical to identification. We cannot stress strongly enough that the findings represented here indicate changes in inclusions that have occurred due to exposure to extreme heat—heat higher than is typical for what we refer to as standard heat treatment (i.e., above 1780°C). While actual temperature data from Thai treaters is unavailable, we have observed alterations in inclusions that we rarely see with standard heat treatment. Such evidence cannot unequivocally prove beryllium diffusion. However, these types of features, considered together with the other evidence outlined in this article, can provide a strong indication that a stone has been Be-diffusion treated.

Included Crystals. Almost all of the Madagascar samples contained small crystals of zircon, which is very common in corundum from that locality (see, e.g., Schmetzer, 1999). In all the Be-diffused samples that contained zircon inclusions, we found that those inclusions were always significantly altered. What were once transparent subhedral crystals (rounded grains, as shown in figure 41) were transformed into opaque white irregularly shaped masses, often with a crackled appearance and a gas bubble in the center (figure 42 and chart figure C-7). We have seldom seen the destruction of zircon inclusions in sapphires that have been subjected to typical heat treatments, regardless of their locality of origin. The fact that *all* such inclusions in Be-diffused stones are significantly altered is important. It means that the temperatures being used for Be diffusion are significantly higher than those used for standard heat treatment. Therefore, if zircon crystals appear to be unaltered, it is unlikely that the sapphire host has been subjected to the high temperatures typically used for Be diffusion (Butterman and Foster, 1967).

Figure 43 shows the Raman spectra of (A) a zircon inclusion inside a natural pink sapphire and (B) a zircon in the same sapphire after Be-diffusion treatment. Spectrum A has strong Raman scattering at 1018, 983, 441, 364, 224, and 200 cm^{-1}. In spectrum B, all these peaks are gone, which indicates that a phase transformation has occurred. It is very likely that the peaks at 192 and 181 cm^{-1} are from ZrO_2 (baddeleyite). None of the other peaks matched any minerals in our database that could

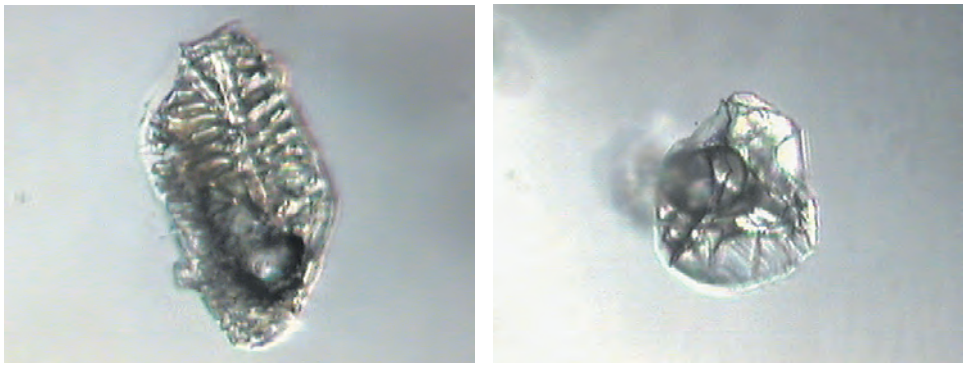

Figure 42. At high temperatures, zircon inclusions become significantly altered. Typically, they are transformed into opaque irregular masses, often with a crackled appearance and a gas bubble in the middle. Photomicrographs by Ken Scarratt; magnified 40×.

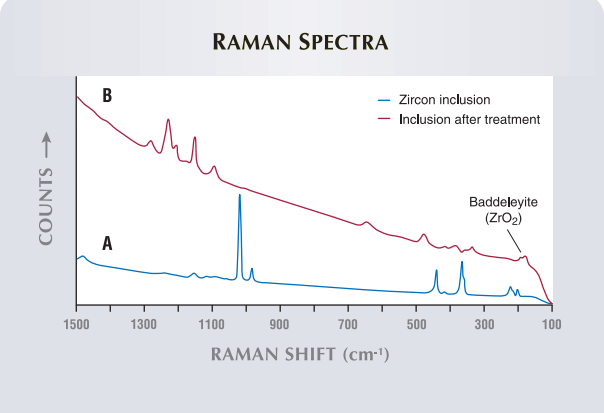

Figure 43. Shown here are the Raman spectra of (A) a zircon inclusion inside a natural pink sapphire, and (B) a similar inclusion in the same sapphire after Be-diffusion treatment. Due to partial melting and reaction with the surrounding corundum, the zircon in the Be-diffused sample was transformed to ZrO_2 (baddeleyite) and an Al_2O_3-SiO_2-rich glass.

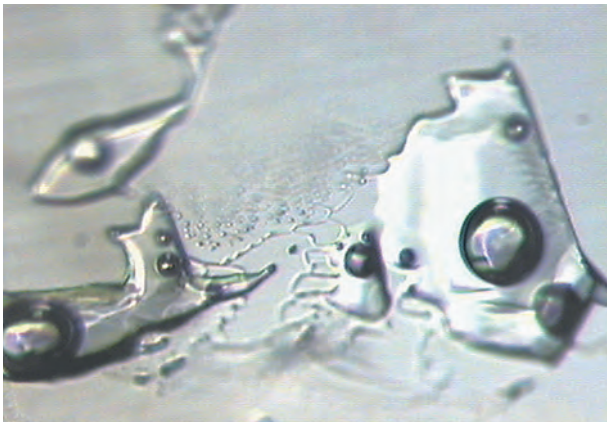

Figure 44. These former mineral inclusions were reduced to a glass-like melt containing gas bubbles after the host sapphire was Be-diffusion treated. Photomicrograph by Ken Scarratt; magnified 40×.

crystallize from the partial melt (such as quartz, tridymite, cristobalite, or mullite). These results indicate that the partial melt was cooled rapidly, and the zircon inclusion eventually transformed into ZrO_2 and an Al_2O_3-SiO_2-rich glass, following the Be-diffusion treatment. These findings are in agreement with those recently published by Rankin and Edwards (2003), who provide an in-depth discussion of what happens to zircon crystals at such high temperatures (see also Butterman and Foster, 1967).

Note that the melt created by these highly altered inclusions often flows into the surrounding strain haloes. As it cools within the halo, it forms the phases mentioned above and creates crossing fern-like structures that are reminiscent of the structure of devitrified glass (see chart figure C-10). These recrystallized haloes were seen in many of the Be-diffused stones, but they were particularly common in the orange, yellow, and pink-orange samples. A Raman spectrum of the substance within the halo exactly matched spectrum B in figure 43, indicating that it, too, was caused by the destruction of zircon.

Other types of crystals were seen in many of the samples tested, but in all cases they were damaged or significantly altered by the treatment, and in most cases they were visually unidentifiable, shapeless white masses (see chart figure C-28). We also saw numerous instances of large gas bubbles that were trapped in internal cavities filled with what appeared to be a transparent glass (figure 44).

Internal Diffusion. We saw evidence of internal lattice diffusion (i.e., the diffusion of a color-causing agent from an inclusion into the surrounding stone; Koivula, 1987) in many of our study samples, particularly in the orange, yellow, and red colors. This phenomenon generally occurs in association with rutile (TiO_2), and is extremely common in blue sapphires that have undergone standard heat treatment. At high temperature, rutile inclusions break down and release Ti, which diffuses into the structure of the corundum, reacts with existing Fe, and produces a localized blue coloration (see chart figures C-17 and C-18).

In many of the untreated Songea rubies and sapphires we examined, the rutile inclusions were in the form of euhedral crystals. In untreated stones from Madagascar, they appeared mostly as needles or clouds of fine, dust-like particles, as are commonly seen in corundum samples from many other localities. However, all of the Be-diffused stones from Songea in this study that contained rutile crystals showed a typical internal diffusion pattern consisting of a hexagonal or irregularly shaped crystal surrounded by a spherical blue halo (figure 45). The blue color contrasted sharply with the yellow, orange, or orangy red bodycolor of the stones. Some of the areas of spotty blue coloration created by rutile silk in Be-diffused stones from Madagascar still contained a visible pinpoint inclusion (chart figure C-19).

The important observation is that although internal diffusion is quite common in heat-treated blue sapphire, it is not at all common in yellow, orange, and red corundum. While it is true that yellow

BOX C: A PRACTICAL GUIDE TO RECOGNIZING BERYLLIUM-DIFFUSED RUBIES AND SAPPHIRES

The most critical issue for gemologists and the gem trade is how to separate these treated stones from natural-color corundum and corundum that has been heated by "standard" methods, without the addition of external elements. Although our research has shown that all the Be-diffused stones can be identified by mass spectroscopy, especially SIMS analysis, this technique is expensive and time consuming. However, we have found many other, more readily obtainable clues that provide either proof or strong indication of Be-diffusion treatment.

This box and the accompanying chart summarize the clues a gemologist can use to help determine if a sapphire or ruby has—or has not—been subjected to Be diffusion. While we believe these indicators to be common to all colors of Be-diffused corundum, to date we have not examined a sufficient number of Be-diffused blue sapphires to draw general conclusions about them. Observations requiring magnification are best seen with a gemological microscope. All numbers in parentheses refer to images on the chart.

DIAGNOSTIC EVIDENCE

Color Zoning – The only diagnostic evidence of Be-diffusion treatment immediately available to the gemologist is the presence of a color zone that conforms to the external faceted shape of the stone. This color zone may be seen in all types of Be diffusion–treated corundum and can penetrate to any depth, including throughout the gem (figure C-1). The Be-diffused conformal zone is yellow, orange, or occasionally colorless (C-2). It surrounds central cores that are either colorless or some other color, most often pink or red (C-3). It also may be seen to overlay natural zoning (C-4). Observation of this feature requires the use of immersion, with methylene iodide (what gemologists call 3.32 liquid) the best medium.

HIGHLY INDICATIVE EVIDENCE

The features in this section do not *prove* that a stone has been Be-diffusion treated. However, they do prove that it was subjected to very high temperatures (i.e., higher than those typically used for the standard heat treatment of corundum) and are a strong indication that Be-diffusion treatment may have occurred. Therefore, observation of one or more of the following features in a ruby or sapphire means that the color origin is highly suspect.

Highly Altered Zircon Inclusions – Zircon crystals in corundum usually survive standard heat treatment, retaining their initial appearance as small transparent angular or rounded grains (C-5). The extreme alteration of such crystals to white, formless masses (C-6)—often containing a gas bubble (C-7)—is an excellent indicator that the stone has been exposed to very high temperatures.

Internal Recrystallization – Several forms of internal recrystallization occur as a result of the extreme temperatures used in Be-diffusion treatment. One of these relates to the zircon inclusions mentioned above. Discoid fractures around zircon crystals are commonly created during normal heat treatment as the crystal expands, even when the inclusion itself is not damaged (C-8); the circular fractures around zircons and other crystals are often glassy and reflective (C-9). Such fractures also often occur around zircon crystals during Be-diffusion treatment. However, as the zircon is destroyed, the resulting fluid melts and flows into the planar fractures of the discoid. Then, as the stone cools, the melt partially recrystallizes, leaving a characteristic appearance that we had not seen in sapphires prior to this new treatment: a plane of transparent material interwoven with fern-like patterns reminiscent of the structure seen in devitrified glass (C-10), occasionally displaying iridescent colors (C-11). The discoids also may contain areas healed by the regrowth of corundum (C-12), and near their center is always a white mass (usually with a gas bubble) that used to be a zircon crystal (C-13).

The second type of recrystallization involves the mineral boehmite. Recrystallized corundum in the channels left behind by destroyed boehmite inclusions often has a characteristic "roiled" appearance (C-14), particularly in transmitted light. These now-filled channels often contain voids that may be spherical (C-15) or have a bone-like shape (C-16).

Internal Diffusion – Internal lattice diffusion around rutile crystals and "silk" is very common in heat-treated blue sapphires. This typically manifests itself as roughly spherical blue haloes around the crystals (C-17) and spotty blue coloration where the rutile "silk" used to be (C-18). In our experience, however, this phenomenon is extremely rare in rubies and yellow-to-orange sapphires (C-19) since these stones are heated in an oxidizing atmosphere that usually removes blue color. Its presence in these colors can be considered a direct result of exposure to high temperatures. However, since yellow sapphires from some localities (such as Montana) are routinely heated—but not diffused—at temperatures high enough to cause some spotty blue coloration, these characteristics indicate the possibility—but not proof—of Be diffusion.

Synthetic Overgrowth – Synthetic corundum can grow in any high-temperature treatment environment. However, the appearance of synthetic overgrowth on faceted Be-diffused rubies and sapphires is different from any we have seen before. Specifically, remnants of synthetic overgrowth occasionally have been seen in surface-reaching cavities as tiny platelets, but not covering entire facets. Although this synthetic material is often removed during finishing, portions remain on the surfaces of some stones, particularly those that are yellow to orangy red, providing an important clue to the use of high heat.

The synthetic crystals that grow during Be-diffusion treatment are often randomly oriented, tend to be platy

and hexagonal in shape (C-20), and are much larger and far more numerous than any typically found on stones heat treated by standard methods. When they grow together, they form a solid layer that often looks like an aggregation of irregular blocks (C-21), sometimes with tiny voids between them and cloud-like inclusions along the crystal interfaces (C-22). This tends to create a roiled appearance in the surface layer (C-23). While this usually can be seen with darkfield illumination, it is even more readily visible with transmitted light (C-24). Cross-polarized light also helps reveal such features, due to the randomness of the crystal growth. Since the orientation of many of the synthetic crystals is different from that of the natural host, in crossed polarizers they may appear light while the host material is dark (C-25).

We have recently noted increased synthetic growth on the surfaces of a number of Mong Hsu rubies, sometimes lining cavities and sometimes having the same appearance as that found on Be-diffused stones (C-26). The cavities exhibited linings of tiny hexagonal platelets and were often filled with glass residues. This indicates that some of these stones are now being treated at higher temperatures than were typically used before. However, we have not seen this type of growth in yellow and orange heat-treated sapphire that has not been subjected to Be-diffusion treatment.

Other Inclusions – Other unidentifiable severely damaged crystals that do not appear to have been zircons have been noted in some Be-diffused corundum (C-27). Although the original form of these white, shapeless masses is unrecognizable, the sheer amount of damage (C-28) is clear evidence of exposure to extreme temperatures. This is also true of internal cavities that are now filled with a transparent glass-like material containing spherical gas bubbles (C-29).

EVIDENCE THAT IS NOT INDICATIVE

Some features of Be-diffused corundum overlap too much with corundum that has not been treated by this process to help in identification, although they may suggest that a stone is suspect.

Color – The colors produced by Be diffusion are often very saturated and "unnatural" (C-30). Yet all of the colors produced by Be diffusion can occur naturally or as a result of standard heat treatment (C-31). Thus, for any individual stone, color by itself does not indicate Be diffusion, but it can be a reason for further testing.

Be diffusion produces colors in rubies that are often a slightly orangy red, or occasionally even pure red (figure C-32). These colors mimic many iron-rich rubies that are found in Africa and elsewhere.

Healed Fractures – Artificial healing of fractures clearly occurs during the Be-diffusion process (C-33). However, it also commonly occurs during the heating of rubies, particularly from Mong Hsu. Therefore, it cannot be used to identify the presence of Be diffusion.

Dissolution – Dissolution of the surface is very common on Be-diffused stones. Surfaces that have not been repolished often have a melted appearance (C-34). However, this is a common feature on most corundums that have been heated at high temperatures, particularly when fluxes are used, so it is not distinctive of Be diffusion.

INDICATIONS OF NO EXPOSURE TO VERY HIGH TEMPERATURES

The presence of these inclusions proves that the stone has *not* been exposed to high heat and therefore could not be Be diffused.

CO_2 Inclusions – Internal "voids" that contain water and a bubble of carbon dioxide (CO_2) are quite common in sapphires from some localities, particularly Sri Lanka (C-35). Because CO_2 expands when heated, these inclusions cannot survive the very high temperatures necessary for Be diffusion. Therefore, the presence of undamaged inclusions would prove that a stone has not been Be-diffusion treated.

Internal voids filled with other liquids will also not survive high-temperature heat treatment. The presence of undamaged liquid-filled voids of any kind proves that no Be treatment has occurred (C-36).

Included Crystals – As discussed above, the presence of undamaged zircon crystals in a sapphire is a good indication that Be diffusion treatment has not taken place. Likewise, in our experience, it is unlikely that any crystalline inclusion could survive the temperatures required for Be diffusion without being significantly altered. Therefore, the presence of transparent, angular, or rounded solid grains of any mineral would be an excellent indication that Be diffusion has not taken place (C-37 and 38).

Rutile Needles – Needle-like inclusions of rutile, often referred to as "silk," are common in corundum from many localities. These needles usually survive the lower-temperature heat treatments that are performed on some sapphires. However, they typically do not survive the higher-temperature treatments to which most blue sapphires and rubies are subjected, including the very high temperatures necessary for Be-diffusion treatment. The presence of unaltered rutile needles means that a stone has not been exposed to this (or any other) high-temperature treatment (C-39).

SEND IT TO A LABORATORY

What if you have a sapphire that is colored throughout and does not show any of the indications listed above? These are the most difficult situations. We recommend that you send it to a qualified gemological laboratory and have its chemistry analyzed by the techniques mentioned in this article. We will continue to investigate alternative methods to identify this treatment process.

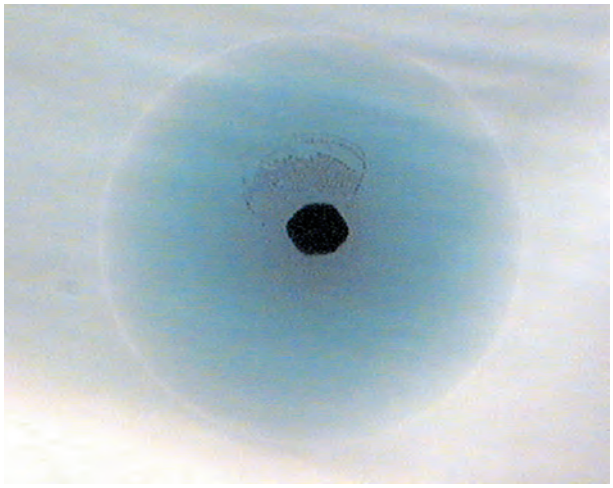

Figure 45. All the Be-diffused sapphires in this study that contained rutile crystals exhibited blue internal diffusion haloes around those crystals, which is very unusual in yellow and orange sapphires. Photomicrograph by Ken Scarratt; magnified 20×.

sapphire from some localities (e.g., Montana) is routinely heated to temperatures high enough (without adding chemicals) to cause such spotty blue coloration, this phenomenon is seen only rarely in heat-treated stones. Its presence does not unequivocally prove beryllium diffusion, but it does provide solid evidence of exposure to very high temperatures.

Flux-Assisted Synthetic Growth. During flux-assisted heat treatment (with or without diffusion), material from the surface of the corundum (as well as the alumina crucible and the boehmite inclusions) will dissolve to some degree into the molten flux (which may itself contain alumina). On cooling, the flux becomes supersaturated in alumina and crystallizes out onto the nearest convenient surface, often on the stones themselves (figure 46 and chart figure C-20).

We noted synthetic corundum overgrowth (identified by Raman spectroscopy and microprobe) on the surfaces of some of the yellow, orange, and orangy red Be diffusion–treated samples in this study. The overgrowth was particularly obvious on rough or preformed samples and often remained after the stones were recut following processing. The extent of this overgrowth ranged from single small areas (usually around the girdle) to numerous large areas covering 10–20% of the stone's surface. The typical appearance of this overgrowth is depicted in figure 47 (McClure, 2002a; Scarratt, 2002a; Moses et al., 2002). The

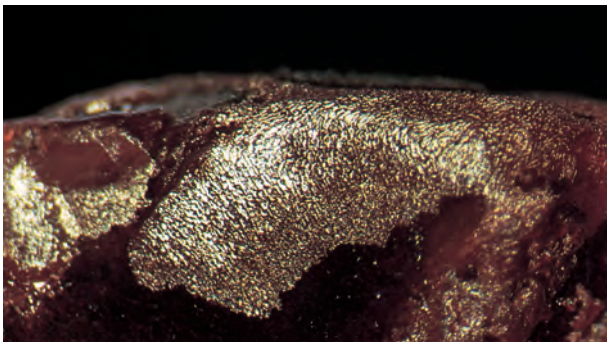

Figure 46. Large areas of platy synthetic corundum crystals were present on the surface of some Be-diffused samples examined for this study. Photomicrograph by Shane F. McClure; magnified 20×.

"blocky" texture may be observed even at low-power (10×) magnification with transmitted light, but it may be missed if only reflected light is used to examine the specimen.

Pre-existing fractures in corundum—as well as those created during Be diffusion—and boehmite channels are often sealed, or "healed," by the same process. The molten flux enters the fracture or channel, and the surfaces of the fracture or channel dissolve into the flux, where the dissolved material is held in solution until the temperature is reduced. On cooling, the alumina then crystallizes out of the flux onto the walls of the fracture or channel, sealing it while at the same time trapping residues such as gas bubbles, flux remains, and glass. This "flux-assisted healing" of fractures was well documented in rubies even before the

Figure 47. Blocky synthetic overgrowth produced during the Be-diffusion process was still present on the surface of some treated stones, even after repolishing. Photomicrograph by Ken Scarratt; transmitted light, magnified 30×.

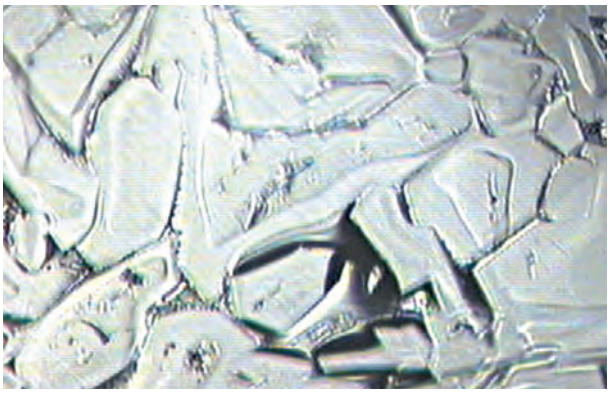

introduction of the new Be-diffusion treatment (Hänni, 2001).

In the Be-diffused stones, the artificially healed fractures (figure 48) often resembled the "fingerprints" or "feathers" seen in flux- or hydrothermally grown synthetic rubies and sapphires. A "roiled" appearance could be seen within the healed boehmite channels, which were aligned with edges of intersecting parting planes. These tubes often contained high-relief internal cavities that varied from spherical to a "dog bone" shape (see chart figures C-15 and C-16).

These observations are not surprising, as the conditions and equipment used to heat treat or lattice diffuse elements into corundum closely resemble those used for corundum synthesis, except that the production of flux-grown synthetic corundum involves lower temperatures (around 1300°C) and the use of platinum crucibles rather than alumina ones (Nassau, 1980).

UV-Vis-NIR Spectroscopy. As discussed earlier, UV-Vis-NIR spectroscopy was used to confirm the trapped-hole nature of color in these Be-diffused stones, but we have not found it useful as an identification method. We have examined the UV and visible-range absorption spectra of dozens of samples, both at room temperature and at liquid-nitrogen temperature, but have failed to find a Be-diffusion identification criterion. The difficulty is that there appears to be little difference in the spectra of trapped holes caused by naturally occurring magnesium and those induced by beryllium diffusion. This method is therefore of no use in the identification of Be-diffusion treatment.

Infrared Spectroscopy. Much natural corundum contains detectable quantities of hydrogen, which can be present in several forms (Rossman, 1988). Hydrogen can bond with oxygen in the lattice to form O-H, resulting in sharp absorption bands at 3367, 3310, 3233, and 3185 cm^{-1} (Beran, 1991). Hydrogen can also exist in corundum as H_2O, leading to a broad absorption band at ~3400 cm^{-1}. It can also be present as water within fluid inclusions, and, finally, it can exist as a component of an included solid phase, such as diaspore (Smith, 1995), which is one of the hydroxides of aluminum. Since corundum is transparent from the UV region to 2000 cm^{-1} (5000 nm) in the infrared, even trace amounts of hydrogen are detectable using infrared spectroscopy. Some of the variations observed in the IR spectra of natural sapphires are shown in figure 49.

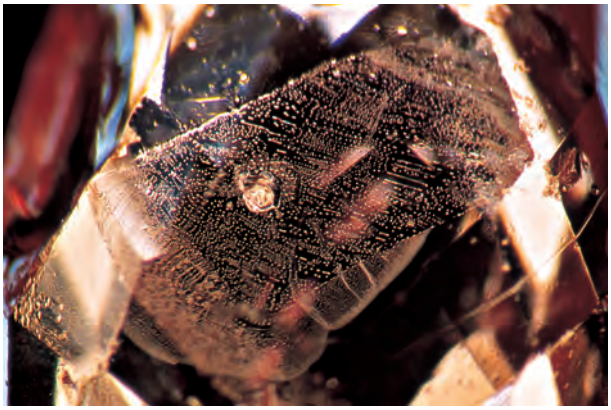

Figure 48. Healed fractures such as these were seen in many of the Be-diffused corundum samples we examined. They often appeared similar to those found in flux- or hydrothermally grown synthetic rubies and sapphires. Photomicrograph by Shane F. McClure; magnified 25×.

During the course of this study, we collected IR spectra on 50 Be-diffused sapphires. In none of these spectra did we observe hydrogen-related features. This result was expected, since hydrogen rapidly diffuses out of corundum at high temperatures (e.g., 1800°C) in a hydrogen-free atmosphere (i.e., the oxygen atmosphere used for Be diffusion). An example of this effect is illustrated in figure 50. The blue spectrum shows the O-H absorption of a natural

Figure 49. The O-H infrared absorptions in sapphire may vary in appearance, as illustrated by the selection of five spectra shown here. The top four spectra are derived from heat-treated blue sapphires, and the bottom spectrum is from an unheated yellow sapphire.

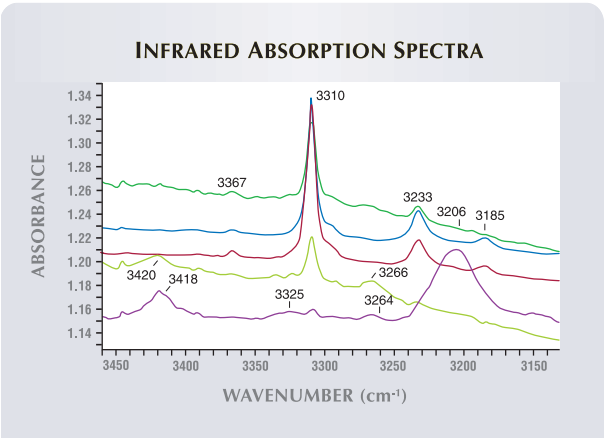

pink sapphire from Vietnam. After Be diffusion at 1800°C for 33 hours in an oxygen atmosphere (red spectrum), the O-H absorption features have entirely disappeared. Figure 51 shows the H_2O absorption band (Rossman, 1988) in a natural light yellow sapphire of unknown origin (blue spectrum). After the same Be diffusion parameters noted above, the H_2O absorption features are absent (red spectrum).

As shown earlier, some types of dark blue basaltic sapphire can be greatly lightened by a two-step process of Be diffusion followed by normal heat treatment in a reducing environment. Because the reduction heat treatment is carried out in an atmosphere that contains hydrogen, the hydrogen will diffuse back into the crystal and appear in the absorption spectrum as O-H, with the absorption features enumerated above. Thus, an attractive blue Be-diffused sapphire could exhibit the O-H absorption features of a natural-color sapphire or one that has been heat treated without diffusion. Consequently, the presence of O-H absorption features in a blue stone is not evidence that it has *not* been Be diffused. This is only an issue in blue sapphire, since heat treatment of a yellow or orange stone in a reducing atmosphere will remove the Be-induced color.

Our data show that a ruby or a yellow, orange, or orange-pink sapphire that has undergone Be diffusion contains no structurally bonded hydrogen and little if any molecular water. However, this tells us only that the stones have been heated in an oxidizing atmosphere, the same atmosphere required for Be-diffusion treatment. It does not necessarily mean that Be diffusion is involved. Still, it can be a helpful piece of data when combined with other factors.

Raman Spectroscopy. No additional peaks were discovered and no changes in the normal corundum spectrum were observed in specimens analyzed before and after Be diffusion treatment.

Raman analysis also proved that the overgrowth seen on some of the samples was indeed (synthetic) corundum. An unexpected result was the identification of a tiny grain of material on the surface of one stone as synthetic cubic zirconia, the feed source of which may have been a zircon inclusion or a flux additive.

Chemistry. EDXRF spectra on stones that were not re-polished following Be diffusion consistently revealed the presence of both Ca and Zr, elements that are not typically found in corundum. The Zr may be related to exposed zircon inclusions or to zircons that were accidentally included in the heat-treatment process. The Ca may indicate that calcium borate is a component of the flux mixture (see "Beryllium Diffusion into Corundum: Process and Results" section).

Figure 50. The infrared spectrum of a natural-color pink sapphire from Vietnam containing hydrogen as O-H (blue) shows strong absorption bands at 3367, 3310, 3233, and 3185 cm^{-1}. After Be diffusion at 1800°C for 33 hours in an oxidizing atmosphere, these hydrogen-related bands were eliminated (red).

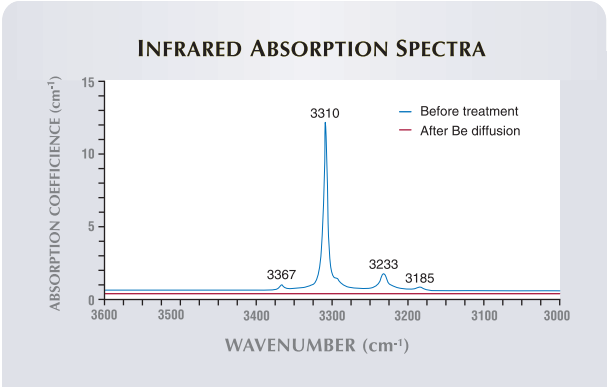

Figure 51. This infrared spectrum of a natural-color yellow sapphire from an unknown source (blue) shows a broad absorption band centered at about 3300 to 3400 cm^{-1} that is indicative of molecular water (H_2O), possibly contained in the stone as an inclusion. After Be diffusion at 1800°C for 33 hours in an oxidizing atmosphere, this H_2O-related absorption was removed (red).

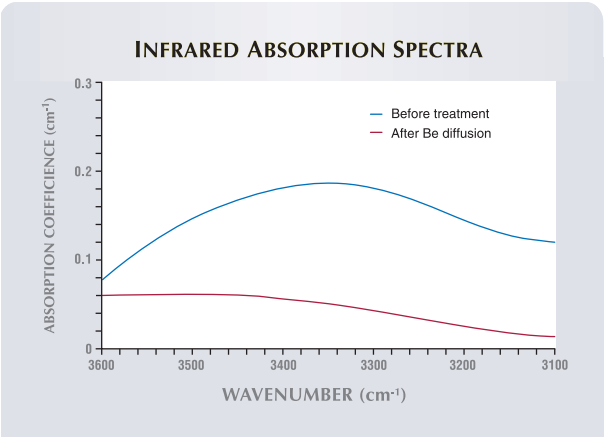

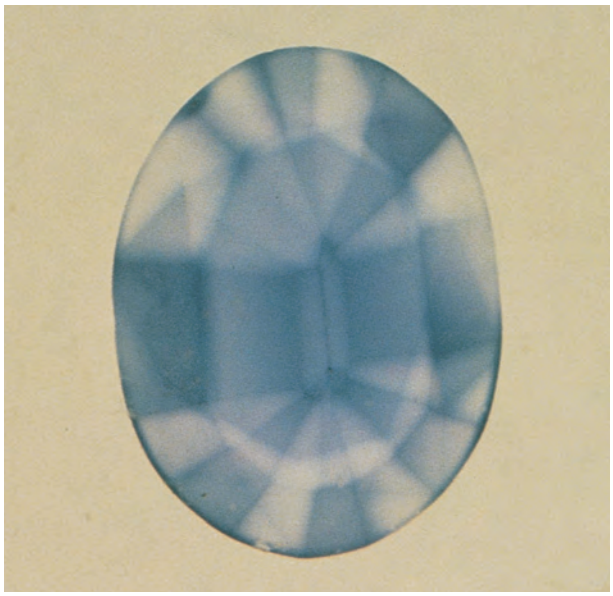

Figure 52. Titanium-diffused sapphires often show patchy surface coloration in immersion, caused by the shallow penetration depth of Ti. This is not seen in Be-diffused corundum. Photo by Shane F. McClure.

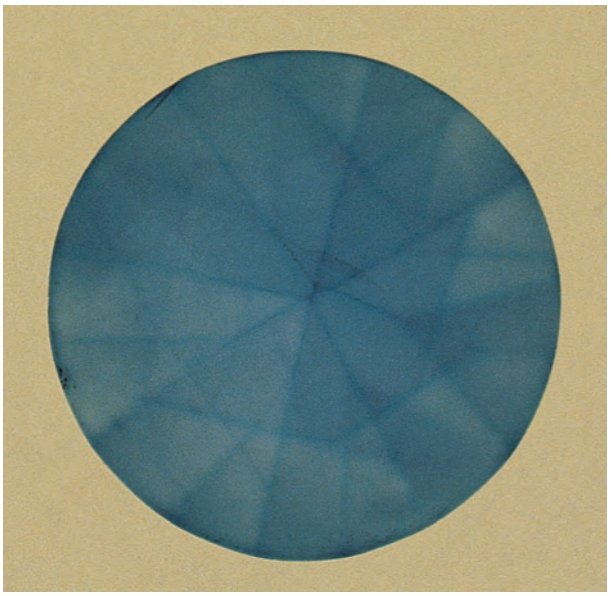

Figure 53. The facet junctions of this 1.77 ct Ti-diffused sapphire appear darker blue when seen in immersion. This phenomenon is not seen in Be-diffused corundum. Photo by Shane F. McClure.

SIMS analysis readily identified the presence of beryllium at the surface of all the samples of Be-diffused rubies and sapphires analyzed. Table 7 shows representative analyses[2] of a variety of our corundum samples (with full analyses given in the data depository SIMS table). When there is no Be in the stone, the SIMS analysis indicates about 1.5 ppma because of interference from aluminum ions. This sets the lower limit of what can be measured, and thus a measurement of 5 ppma or more gives high confidence that a stone contains beryllium. The Be concentration for this process ranges from approximately 10 to 35 ppma. Consequently, our data confirmed that very little Be is needed to affect the color of corundum. If measurements are much below 10 ppma, the sample should be re-measured on another facet. Overall, these analyses demonstrate a clear correlation between color modification and elevated Be content.

Comparison to Ti Diffusion Treatment

There are definite differences in diagnostic features between sapphires that have been diffusion treated with titanium (see, e.g., Kane et al., 1990) and those that have been diffused with beryllium. In the earlier diffusion-treated stones, the color-causing elements (mainly Ti to produce blue) had limited penetration into the surface of the treated stone (again, see figure 16). However, Be diffuses much faster than Ti (see Appendix), so the depth of the color layer produced can vary greatly, even extending throughout the stone.

Ti-diffused corundum will typically show patchy surface coloration with immersion (figure 52), since the very shallow color layer is often cut through during repolishing. Immersion will also reveal color concentrations at facet junctions and high relief (figure 53), as well as "bleeding" of color into the stone from the surfaces of cavities, fractures, and fingerprints (figure 54). None of these features has been seen in stones that have been diffused with Be. In contrast, the layer of color conforming to the outside shape of the stone is usually *not* visible in faceted Ti-diffused sapphires, even with immersion. However, this surface-conformal

[2] The very first analyses were conducted and published (McClure et al., 2002) without the benefit of a Be-in-sapphire analytical standard with which to calibrate the SIMS equipment. Those analyses indicated a Be content roughly 10 times higher than we now know to be correct. An accurate Be-in-sapphire standard was then prepared by one of the authors (SN) and analyzed at Evans East, which allowed the previous data to be recalculated (see, e.g., Wang and Green, 2002a). Although the precise concentrations changed for all the samples reported, the ratio of beryllium content between known treated stones and known natural-color stones remained the same. Thus, the original correlation of elevated Be content to color modification in treated stones was correct, though the absolute Be concentration was not. Since April 2002, all analyses have been run with the Be-in-sapphire standard. All other elements in the table are also calibrated by element-in-sapphire standards.

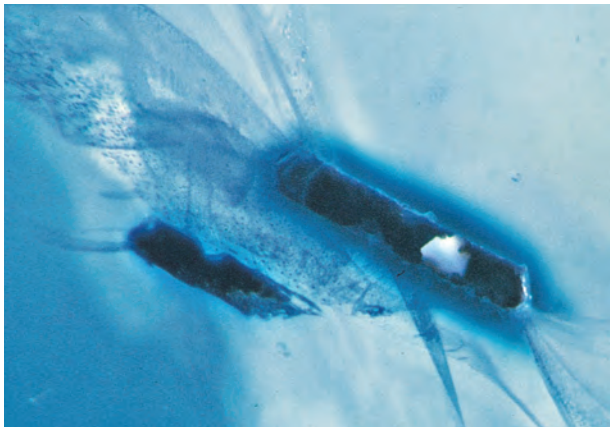

Figure 54. "Bleeding" of color into surface-reaching fractures and cavities is often visible in sapphires that have been diffused with Ti. This was not seen in any of the Be-diffused samples examined in this study. Photomicrograph by John Koivula; magnified 15×.

layer is easily visible—when present—in stones that have been Be diffused (figure 55).

WHERE DO WE GO FROM HERE?

We have been investigating other nontraditional methods of Be detection with the goal of developing a low-cost screening methodology for these treated stones. We have no solution yet, but outline below a number of possibilities that are being studied. We hope that this discussion will stimulate gemologists around the world to focus their creative talents on this problem.

Figure 55. The actual surface-conformal color zone that is produced by Ti diffusion is usually not visible, even in immersion, as seen with the stone on the right in this image. This is distinctly different from the Be-diffused stones, in which the surface-related color layer (if present) is often easily seen with immersion (left). Photomicrograph by Shane F. McClure; magnified 10×.

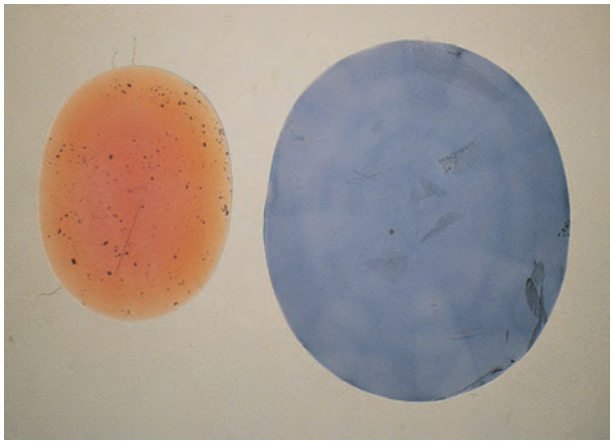

Electrical Conductivity. Magnesium at 15–40 ppma in corundum gives rise to measurable electrical conductivity as the temperature is raised moderately above room temperature (Ramírez et al., 2001; Tardío et al., 2001a,b,c). A similar effect should be produced by beryllium. The trapped holes induced by Mg^{2+} (and potentially by Be^{2+}), which are responsible for color formation in corundum, also give rise to electrical conductivity when the stones are heated. One of the authors (OB) performed initial experiments on a Be-diffused cube of Czochralski-grown sapphire using electrically conductive epoxy for electrodes. Be-diffused synthetic sapphire was chosen to eliminate possible interference with other impurities. Measurable conductivity was achieved at about 160°C over a range of 500 to 3,000 volts, similar to what was observed by Tardío et al. (2001a,c).

Measurements were then made on two natural faceted sapphires—a 1.6 ct Be-diffused yellow, and a 5.46 ct heat-treated but not Be-diffused yellow. The Be-diffused sample showed conductivity of two to three orders of magnitude higher than the non-Be-diffused sapphire, providing some indication that this method has potential.

There are many issues that will have to be addressed before the value of this technique can be determined. It will be necessary to prove that the conductivity measured is a bulk conductivity and not surface conductivity that would only be dependent on stone finish and the size of the stone. A practical method of applying electrical contacts will have to be developed. A significant amount of data will have to be acquired on the effects of geometry and beryllium concentration to prove that Be can be identified independently from naturally occurring Mg, and to delineate regions of validity and regions of uncertainty. In principle, though, it is a technique that could be automated.

Low-Temperature Heating. During discussions of the Be-diffusion problem with Thomas R. Anthony of General Electric Co. (pers. comm., 2002), he suggested that the Be-induced color modification may not be stable at temperatures in the range of 400°–600°C. It is known that the absorption due to the Fe^{2+}-Ti^{4+} pair is substantially

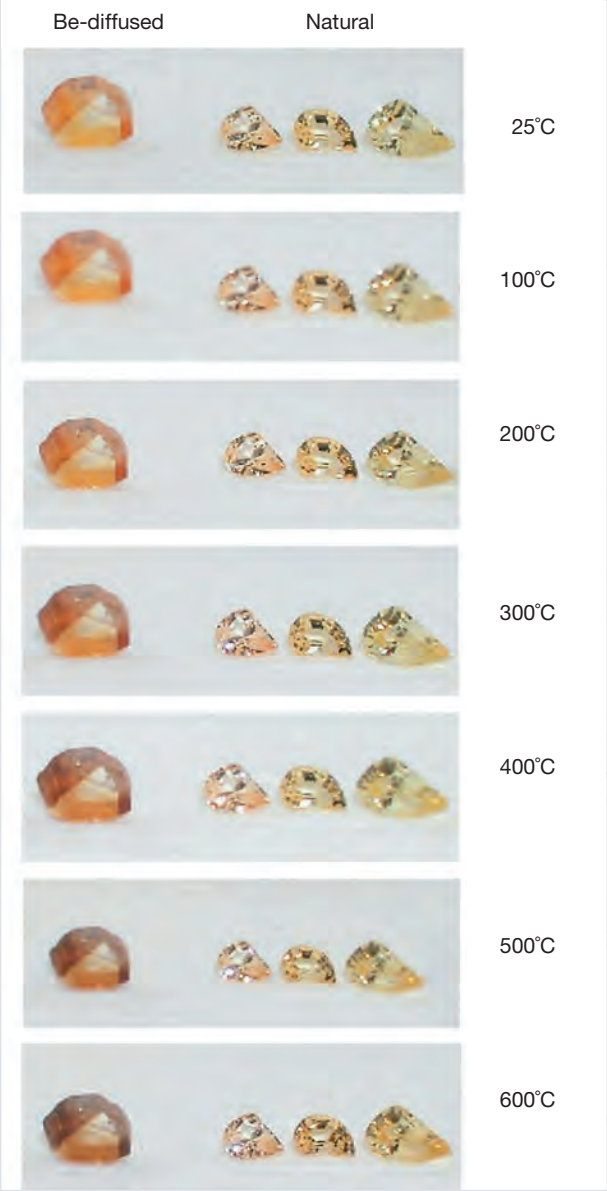

Figure 56. These photos show a Be-diffused sapphire on the left (0.95 ct) and three non-diffused (Fe-colored) sapphires on the right (0.28–0.33 ct). Note that at about 400°C, the Be-diffused sapphire took on a distinct brown coloration, whereas the natural sapphires did not show any change. Photos by Wuyi Wang.

reduced at temperatures of 500°C and above, and the Be-induced trapped-hole coloration could exhibit similar, useful color alterations with temperature. These "thermochromic" effects are a common property of minerals. With increasing temperature, absorption bands become broader and shift to a lower energy (i.e., higher wavelength).

The Be trapped-hole center causes selective absorption from 600 nm to the high-energy side, producing additional yellow coloration. However, color appearance varies depending on the color center involved, so this yellow color differs in tone from that typically caused by Fe in natural corundum. Because of the different natures of these two absorbing centers (Burns, 1993), they could react differently to heat. Therefore, heating Be-diffused sapphires and natural sapphires with similar (or even identical) colors could reveal a temperature range within which the colors of treated and untreated corundum temporarily become very different, possibly yielding a useful method of identification.

To test this idea, a natural colorless corundum was Be diffused at 1800°C for 33 hours at a high oxygen partial pressure. It turned intense yellow due to formation of Be trapped-hole centers. It was then heated to 600°C with three other natural yellow sapphires colored by Fe. The Be-diffused yellow sapphire began to exhibit a strong brown coloration starting at about 400°C (figure 56). Figure 57 shows the changes in its absorption spectrum over the range from room temperature to 600°C. The shift in coloration from yellow to brown is a result of the increasing absorption in the red region of the spectrum. The original color was restored after cooling. The three naturally Fe-colored sapphires showed no visual changes in color when heated.

Figure 57. The absorption spectrum of the Be-diffused yellow sapphire in figure 56 changed as the temperature increased. The increased absorption in the red at high temperature is responsible for the brown coloration.

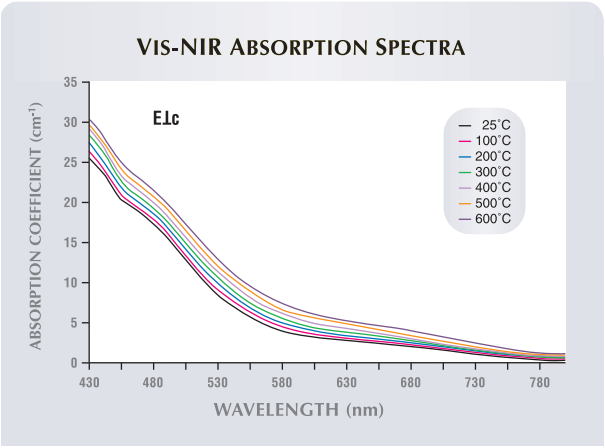

More than 30 pinkish orange Be-diffused sapphires also were tested for visual color change on heating, and all exhibited a strong brown coloration at ~500°C. Hughes (1987b, 1988) noted that heat-treated yellow sapphires from Sri Lanka (Mg^{2+} trapped-hole coloration) shift to a darker, browner color when heated to moderate temperatures. Thus it remains to be determined if this heating process can distinguish the yellow Be-induced coloration from the yellow Mg-induced coloration of heat-treated yellow sapphire.

It is important to note that this procedure also requires several caveats, and may not apply across the full range of colors and types of corundum being treated by the new diffusion process. However, if applicable, it may provide a means to rapidly identify large groups of treated sapphires—both loose and mounted in jewelry, since the temperature range being used would not affect the metals used in jewelry.

Luminescence to Ultraviolet Radiation. Recent work outlined in Fritsch et al. (2003) has noted differences in luminescence to ultraviolet radiation that may provide helpful indications for identifying Be-diffusion treatment, particularly using a specialized microscope for viewing this property that was designed by Franck Notari of GemTechLab in Geneva. Junko Shida, of the Gemmological Association of All Japan, recently presented useful fluorescence observations to members of the Laboratory Manual Harmonization Committee that she and her staff had made when examining Be-diffused corundum using laser tomography. They found that, with this technique, the Be-diffused areas fluoresced a distinctive orange (J. Shida, pers. comm., 2003).

DURABILITY AND STABILITY OF THE TREATMENT

One of the first questions most jewelers and gemologists ask about a gemstone enhancement is: Is the process permanent and stable when subjected to typical jewelry cleaning and repair procedures? To address this question, we tested three faceted Be diffusion–treated orange to pinkish orange sapphires (all of which had been treated in Thailand) to determine the durability and stability of this process under a wide range of conditions to which sapphires might be subjected during jewelry manufacturing or routine cleaning and repair. The samples used were: (1) a 1.12 ct medium dark pinkish orange oval mixed-cut, (2) a 0.43 ct dark orange oval mixed-cut, and (3) a 0.83 ct intense reddish orange princess cut. All three sapphires were mounted in 14k gold rings (the first in a four-prong white head, the second in a six-prong yellow head, and the third in a four-prong yellow head) before the durability testing began. Details on the tests used and the results observed are provided in the durability table of the *G&G* Data Depository (http://www.gia.edu/GemsandGemology).

Given the low concentrations of Be required to change the color of corundum, we did not expect these diffused stones to behave any differently from natural-color or heat-treated samples. Indeed, Be-diffusion treatment did not appear to have any impact on the durability or stability of the three samples tested when exposed to routine cleaning and jewelry repair procedures. Neither ultrasonic nor steam cleaning produced any damage in the treated stones, which were examined with magnification both before and after the cleaning procedure.

In addition, these three Be-diffused stones showed little or no surface etching as a result of retipping. However, it is well known that the use of borax-containing chemicals (both fire coat and flux) contributes to moderate to severe surface etching of corundum, so other researchers may find different results using a different flux or higher temperatures. The best way to avoid this potential problem is to unmount the stone for any repair procedure that would expose it to heat.

If etching due to exposure to borax-containing compounds is severe enough, the stone might have to be repolished. Of particular importance for diffusion-treated stones with shallow color layers is the fact that repolishing or recutting could remove some or all of the diffused layer, resulting in a significant change in the appearance of the stone (figure 58). This precaution is especially pertinent to Be diffusion–treated stones in the orangy pink color range, which may have a shallow color penetration. Therefore, we recommend great caution in repolishing or recutting Be diffusion–treated stones.

LABORATORY NOMENCLATURE AND TRADE DISCLOSURE RECOMMENDATIONS

As with other gem treatments, a clear declaration of the lattice diffusion process is necessary,

Figure 58. To illustrate the consequences of recutting incompletely Be-diffused stones, we took one of these two closely matched treated sapphires and had it recut as if it had been chipped and needed significant repair. The 0.71 ct stone on the right side of the pair was recut to 0.40 ct, and clearly has lost most of its orange component. Photos by Maha Tannous.

whether Be or Ti is involved, to insure trade stability and to maintain consumer confidence in gems. In the case of the two gemological laboratories represented by authors of this article, GIA and AGTA, laboratory reports indicate the exposure of a gem to a treatment process such as lattice diffusion, and note if synthetic corundum is present on the surface. This is consistent with the nomenclature adopted by the Laboratory Manual Harmonization Committee (LMHC), of which our two labs are members. For lattice diffusion, the LMHC conclusion states that the stone shows: ". . . indications of heating, color induced by lattice diffusion from an external source." For the flux-assisted healing of fractures, a quantitative descriptor (such as minor, moderate or significant) is applied, as is commonly used for heat-treated rubies.

It is also important that synthetic overgrowths on corundum are properly characterized and declared on laboratory reports. The reasons for this closely parallel those for clearly describing the filling of cavities and fractures with glass on reports and, as a consequence, within the industry (Kane, 1984; Scarratt and Harding, 1984; Scarratt et al., 1986; Hughes, 1987a; Scarratt, 1988, 2000; "Glass filled rubies . . . ," 1994; "Glass filling . . . ," 1994; Robinson, 1995). Specifically, synthetic overgrowths created during the Be-diffusion process: (1) are created artificially and, therefore, are unnatural additions to the stone; and (2) unnaturally increase the weight of a finished stone by both adding the weight of the synthetic material and allowing a larger stone to be cut than would otherwise be possible.

Gem dealers and retailers often need more descriptive terminology to communicate with the consumer. In some instances, one could say that beryllium was introduced into the stone to create colors that are otherwise very rare in nature. A simple and accurate description might be "artificially colored with beryllium." Additional disclosure information is needed for those stones where repolishing may affect the color or where synthetic material may be present on the surface.

SUMMARY AND CONCLUSIONS

We have shown that the "new process" from Thailand is the diffusion of beryllium into ruby and sapphire at very high temperatures in an oxygen atmosphere. Unlike the much older titanium diffusion process, which produced a thin blue layer under the surface, Be diffusion can penetrate deeply, sometimes coloring the entire volume of the stone. We have shown that beryllium diffused into corundum, at high temperature, is the sole cause of the color modifications observed. A wide variety of colors are produced by this process, depending on how the Be trapped-hole pair interacts with the internal chemistry of the stone. Thus far, the colors produced or modified by this process are predominantly yellow, yellowish orange, orangy pink to pinkish orange, orange, and orange-red to red (ruby). Many are very attractive, and have excellent commercial potential (figure 59). We have also shown that some types of dark blue basaltic sapphire can be lightened very significantly by Be diffusion. Thus, the majority of sapphire colors in the marketplace could potentially be products of the Be-diffusion process.

However, color modifications are not the only important consequences of this process. We have

Figure 59. As shown by this attractive jewelry, Be-diffused sapphires clearly have significant commercial potential, as long as they are properly disclosed. Photo by Myriam Naftule Whitney; courtesy of Nafco Gems.

noted significant amounts of synthetic corundum overgrowth on many of these stones, much of which may remain after re-cutting. Some faceted stones have shown 10–20% of the surface covered with this synthetic material, raising questions concerning just how "natural" such a stone is. In addition, fractures and boehmite channels are often sealed or "healed" by this process

Identification of Be diffusion–processed stones ranges from very simple observations to quite complex chemical analyses. Standard gemological properties are not changed by Be diffusion, nor does the durability of the stone appear to be affected. If the diffusion layer penetrates only a portion of the radius of the stone, it may be seen easily by immersion in a high R.I. liquid with diffuse background illumination. Observation of a three-dimensional surface-conformal color layer is considered proof that the stone has been diffused. If there is only a portion of a color layer, however, because the stone was recut or originally diffused in the rough, care must be taken not to confuse Be-diffusion treatment with natural color zoning.

In some sapphires, diffusion fully penetrates the stone—and identification becomes substantially more difficult. However, the inclusion scene may provide important indicators of the high heat required for Be-diffusion treatment. Careful examination with magnification and diffuse reflected light may reveal synthetic growth on surfaces and in healed fractures and channels. Highly altered zircon inclusions are also indicative of the very high temperatures used in this process, as is the replacement of boehmite with synthetic material. Internal diffusion, in the form of blue halos around rutile crystals in yellow and red corundum, is another important indicator. Although these features do not prove Be diffusion, they do indicate that the stone should be subjected to additional testing.

SIMS and LA-ICP-MS can both unequivocally identify the presence of beryllium in color-altering concentrations (5–30 ppma). While these are expensive tests, they are necessary for potentially high-value stones that do not exhibit a surface-conformal color layer.

As a part of the study of this process we have decided to replace the term *surface diffusion*, which has been used by gemologists and some laboratories for years, with *lattice diffusion* to be consistent with the usage in other scientific disciplines. In their official reports, both the GIA laboratory and AGTA-GTC describe Ti- and Be-diffused stones with the wording ". . . indications of heating, color induced by lattice diffusion from an external source." Thus, both the earlier titanium blue diffusion and the new beryllium diffusion are described the same way, as they are exactly the same process, just different diffusing elements.

The implications of Be diffusion to the entire gem community (from miner to consumer) are

quite far reaching. It appears that virtually any color of ruby and sapphire can be reproduced by the Be-diffusion process. Transparent corundum actually is a common commodity. Only corundum in attractive colors and color saturation levels is rare. There are large deposits of sapphire that can produce large stones in unmarketable colors. Conventional heat treatment can improve only a very small percentage of such material. However, it appears that much, if not most, of this material can be Be diffused to produce attractive colors (figure 60). We have observed that Be diffusion beneficially affects 50–95% of mine run material, not just a small portion. Thus, if we cannot develop a simple low-cost detection method, gem sapphire will become as common as blue topaz, supply will exceed demand, and prices will fall radically, damaging the entire gem trade. Today, there is no simple, low-cost alternative to SIMS or LA-ICP-MS, but we are working on the problem and strongly encourage others to do so as well.

Technology will always advance, and attempting to slow or stop it is as rewarding as trying to sweep back the sea with a broom. However, as a community we need to come together to understand each new process as it is developed, and bring it to the gem market with full disclosure, allowing an informed marketplace to determine value. Only in this way can our miners, treaters, dealers, and jewelers prosper. Only in this way will the consumer show us the trust and support we have enjoyed in the past.

Figure 60. Many attractive sapphire colors that were previously very rare will now be made abundant with Be diffusion, opening up uses in jewelry designs that were previously not available. The total weight of the Be-diffused sapphires in this pin is 3.50 ct. Photo by Myriam Naftule Whitney; courtesy of Nafco Gems.

ABOUT THE AUTHORS

Dr. Emmett (jlemmett@earthlink.net) is a principal of Crystal Chemistry, Brush Prairie, Washington; Mr. Scarratt is laboratory director, AGTA Gemological Testing Center, New York; Mr. McClure is director of Identification Services, GIA Gem Laboratory, Carlsbad, California; Mr. Moses is vice president for Identification and Research, GIA Gem Laboratory, New York; Mr. Douthit is a principal of Crystal Chemistry, Los Altos, California; Mr. Hughes is the author of Ruby & Sapphire *and webmaster at Palagems.com, based in Fallbrook, California; Dr. Novak is manager of Dynamic SIMS Services, Evans East, East Windsor, New Jersey; Dr. Shigley is director of GIA Research in Carlsbad; Dr. Wang is a research scientist, GIA Gem Laboratory, New York; Mr. Bordelon is a gem merchant and designer/manufacturer of gemological instruments in New Orleans, Louisiana; and Mr. Kane is president, Fine Gems International, Helena, Montana.*

ACKNOWLEDGMENTS: The authors thank gem dealers Terry Coldham, Mark Smith, Joe Belmont, Tom Cushman, Rudi Wobito, Hans-Georg Wild, Markus Wild, Bill Larson, Eric Braunwart, Santpal Sinchawla, Jeff Bilgore, and Roland Naftule for graciously supplying stones and other materials for these experiments. They thank Junko Shida for details on the Gemological Association of All Japan's experience with laser tomography and supply of, and information concerning, Be-diffused blue sapphires. A number of stimulating conversations with Professor George Rossman of the Division of Geological and Planetary Sciences at the California Institute of Technology, Pasadena, California, are also greatly appreciated, as are conversations with Milan Kokta and Jennifer Stone-Sundberg of Sant-Gobain Crystals and Detectors, Washougal, Washington. Yianni Melas provided invaluable assistance in the early stages of this research. Dr. Thomas R. Anthony of the General Electric Company, Schenectady, New York, is also thanked for his assistance. Garth Billings and Dave Witter are thanked for their support of the experiments. Don and Corey Johnson of Eaton-Turner Jewelry, Helena, Montana, kindly provided assistance with the durability testing. Thomas Moses, Shane McClure, and Kenneth Scarratt acknowledge with thanks the aid of their laboratory staff members. John Emmett, Troy Douthit, and Owen Bordelon express their appreciation to the AGTA for partial financial support of their work.

APPENDIX: WHAT IS DIFFUSION?

The motion of atoms through solids is fundamental to our technological society. The heat treatment and case hardening of steels, the doping of semiconductors for integrated circuits, and the production of padparadscha-like colored sapphires from pink ones all rely on the transport of atoms through solids. The mechanism by which atoms or ions move through solids is known as *diffusion*.

How actually does an atom move through a solid that is, after all, solid? It turns out that even the most perfect crystal has places in its lattice where atoms are missing. These holes are termed "vacancies." In the case of corundum, which is made up of aluminum and oxygen atoms, even the most perfect crystal sample will have missing aluminum and oxygen atoms, and the higher the temperature the more missing atoms there will be. A foreign ion can move through solid corundum by jumping from one vacancy to the next. Since the vacancies are randomly distributed, the diffusing ion will "random walk" through the crystal, sometimes moving forward or back, up or down, or right or left. Averaged over a large number of jumps, the ion always moves away from regions of high concentration of diffusing ions to regions of low concentration. Jumping requires energy, which is supplied by heat, so an ion makes more jumps per second at high temperatures than at low temperatures. Thus, diffusion rates increase dramatically with temperature due to the increase in the number of both vacancies and jumps per second.

All types of heat treatment of corundum involve some type of diffusion process. It is the movement of preexisting ions that makes heat treatment work. For example, the dissolution of rutile needles into the host corundum crystal is simply titanium diffusing into corundum (and aluminum diffusing into rutile) at high temperature. In this case, the diffusion involves ions that are already in the host corundum (Koivula, 1987). In this article, however, we are primarily concerned with the diffusion of a foreign element (Be) into corundum from an outside source. Thus, *diffusion* is the physical process, and *diffusion treatment*—the term we use to describe the enhancement method in this article—refers to artificially coloring a gem.

How fast does diffusion occur? In corundum it depends on the size (ionic radius) of the diffusing ion relative to the size of the vacancy, the ionic charge of the diffusing ions, the temperature during treatment, and a variety of other less important factors. Because of the "random walk" nature of diffusion, the depth of penetration does not increase linearly with time. Rather, it increases with the square root of time. This means that if the penetration depth of a given ion at a given temperature is 1.0 mm in one hour, it will be 3.16 mm in 10 hours, and 10 mm in 100 hours. Thus at a particular temperature we can say that the diffusion depth x (in cm) is related to time by

$$x = \sqrt{Dt}$$

where D is the diffusion coefficient in units of cm^2/sec, and t is the time in seconds over which the diffusion is conducted. The diffusion coefficient D is a measure of the ease with which an ion moves through the corundum lattice. At 1750°C, for example, the diffusion coefficients for the following ions are approximately: $H^+ \sim 10^{-5}$, $Be^{2+} \sim 10^{-7}$, $Ti^{4+} \sim 10^{-9}$, and $Cr^{3+} \sim 10^{-13}$ cm^2/sec. Diffusion coefficients increase exponentially with temperature.

Figure Ap-1 shows the concentration profiles at three different times for beryllium (assuming $D = 10^{-7}$ cm^2/sec at 1750°C). The shape of these curves is typical of the diffusion process. If we wish to fully saturate a stone with a foreign ion, we need to know how long it will require. Figure Ap-2 is a plot of the average concentration in a spherical sample as a function of time t, the diffusion coefficient D, and the diameter d, of the stone. Continuing our example, if we assume D to be 10^{-7} cm^2/sec, then it will require 97 hours to completely saturate a 5-mm-diameter spherical sample of corundum, but 75% of complete saturation can be achieved in about 16 hours, which is one-sixth of the time for complete saturation.

What determines the magnitude of the diffusion coefficients, which, as we have noted, can vary over many orders of magnitude from element to element? At a given temperature, aliovalent ions (see "Color in Corundum" section) exhibit diffusion coefficients in relatively pure corundum that are between 1,000 and 10,000 times those of isovalent ions. As discussed above, a diffusing ion requires vacancies into which to jump in order to move. In pure corundum, or corundum containing only isovalent impurities, vacancies occur only from heating the lattice. These thermally induced vacancies exist only in extremely low concentrations, even at very high temperatures. Thus the diffusion of isovalent ions is very slow. In contrast, aliovalent ions make their own vacancies and do not have to rely on thermally induced vacancies. This is due to the fact that aliovalent ions must be charge compensated to dissolve into

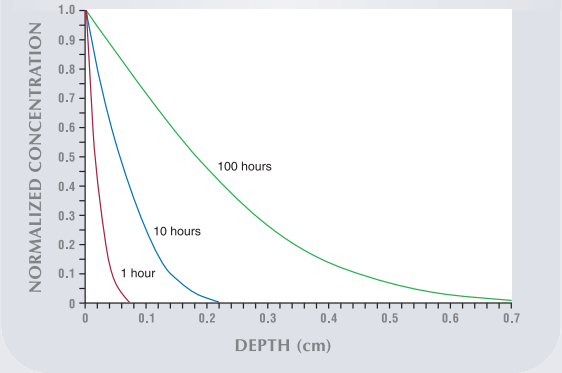

Figure Ap-1. The depth of beryllium diffusion into sapphire is shown here calculated for three different processing times—1 hour, 10 hours, 100 hours. Diffusion depth does not increase linearly with time, but with the square root of time.

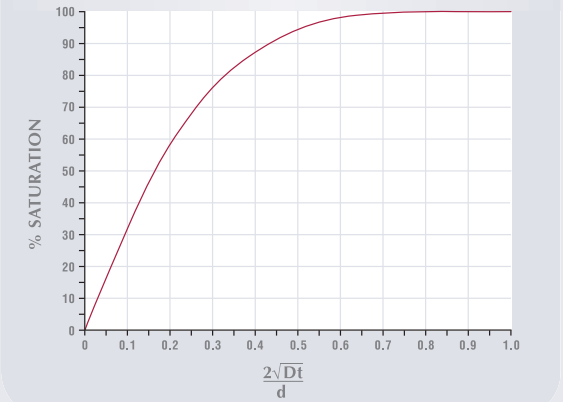

Figure Ap-2. This diagram shows the time required to saturate, by diffusion, a sphere of material of diameter d *in cm.* D *is the diffusion coefficient in units of* cm^2*/sec, and* t *is the diffusion time in seconds. Note that to achieve 100% saturation requires approximately six times as long as to achieve 75% saturation. An example of how to use this graph is as follows: Suppose that we wish to determine the degree of Be saturation (and thus color saturation) that will be achieved in a 5-mm-diameter sapphire that we will Be diffuse for 25 hours at 1750°C. Thus* d = 5 mm (or 0.5 cm), t = 25 hours (or 90,000 seconds), *and* D = 10^{-7} cm^2*/sec (or 0.0000001* cm^2*/sec). Putting these numbers into the relation on the horizontal axis,* $2\sqrt{Dt}/d$*, we get 0.375. A value of 0.375 on the horizontal axis corresponds to about 85% saturation. Note that the curve is very general in that it applies to any ion at any temperature diffusing into any spherical host, as long as the diffusion coefficient is known at the temperature of interest.*

the corundum lattice (see "Color in Corundum" section). In diffusion situations, this charge compensation is usually accomplished by the formation of vacancies. For example, to place three Ti^{4+} ions in the corundum lattice requires the formation of one aluminum vacancy to charge compensate them. At any measurable Ti^{4+} concentration, therefore, the concentrations of these vacancies exceeds by orders of magnitude the concentration of thermally induced vacancies. Thus the aliovalent ion can diffuse orders of magnitude faster than isovalent ions.

Ion size, or the effective "radius" of an ion, has a strong effect on the diffusion coefficient. The effective radius (Shannon, 1976) of the Al^{3+} site in corundum is 53 picometers (1 pm = 10^{-12} meters). Be^{2+} on this site, at 45 pm, is much smaller. Mg^{2+} on this site, at 72 pm, is much larger. Ando (1987) determined that the diffusion coefficient of Mg^{2+} in sapphire—at low concentrations and at 1800°C—is about 2.5 × 10^{-10} cm^2/sec. Our estimate of the Be^{2+} diffusion coefficient (see "Beryllium Diffusion into Corundum: Process and Results" section) at the same temperature, based on the depth of the color boundary, is roughly 10^{-7} cm^2/sec—400 times greater than that of Mg^{2+}. Recently there has been concern in the gemological community about the possibility that boron or lithium might be diffused into sapphire (see, e.g., Shor, 2003). Diffusion coefficients for B^{3+} and Li^{+} in corundum have not been measured, but boron is both isovalent and very small (27 pm), so its diffusion coefficient is hard to estimate but is expected to be smaller than that of titanium or magnesium because it is isovalent. Thus Be^{3+} would diffuse much more slowly than Be^{2+}. Lithium is both large (76 pm; very close to the size of Mg^{2+}) and aliovalent and could be expected to diffuse somewhat like magnesium or titanium.

In most diffusion situations, the concentration of the diffusing ion is much higher in the flux or other carrier outside the crystal, than just inside the crystal. The concentration just inside the crystal is not determined by the concentration outside, but by the solubility of the foreign ion in corundum. The solubility of foreign ions in corundum also increases with temperature. Solubilities vary widely; for example, at 1750°C, titanium solubility is a several hundred ppma while that of beryllium is a few tens of ppma.

A good overall reference on diffusion is Borg and Dienes (1988).

REFERENCES

Ando K. (1987) Magnesium-impurity diffusion in Al_2O_3 single crystals. Nonstoichiometric compounds. In C.R.A. Catlow and W.C. Mackrodt, Eds., *Advances in Ceramics*, Vol. 23, American Ceramic Society, Westerville, OH, pp. 149–158.

Beesley C.R. (1982) The alchemy of blue sapphire. *Jewelers' Circular-Keystone*, Vol. 153, No. 8, pp. 102–103.

Beran A. (1991) Trace hydrogen in Verneuil-grown corundum and its colour varieties: An IR spectroscopic study. *European Journal of Mineralogy*, Vol. 3, No. 6, pp. 971–975.

Boiko B.B., Shkadarevich A.P., Zhdanov É.A., Kalosha I., Koptev V.G., Demidovich A.A. (1987) Lasing due to color centers in an Al_2O_3:Mg crystal. *Soviet Journal of Quantum Electronics*, Vol. 17, No. 5, pp. 581–582.

Borg R.J., Dienes G.J. (1988) *An Introduction to Solid State Diffusion*. Academic Press, San Diego, CA, 360 pp.

Bube R.H. (1992) *Electrons in Solids*, 3rd ed. Academic Press, San Diego, CA, 329 pp.

Burns R.G. (1981) Intervalence transitions in mixed-valence minerals of iron and titanium. *Annual Review of Earth and Planetary Sciences*, Vol. 9, pp. 345–383.

Burns R.G. (1993) *Mineralogical Applications of Crystal Field Theory*. Cambridge University Press, Cambridge, UK.

Butterman W.C., Foster W.R. (1967) Zircon stability and the ZrO_2-SiO_2 phase diagram. *American Mineralogist*, Vol. 52, No. 5/6, pp. 880–885.

Carr R.R., Nisevich S.D. (1975) *Altering the appearance of sapphire crystals*. U.S. patent 3,897,529, issued July 29.

Carr R.R., Nisevich S.D. (1976) *Altering the appearance of corundum crystals*. U.S. patent 3,950,596, issued April 13.

Carr R.R., Nisevich S.D. (1977) *Altering the appearance of corundum crystals*. U.S. patent 4,039,726, issued August 2.

CGA (2003) Chanthaburi gem traders and heaters agree to disclose beryllium treatment, CGA Press Release, February 20.

Chiang Y.-M., Birnie D.P. III, Kingery W.D. (1997) *Physical Ceramics*. John Wiley & Sons, New York, 522 pp.

Coldham T. (2002) Orange sapphires or just lemons? *Australian Gemmologist*, Vol. 22, No. 7, pp. 288–293.

Crowningshield R. (1966) Developments and highlights at GIA's Lab in New York: Unusual items encountered. *Gems & Gemology*, Vol. 12, No. 3, p. 73.

Crowningshield G.R. (1970) Developments and highlights at GIA's Lab in New York: Unusual fluorescence [sapphire with unusual fluorescence]. *Gems & Gemology*, Vol. 13, No. 4, pp. 120–122.

Crowningshield R. (1979) Developments and highlights at GIA's Lab in New York: Treated blue sapphires. *Gems & Gemology*, Vol. 16, No. 5, p. 147.

Crowningshield R., Nassau K. (1981) The heat and diffusion treatment of natural and synthetic sapphires. *Journal of Gemmology*, Vol. 17, No. 8, pp. 528–541.

Dodd D.M., Wood D.L., Barns R.L. (1964) Spectrophotometric determination of chromium concentration in ruby. *Journal of Applied Physics*, Vol. 35, No. 4, pp. 1183–1186.

Dutt B.V., Kröger F.A. (1975) High-temperature defect structure of iron-doped α-Alumina. *Journal of the American Ceramic Society*, Vol. 58, No. 11/12, pp. 474–476.

Eigenmann K., Kurtz K., Günthard H.H. (1972) The optical spectrum of α-Al_2O_3:Fe^{3+}. *Chemical Physics Letters*, Vol. 13, No. 1, pp. 54–57.

El-Aiat M.M., Kröger F.A. (1982) Hydrogen donors in α-Al_2O_3. *Journal of Applied Physics*, Vol. 53, No. 5, pp. 3658–3667.

Emmett J.L., Douthit T.R. (1993) Heat treating the sapphires of Rock Creek, Montana. *Gems & Gemology*, Vol. 29, No. 4, pp. 250–272.

Emmett J.L. (1999) Fluxes and the heat treatment of ruby and sapphire. *Gems & Gemology*, Vol. 35, No. 3, pp. 90–92.

Emmett J.L., Douthit T.R. (2002a) Beryllium diffusion coloration of sapphire: A summary of ongoing experiments. American Gem Trade Association, http://agta.org/consumer/gtclab/treated-sapps04.htm.

Emmett J.L., Douthit T.R. (2002b) Understanding the new treated pink-orange sapphires. Pala International, http://palagems.com/treated_sapphire_emmett.htm.

Ferguson J., Fielding P.E. (1971) The origins of the colours of yellow, green and blue sapphires. *Chemical Physics Letters*, Vol. 10, No. 3, pp. 262–265.

Ferguson J., Fielding P.E. (1972) The origins of the colours of natural yellow, blue, and green sapphires. *Australian Journal of Chemistry*, Vol. 25, pp. 1371–85.

Fritsch E., Chalain J.-P., Hänni H., Devouard B., Chazot G., Giuliani G., Schwarz D., Rollion-Bard C., Garnier V., Barda S., Ohnenstetter D., Notari F., Maitrallet P. (2003) Le nouveau traitement produisant des couleurs orange à jaune dans les saphirs (French with English abstract). *Revue de Gemmologie*, No. 147, pp. 11–23.

Fritsch E., Rossman G.R. (1987) An update on color in gems. Part 1: Introduction and colors caused by dispersed metal ions. *Gems & Gemology*, Vol. 23, No. 3, pp. 126–139.

Fritsch E., Rossman G.R. (1988) An update on color in gems. Part 2: Colors involving multiple atoms and color centers. *Gems & Gemology*, Vol. 24, No. 1, pp. 3–15.

GIT (2002) GIT information on heat-enhanced orange-pink (padparadscha-like) sapphires from Madagascar. Gem and Jewelry Institute of Thailand, http://www.git.or.th (document no longer available online; hard copy on file with authors).

Glass filled rubies increasing (1994) *Jewellery News Asia*, No. 119, pp. 66–70.

Glass filling in ruby from Burma (1994) *Indian Gemmologist*, Vol. 4, No. 1, pp. 1, 24.

Häger T. (1992) Farbgebende und "farbhemmende" Spurenelemente in blauen Saphiren. *Berichte der Deutschen Mineralogischen Gesellschaft, Beihefte zum European Journal of Mineralogy*, Vol. 4, p. 109.

Häger T. (1993) Stabilisierung der Farbzentren von gelben natürlichen Saphiren. *Berichte der Deutschen Mineralogischen Gesellschaft, Beihefte zum European Journal of Mineralogy*, Vol. 5, p. 188.

Häger T. (1996) *Farbrelevante Wechselwirkungen von Spurenelementen in Korund*. Dissertation, Universität Mainz, Mainz, Germany.

Häger T. (2001) High temperature treatment of natural corundum. *International Workshop on Material Characterization by Solid State Spectroscopy: The Minerals of Vietnam*, April 4–10, Institute of Materials Science, Hanoi.

Hänni H.A. (2001) Beobachtungen an hitzesehandeltem Rubin mit künstlicher Rissheilung. *Zeitschrift der Deutschen Gemmologischen Gesellschaft*, Vol. 50, No. 3, pp. 123–136.

Hänni H.A. (2002) Orange treated sapphire—towards finding a name for a new product. *Journal of the Gemmological Association of Hong Kong*, Vol. 23, pp. 23–28.

Hänni H.A., Pettke T. (2002) Eine neue Diffusionsbehandlung liefert orangefarbene und gelbe Saphire. *Zeitschrift der Deutschen Gemmologischen Gesellschaft*, Vol. 51, No. 4, pp. 137–152.

Hervig R.L. (2002) Beryllium analysis by secondary ion mass spectrometry. In E.S. Grew, Ed., *Beryllium: Mineralogy, Petrology, and Geochemistry, Reviews in Mineralogy and Geochemistry*, Vol. 50, Mineralogical Society of America, Washington, DC, pp. 319–332.

Hughes R.W. (1987) Glass infilling of cracks in ruby. *ICA Lab Alert*, Vol. 4, p. 1.

Hughes R.W. (1988) Identifying yellow sapphires—two important techniques. *Journal of Gemmology*, Vol. 21, No. 1, pp. 23–25.

Hughes R.W. (1991a) Thailand taking the heat. *JewelSiam*, Vol. 2, No. 2, pp. 42–48.

Hughes R.W. (1991b) There's a rumble in the jungle—The sapphire facelift face-off. *Gemological Digest*, Vol. 3, No. 2, pp. 17–31.

Hughes R.W. (1997) *Ruby & Sapphire*. RWH Publishing, Boulder, CO, 511 pp.

Hughes R.W. (2002) The skin game: Orange sapphire treatment raises controversy. *The Guide*, Vol. 21, No. 2, pp. 3–7.

Kane R.E. (1984) Natural rubies with glass-filled cavities. *Gems & Gemology*, Vol. 20, No. 4, pp. 187–199.

Kane R.E., Kammerling R.C., Koivula J.I., Shigley J.E., Fritsch E. (1990) The identification of blue diffusion-treated sapphires. *Gems & Gemology*, Vol. 26, No. 2, pp. 115–133.

Keller P.C. (1982) The Chanthaburi-Trat gem field, Thailand. *Gems & Gemology*, Vol. 18, No. 4, pp. 186–196.

Khattak C.P., Schmid F. (1984) Growth of large-diameter crystals by heat exchanger method for optical and laser applications. In S. Musikant, Ed., *Proceedings of the SPIE Conference on Advances in Optical Materials*, 260 pp.

Khattak C.P., Scoville A.N., Schmid F. (1986) Recent developments in sapphire growth by heat exchanger method (HEM). In R.W. Schwartz, Ed., *Proceedings of the SPIE Conference on Infrared and Optical Transmitting Materials*, 181 pp.

Kingery W.D., Bowen H.K., Uhlmann D.R. (1976) *Introduction to Ceramics*. John Wiley & Sons, New York, 1032 pp.
Kizilyalli M., Corish J., Metselaar R. (1999) Definitions of terms for diffusion in the solid state. *Pure and Applied Chemistry*, Vol. 71, No. 7, pp. 1307–1325.
Koivula J.I. (1987) Internal diffusion. *Journal of Gemmology*, Vol. 20, No. 7/8, pp. 474–477.
Koripella C.R., Kröger F.A. (1986) Electrical conductivity of Al_2O_3: Fe + Y. *Journal of the American Ceramic Society*, Vol. 69, No. 12, pp. 888–896.
Krebs J.J., Maisch W.G. (1971) Exchange effects in the optical-absorption spectrum of Fe^{3+} in Al_2O_3. *Physical Review B*, Vol. 4, No. 3, pp. 757–769.
Kröger F.A. (1974) *The Chemistry of Imperfect Crystals*. North-Holland Publishing Co., Amsterdam, The Netherlands, 988 pp.
Kröger F.A. (1984) Defect related properties of doped alumina. *Solid State Ionics*, Vol. 12, pp. 189–199.
Kvapil J., Perner B., Sulovsky J., Kvapil J. (1973) Colour centre formation in corundum doped with divalent ions. *Kristall und Technik*, Vol. 8, No. 1/3, pp. 247–251.
Lee C.H., Kröger F.A. (1985) Electrical conductivity of polycrystalline Al_2O_3 doped with silicon. *Journal of the American Ceramic Society*, Vol. 68, No. 2, pp. 92–99.
Leta D.P., Morrison G.H. (1980) Ion implantation for in-situ quantitative ion microprobe analysis. *Analytical Chemistry*, Vol. 52, pp. 277–280.
McClure D.S. (1962) Optical spectra of transition-metal ions in corundum. *Journal of Chemical Physics*, Vol. 36, No. 10, pp. 2757–2779.
McClure S.F. (2002a) Gem Trade Lab Notes: Bulk-diffusion treated sapphire with synthetic overgrowth. *Gems & Gemology*, Vol. 38, No. 3, pp. 255–256.
McClure S.F. (2002b) Swarovski scientists identify possible source of beryllium in new treated sapphires. *GIA Insider*, May 3, 2002, http://www.gia.edu/newsroom/issue/2798/1046/insider_newsletter_details.cfm#3.
McClure S.F., Kammerling R.C., Fritsch E. (1993) Update on diffusion-treated corundum: Red and other colors. *Gems & Gemology*, Vol. 29, No. 1, pp. 16–28.
McClure S.F., Moses T., Wang W., Hall M., Koivula J.I. (2002) Gem News International: A new corundum treatment from Thailand. *Gems & Gemology*, Vol. 38, No. 1, pp. 86–90.
Mohapatra S.K., Kröger F.A. (1977) Defect structure of α-Al_2O_3 doped with magnesium. *Journal of the American Ceramic Society*, Vol. 60, No. 3/4, pp. 141–148.
Moon A.R., Phillips M.R. (1994) Defect clustering and color in Fe, Ti: α-Al_2O_3. *Journal of the American Ceramic Society*, Vol. 77, No. 2, pp. 356–357.
Moses T.M., Hall M., Wang W. (2002) Gem Trade Lab Notes: More bulk diffusion—rubies and orange sapphires. *Gems & Gemology*, Vol. 38, No. 4, pp. 342–344.
Nassau K. (1980) *Gems Made by Man*. Chilton Book Co., Radnor, PA.
Nassau K. (1983) *The Physics and Chemistry of Color*. John Wiley & Sons, New York, 454 pp.
Nelson D.F., Sturge M.D. (1965) Relation between absorption and emission in the region of the R lines of ruby. *Physical Review*, Vol. 137, No. 4A, pp. 1117–1130.
Pauling L. (1956) *General Chemistry*. W. H. Freeman and Co., San Francisco, CA, 710 pp.
Peretti A., Günther D. (2002) The color enhancement of fancy sapphires with a new heat-treatment technique (Part A). *Contributions to Gemology*, Vol. 1, pp. 1–48.
Pisutha-Arnond V., Häger T., Wathanakul P., Atichat W. (2002) Lab News: A brief summary on a cause of colour in pink-orange, orange and yellow sapphires produced by the new heating technique. Gem and Jewelry Institute of Thailand Gem Testing Lab, http://www.git.or.th/eng/eng_lab/eng_lab_news/eng_news_on_22_november_2002.htm.
Proust M.A. (2002) New sapphire treatment still a mystery. *Colored Stone*, Vol. 15, No. 2, pp. 12–13.
Qi L., Yuan X., Lin S., Wang Z. (2002) Colouring mechanism of high-temperature heat-treated orange sapphire in Madagascar [in Chinese]. *Journal of Gems & Gemology*, Vol. 4, No. 4, pp. 1–5.
Ramírez R., Tardío M., González R., Kokta M.R., Chen Y. (2001) Electroluminescence in magnesium-doped Al_2O_3 crystals. *Radiation Effects & Defects in Solids*, Vol. 154, pp. 295–299.
Rankin A., Edwards W. (2003) Some effects of extreme heat treatment on zircon inclusions in corundum. *Journal of Gemmology*, Vol. 28, No. 5, pp. 257–264.
Robinson N.L. (1995) Thais get burned by glass fillings. *Colored Stone*, Vol. 8, No. 4, pp. 1, 6.
Rossman G.R. (1988) Vibrational spectroscopy of hydrous components. In Hawthorne F.C., Ed., *Spectroscopic Methods in Mineralogy*, *Reviews in Mineralogy*, Vol. 18, Mineralogical Society of America, Washington, DC, pp. 193–206.
Scarratt K. (1983) Notes from the Laboratory: Diffusion treated corundum. *Journal of Gemmology*, Vol. 18, No. 6, pp. 523–530.
Scarratt K. (1988) Notes from the laboratory: Glass filled feathers and cavities in ruby. *Journal of Gemmology*, Vol. 21, No. 3, pp. 131–139.
Scarratt K. (2000) Gem News: Heat-treated rubies: Glass or not glass? *Gems & Gemology*, Vol. 36, No. 1, pp. 75–76.
Scarratt K. (2002a) Is it pink or is it padparadscha? *Rapaport Diamond Report*, Vol. 25, No. 5, pp. 103, 105, 109.
Scarratt K. (2002b) Orange-pink sapphire alert. American Gem Trade Association, http://www.agta.org/consumer/gtclab/orangesapphirealert.htm.
Scarratt K., Harding R.R. (1984) Glass infilling of cavities in natural ruby. *Journal of Gemmology*, Vol. 19, No. 4, pp. 293–297.
Scarratt K., Harding R.R., Din V.K. (1986) Glass fillings in sapphire. *Journal of Gemmology*, Vol. 20, No. 4, pp. 203–207.
Schmetzer K. (1981) The colour of natural corundum. *Neues Jahrbuch für Mineralogie, Monatshefte*, No. 2, pp. 59–68.
Schmetzer K. (1999) Ruby and variously colored sapphires from Ilakaka. *Australian Gemmologist*, Vol. 20, No. 7, pp. 82–84.
Schmetzer K., Bosshart G., Hänni H.A. (1983) Naturally-coloured and treated yellow and orange-brown sapphires. *Journal of Gemmology*, Vol. 18, No. 7, pp. 607–622.
Shannon R.D. (1976) Revised effective ionic radii and systematic studies of interatomic distances in halides and chalcogenides. *Acta Crystallographica*, Vol. A32, pp. 751–767.
Shor R. (2003) Gem News International: AGTA corundum panel. *Gems & Gemology*, Vol. 39, No. 1, pp. 58–59.
Smith C.P. (1995) A contribution to understanding the infrared spectra of rubies from Mong Hsu, Myanmar. *Journal of Gemmology*, Vol. 24, No. 5, pp. 321–335.
Smith G., Strens R.G.J. (1976) Intervalence-transfer absorption in some silicate, oxide and phosphate minerals. In R.G.J. Strens, Ed., *Physical Chemistry of Rocks & Minerals*, John Wiley & Sons, New York, pp. 584–612.
Smyth D.M. (2000) *The Defect Chemistry of Metal Oxides*. Oxford University Press, New York.
Tardío M., Ramírez R., González R., Chen Y., Kokta M.R. (2001a) Electrical conductivity in magnesium-doped Al_2O_3 crystals at moderate temperatures. *Radiation Effects & Defects in Solids*, Vol. 155, pp. 409–413.
Tardío M., Ramírez R., González R., Chen Y., Kokta M.R. (2001b) Enhancement of electrical conductivity in α-Al_2O_3 crystals doped with magnesium. *Journal of Applied Physics*, Vol. 90, No. 8, pp. 3942–3951.
Tardío M., Ramírez R., González R., Chen Y., Kokta M.R. (2001c) High temperature semiconducting characteristics of magnesium-doped α-Al_2O_3 single crystals. *Applied Physics Letters*, Vol. 79, No. 2, pp. 206–208.
Thailand stands by thermal enhancement claim (2002) *Jewellery News Asia*, No. 220, pp. 80–90.
Themelis T. (1992) *The Heat Treatment of Ruby and Sapphire*. Gemlab Inc., Clearwater, FL, 236 pp.
Themelis T. (2003) *Beryllium-Treated Rubies & Sapphires*. Ted Themelis, Bangkok, Thailand, 48 pp.
Townsend M.G. (1968) Visible charge transfer band in blue sapphire. *Solid State Communications*, Vol. 6, pp. 81–83.
Treated Songea sapphires hit the market (2002) *Jewellery News Asia*, No. 209, p. 62.
Wang H.A., Lee C.H., Kröger F.A., Cox R.T. (1983) Point defects in α-Al_2O_3:Mg studied by electrical conductivity, optical absorption, and ESR. *Physical Review B*, Vol. 27, No. 6, pp. 3821–3841.
Wang W., Green B. (2002a) Gem News International: Update on Be-diffused corundum. *Gems & Gemology*, Vol. 38, No. 4, pp. 363–364.
Wang W., Green B. (2002b) An update on treated natural corundum. *GIA Insider*, December 20, 2002, http://www.gia.edu/newsroom/issue/2798/1482/insider_newsletter_details.cfm#2.
Weldon R. (2002) Corundum conundrum. *Professional Jeweler*, Vol. 5, No. 3, pp. 36–37.

AN IMPORTANT EXHIBITION OF SEVEN RARE GEM DIAMONDS

John M. King and James E. Shigley

From late June to mid-September 2003, seven important gem diamonds went on temporary public display at the Smithsonian Institution in Washington, DC, in an exhibit titled "The Splendor of Diamonds." These diamonds, one colorless and six colored, are some of the rarest in the world: the 203.04 ct D-color De Beers Millennium Star, the 101.29 ct Fancy Vivid yellow Allnatt, the 59.60 ct Fancy Vivid pink Steinmetz Pink, the 27.64 ct Fancy Vivid blue Heart of Eternity, the 5.54 ct Fancy Vivid orange Pumpkin, the 5.51 ct Fancy Deep blue-green Ocean Dream, and the 5.11 ct Fancy red Moussaieff Red. This article provides background information on these spectacular diamonds and a record of some of the gemological observations obtained during their quality grading by GIA.

From June 27 through September 15, 2003, "The Splendor of Diamonds," a collection of unique gem diamonds, is on temporary display at the National Museum of Natural History (NMNH) at the Smithsonian Institution in Washington, DC (see figure 1). This museum is the home of the U.S. national gemstone collection, and is where the famous 45.52 ct blue Hope diamond has resided since its donation by Harry Winston in 1958. Since its renovation in 1997, the Harry Winston Gallery in the Janet Annenberg Hooker Hall of Geology, Gems, and Minerals has been one of the most popular sites in the museum. Typically around two to three million people visit this hall every summer (J. E. Post, pers. comm., 2003).

On only one other occasion has another important diamond been displayed in the same room; this was the historic 41 ct Dresden green diamond, which was exhibited on a rare loan from the Green Vaults in Dresden, Germany, in October 2000 ("Harry Winston . . .," 2000). The exhibition of these seven diamonds in the same setting attests to the rarity of this special collection. "The Splendor of Diamonds" at the NMNH includes the 203.04 ct colorless De Beers Millennium Star as well as six exceptional diamonds that represent some of the rarest of naturally occurring colors. On the initiative of GIA representatives and with the sponsorship of the Steinmetz Group, the seven diamonds were brought together from private collections throughout the world. Each is unique in its combination of size, color, and quality.

Over the years, GIA staff members have examined many important gemstones as part of our laboratory grading services and for research purposes. These opportunities have allowed us to characterize and document the gemological properties of a number of unique diamonds in public and private collections that would otherwise not be available for gemological study. Fryer and Koivula (1986, p. 102), in their account of the examination of four important gemstones on public display for a limited time (the Star of Bombay sapphire, the Portuguese diamond, and the Marie Antoinette diamond earrings), concluded with this statement: "We hope that our examinations will provide a more complete record

See end of article for About the Authors and Acknowledgments.

Authors' note: This article contains a number of photos illustrating subtle distinctions in color. Because of the inherent difficulties of controlling color in printing (as well as the instability of inks over time), the color in an illustration may differ from the actual color of the diamond.

GEMS & GEMOLOGY, Vol. 39, No. 2, pp. 136–143.

Figure 1. This collection of extraordinary gem diamonds is on temporary display at the National Museum of Natural History at the Smithsonian Institution in Washington, DC, during Summer 2003. Counter-clockwise from center, the 203.04 ct De Beers Millennium Star (courtesy of De Beers LV), the 59.60 ct Fancy Vivid pink Steinmetz Pink (courtesy of Steinmetz Group), the 27.64 ct Fancy Vivid blue Heart of Eternity (courtesy of a private collector), the 5.54 ct Fancy Vivid orange Pumpkin (courtesy of Harry Winston Inc.), the 5.11 ct Fancy red Moussaieff Red (courtesy of House of Moussaieff), the 5.51 ct Fancy Deep blue-green Ocean Dream (courtesy of Cora Diamond Corp.), and the 101.29 ct Fancy Vivid yellow Allnatt (courtesy of SIBA Corp.). Photo by Chip Clark, courtesy of the Smithsonian Institution.

on these stones for future researchers, and that the opportunity will become available to provide similar reports on other named pieces as we seek to learn more about these touchstones of gemology." Since then, *Gems & Gemology* has published gemological reports on the Hope Diamond (Crowningshield, 1989), the Dresden Green (Kane et al., 1990), and, most recently, the 128 ct Star of the South (Smith and Bosshart, 2002). The information on the seven diamonds discussed here represents a continuation of this kind of documentation for gemologists and the public.

GIA has issued Diamond Grading or Colored Diamond Grading Reports on all seven of these diamonds. Understanding the importance of the diamonds requires an understanding of their grading, inasmuch as all are extraordinary for their size in their color grades. Colorless to light yellow diamonds are color graded against a set of "master color comparison diamonds," and their color grade is

expressed as a set of letters from "D" to "Z" according to the grading system established by GIA in the early 1950s. For diamonds in the standard colorless to light yellow or brown range, those that are "most colorless" ("D" in the GIA system), like the De Beers Millennium Star, are not common and are typically valued much higher than the next grade.

For colored diamonds, the color grade is by far the most important factor in their value. They are graded using a series of "Fancy" grade terms that refer to a three-dimensional color space. Those diamonds in the "end grades" of Fancy Intense, Fancy Deep, and Fancy Vivid are the most strongly colored and valued. For more information, please see the articles by King et al. (1994, 1998, 2002) which elaborate on GIA's fancy-color diamond grading system.

The following takes a brief look at the known history of each of these special diamonds and summarizes the gemological observations made during grading by GIA.

Figure 2. Shown here is the 777 ct piece of rough from which the 203.04 ct De Beers Millennium Star was cut. Courtesy of Steinmetz Group.

THE DE BEERS MILLENNIUM STAR

In the early 1990s, an unnamed miner in an alluvial digging in the Mbuji-Mayi district of Zaire (now the Democratic Republic of Congo) discovered a 777 ct piece of rough (figure 2), the sixth largest "colorless" gem-quality diamond ever found (Balfour, 2000). De Beers purchased the large crystal fragment on the open market. Following three years of study, planning, and work by the Steinmetz Group on three continents, the original crystal was divided into three parts. The largest diamond cut from this crystal was a 203.04 ct, 54-facet pear-shaped brilliant measuring 50.06 × 36.56 × 18.54 mm. De Beers called it the *De Beers Millennium Star*.

In late 1999, the "De Beers Millennium Jewels" exhibit was unveiled at the Millennium Dome in London. This unique collection of diamonds was assembled to mark the passing of the millennium, an event De Beers had anticipated since purchasing the enormous piece of rough years earlier (Balfour, 2000). The centerpiece of this collection was the De Beers Millennium Star; all would soon be the focus of one the most flamboyant robbery attempts in modern history (see below).

When graded by GIA in 1997, the De Beers Millennium Star was noted to be "D" color and Flawless (no internal or surface clarity characteristics were seen using a binocular microscope and a fully corrected 10× loupe). It exhibits excellent polish and symmetry, and it has no fluorescent reaction when exposed to long-wave ultraviolet (UV) radiation. Large, colorless rough crystals with few or no mineral inclusions are usually type IIa diamonds (see Fritsch and Scarratt, 1992,

for more information on diamond types); the laboratory confirmed that the De Beers Millennium Star is a type IIa.

THE ALLNATT

This strongly colored yellow diamond is thought to have originated from the De Beers mine in South Africa, which produced a number of large yellow diamond crystals during its early years of production (Balfour, 2000). It is named for its former owner, Major Alfred Ernest Allnatt, a British soldier, sportsman, art patron, and noted philanthropist who purchased the diamond in the early 1950s.

Originally the Allnatt weighed 102.07 ct and was graded Fancy Intense yellow when it was purchased at the Christie's Geneva May 1996 auction (for a total price of US$3,043,496). Subsequently, the Allnatt was re-cut in a successful attempt to intensify the color appearance. When graded again by GIA in 2000, it weighed 101.29 ct and was classified as Fancy Vivid yellow. The clarity grade was VS_2.

The Allnatt, a type Ia diamond, is a round-cornered square modified brilliant that measures 24.44 × 23.74 × 21.60 mm. Its shape and cutting style are classic examples of those used in the early 20th century to retain maximum weight from well-formed octahedral rough crystals. Its shape is also probably influenced by the fact that its manufacture pre-dates the use of sawing. Therefore, the diamond naturally retains a closer relationship to the shape of the original piece of rough. It has steep crown and pavilion angles and a small table. In the case of this diamond, these proportions act to intensify the color appearance. When examined by GIA, the Allnatt also was noted to have good polish and good symmetry. When exposed to UV radiation, it exhibited weak blue long-wave fluorescence, and weak orangy yellow short-wave fluorescence, both common reactions in many yellow diamonds (Moses, 1997).

Yellow color in diamond may result from the presence of small amounts of nitrogen occurring either as single atoms or as aggregates of a few atoms at carbon sites in the atomic lattice. The cause of the strong yellow color in this diamond is due to aggregated nitrogen in triples (clusters of three atoms, called the *N3 center*), which is known in traditional gemological terminology as the "cape" absorption series (*GIA Diamond Dictionary*, 1993). Among colored diamonds, yellow and brown are the most common colors, but natural-color diamonds of this size with this strength of yellow are extremely rare. This is one of the largest strongly colored yellow diamonds ever seen in the GIA Gem Laboratory.

THE STEINMETZ PINK

Both intriguing and highly valued, pink diamonds have been treasured for many hundreds of years. Adding to this allure are the few famous pink diamonds with rich histories—such as the approximately 60 ct Nur-Ul-Ain, plundered from Delhi in 1739; the 28.15 ct Agra, believed to have belonged to the first Mogul Emperor Babur in the 15th century; or the 20.53 ct Hortensia, stolen from the French Royal Treasury during the French Revolution (*GIA Diamond Dictionary*, 1993; Bari and Sautter, 2001; King et al., 2002). Pink diamonds were encountered only sporadically until the discovery of the Argyle mine in the 1980s. While some of the small quantities of Argyle pink diamonds recovered thus far occur in very strong colors, these characteristically type Ia diamonds seldom exceed one carat and are often highly included (Shigley et al., 2001). Type IIa pink diamonds occur in larger sizes, but they are not commonly encountered with strong color (King et al., 2002). Therefore, a saturated-color pink diamond of this size is almost unprecedented.

The approximately 100 ct rough from which the Steinmetz Pink was cut was recovered from a mine in southern Africa (Moody, 2003), and the 59.60 ct oval-shaped mixed cut diamond was cut over a period of almost two years by the Steinmetz Group. It was only revealed to the public—around the neck of model Helena Christensen—in May 2003 at its unveiling in Monaco.

The cause of color in pink (and red) diamonds is what scientists call a *color center*—a microscopic imperfection at the atomic level that, in the case of pink diamonds, is thought to be the result of plastic deformation of the diamond's atomic lattice (Harlow, 1998; King et al., 2002). When graded in 2001 by GIA, the Steinmetz Pink was classified

as Fancy Vivid pink and Internally Flawless. It measures 26.93 × 20.64 × 13.68 mm, and displays very good polish and symmetry. When exposed to long-wave UV, it exhibited weak blue fluorescence and, to short-wave, very weak blue fluorescence. To date, it is the largest Fancy Vivid pink diamond graded by GIA.

THE HEART OF ETERNITY

As part of the Millennium Jewels display at London's Millennium Dome, De Beers also assembled an extraordinary group of 11 blue diamonds, with a total weight of 118 carats, known as the Midnight Collection (Balfour, 2000). Like the majority of blue diamonds in recent times, all of these blues were recovered from the Premier mine in South Africa; all 11 were also manufactured by the Steinmetz Group (see figure 3). The largest diamond in this collection was the 27.64 ct Fancy Vivid blue Heart of Eternity (Balfour, 2000).

Despite the enormous security surrounding these diamonds (including a special reinforced concrete viewing vault and 24-hour remote surveillance), this priceless display proved to be too great a temptation to a gang of jewel thieves. On the morning of November 7, 2000, in a scene reminiscent of a James Bond movie, the gang crashed a stolen earthmover into the Millennium Dome, through the outer security and up to the vault, lobbing smoke bombs and firing nail guns as they went. They planned to seize the diamonds and escape in a waiting speedboat down the Thames River. Fortunately for De Beers, Scotland Yard had learned of the plan months beforehand and surrounded the Millennium Jewels display with more than 100 elite undercover officers on the morning of the attempted robbery. When the gang entered the vault, they were trapped and swiftly arrested; the diamonds themselves had previously been replaced with replicas. The would-be thieves received sentences ranging from five to 18 years in prison (see Hopkins and Branigan, 2000; "Gang . . . ," 2001; Branigan, 2002).

Figure 3. Shown here with several other rough crystals is the sawn rough from which the Heart of Eternity was cut (second from left). Photo by John King.

The Heart of Eternity diamond was graded by GIA in 1999. It is the largest Fancy Vivid blue diamond GIA has graded to date. Blue diamonds such as the Heart of Eternity are very rare in nature (King et al., 1998); those with a very strong color such as this one are even more so.

The Heart of Eternity is cut as a heart-shaped modified brilliant measuring 19.25 × 21.76 × 11.43 mm. It exhibits very good polish and good symmetry. When exposed to ultraviolet radiation, it was inert to long-wave UV, but very weak red to short-wave UV. Similar to the Hope diamond (Crowningshield, 1989), when the exposure to short-wave UV was discontinued, the diamond continued to emit strong red phosphorescence lasting for approximately 15 seconds. When examined with magnification, it exhibited small included crystals, pinpoint inclusions, and internal graining. Its clarity grade is VS_2. Color zoning was also observed, appearing as narrow parallel bands of colorless and blue areas. Strategically locating color zoning during the manufacturing process is important to obtain the most saturated, even, face-up color appearance; this was done quite successfully in the Heart of Eternity. As is typical of natural-color type IIb blue diamonds, the Heart of Eternity is electrically conductive. This behavior is the result of small amounts of boron in the diamond's atomic structure, which substitutes for carbon, giving rise to the blue color as well as the conductivity.

In addition to the rare assemblage of the seven diamonds in this exhibition, "The Splendor of Diamonds" also offers an extraordinary opportunity to see three large, strongly colored blue diamonds in close proximity. In the same gallery, the famous Hope (its color grade updated in 1996) is a Fancy Deep grayish blue; nearby in the gem collection is

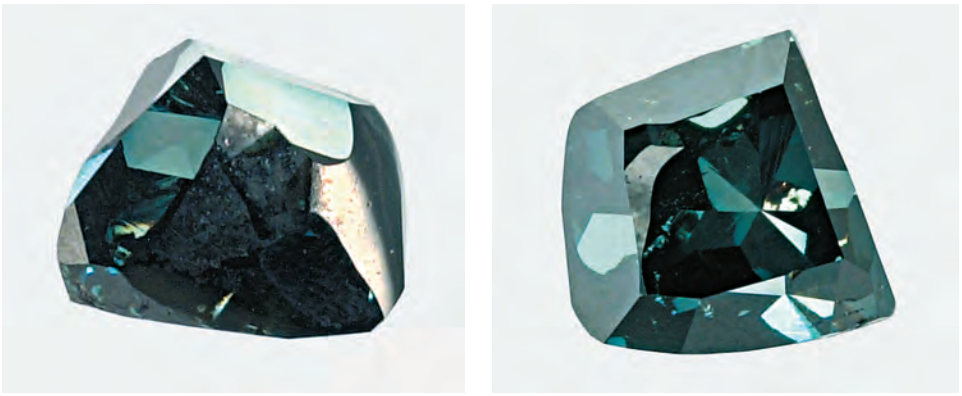

Figure 4. Shown here are two preform stages in the cutting of the 11.17 ct rough from which the 5.51 ct Fancy Deep blue-green Ocean Dream was fashioned. Photo by Elizabeth Schrader.

the 30.62 ct Blue Heart, which was graded Fancy Deep blue (King et al., 1998). While all are of relatively similar tone, subtle differences in saturation account for the differences in color grade.

THE PUMPKIN DIAMOND

Diamonds in the orange hue range are typically dark toned and weak to moderate in saturation. This generally results in a brown or brownish color appearance; an unmodified orange appearance is extremely rare (King and Moses, 1997). Many diamonds in the orange hue range are type Ib, but the Pumpkin was found to be type IIa (King and Moses, 1997).

The Pumpkin diamond was discovered in South Africa in the mid-1990s, and the rough is reported to have appeared predominantly brown with only a hint of orange (W. Goldberg, pers. comm., 1997). After cutting, however, this 5.54 ct gemstone displayed a pure, strongly saturated orange hue. When purchased by Harry Winston Inc. at auction in October 1998, its striking color and the date of the sale—the day before Halloween—led the company to dub it the Pumpkin (Auction report, 1997). It was loaned to actress Halle Berry for the 2002 Academy Awards, the night she won the "Oscar" for Best Actress, the first African-American ever so honored ("The splendor . . . ," 2003).

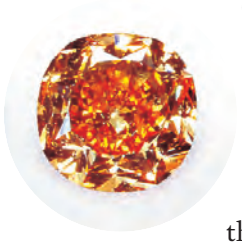

The Pumpkin diamond is fashioned as a cushion-shaped modified brilliant and measures 9.88 × 9.85 × 7.04 mm. The diamond was graded by GIA in 1997 as Fancy Vivid orange. It is one of the largest diamonds of this color ever examined by GIA. As has often been observed in diamonds in this hue range, the Pumpkin diamond displays cloud-like and needle-like inclusions as well as crystals. It exhibits very good polish and good symmetry. When exposed to ultraviolet radiation, the diamond emitted moderate orange fluorescence to long-wave UV, and weak-to-moderate orange fluorescence to short-wave UV. When the UV lamp was turned off, observers noted a weak yellow phosphorescence. Because of the type of reports requested by the clients, clarity grades were not provided for the Pumpkin, Ocean Dream, and Moussaieff Red diamonds.

THE OCEAN DREAM

The 11.17 ct rough from which this diamond was manufactured was recovered in central Africa in 2002. The crystal was polished into a 5.51 ct modified triangular brilliant in New York by Cora Diamond Corp.; it was dubbed the *Ocean Dream* because of its deep, saturated blue-green color.

Because large, natural-color diamonds with this coloration are *extremely* rare, most in the diamond industry associate them with artificial treatment (i.e., irradiation). Not only is such naturally occurring color highly unusual, but it is virtually never seen in diamonds this large.

Natural blue-green to green color in diamonds is the result of exposure to radiation in the earth and the subsequent formation of radiation-induced color centers. In nature, such radiation is typically alpha or beta; the limited penetrating ability of these particles is the reason most rough "green" diamonds have only a thin "skin" of color (Kane et al., 1990). A saturated body color can only be produced by high-energy penetrating radiation such as gamma or neutron, and in nature such sources are very rare, though they are easily produced in a nuclear reactor (Ashbaugh, 1989). Furthermore, these colors tend to be unstable to

heat. For a diamond to acquire a saturated green or blue-green body color in nature, it must remain close to a gamma or neutron source for thousands if not millions of years without being exposed to excessive heat (Ashbaugh, 1989; Kane et al., 1990). It is this very rare set of conditions that makes a diamond like the Ocean Dream almost unique.

Determining the cause of blue-green color—natural or altered—is challenging, as both situations produce similar gemological features (Kane et al., 1990). In addition, important identification criteria may be lost during the process of faceting the diamond, because of the shallowness of the green surface layer typically produced by natural radiation exposure (see Crowningshield, 1963). Determination that the color of the Ocean Dream was natural was aided by numerous examinations of the diamond throughout the cutting process from rough crystal until it was finished (see figure 4). Its origin was confirmed by microscopic examination of gemological features such as color zoning, as well as various spectroscopic results compared to data from smaller blue-green diamonds of known natural color.

When graded by GIA in 2003, this type Ia diamond was classified as Fancy Deep blue-green. It measured 11.49 × 11.47 × 6.47 mm. When exposed to long-wave UV, the Ocean Dream showed a moderate blue reaction. Its reaction to short-wave UV was a weak yellow.

THE MOUSSAIEFF RED

Few gem diamonds that could be described as predominantly red have ever been documented in the jewelry industry. They are so rare that less than two decades ago, Kane (1987) could report that the GIA Gem Laboratory had *never* graded a diamond with an unmodified "red" hue. As recently as 2002, King et al. listed only four Fancy red diamonds in the public domain, one of which was the Moussaieff Red.

Awareness of red diamonds expanded greatly following the 1987 public auction of the 0.95 ct "Hancock Red" (a purplish red stone) for a record $926,316-per-carat price (Kane, 1987). While the Moussaieff Red, a 5.11 ct modified triangular brilliant, may not seem large in comparison to the other gemstones in this collection, for a diamond of this color it is astounding—no other Fancy red diamond reported to date approaches even half its size. To have such a color in a diamond of this size is truly unprecedented. As discussed above and by King et al. (2002), the cause of color in pink and red diamonds is believed to arise from color centers created by plastic deformation.

The Moussaieff Red was fashioned from a 13.90 ct crystal that a Brazilian farmer recovered from an alluvial deposit during the mid-1990s (W. Goldberg, pers. comm., 1997). The finished stone was manufactured by the William Goldberg Diamond Corp. in New York, and measures 11.02 × 10.57 × 6.06 mm. When examined under a UV lamp, it emitted moderate-to-strong blue long-wave UV fluorescence, and weak blue short-wave UV fluorescence. The Moussaieff Red was found to be a type Ia diamond, and at the time of grading in 1997, it was noted to be the largest Fancy red diamond ever documented by GIA.

CONCLUSION

Members of the public have a unique chance to view a collection of superb gem diamonds at the Smithsonian's National Museum of Natural History in Washington, DC, from June 27 through September 15, 2003. The "Splendor of Diamonds" exhibit brings together seven diamonds that are each outstanding examples in terms of their color, quality, and size. Examination of these diamonds allowed GIA to record important information for the science of gemology.

It is difficult to explain to a public audience just how rare the gems in this special collection actually are. In nature, it is challenging for geologists to find diamond-bearing rocks, and all but a few occurrences lack sufficient high-quality diamonds to make them economically feasible to exploit. Even at productive mines, recovery of diamonds is tremendously expensive, and in most instances the number of crystals suitable for manufacturing as gemstones is very limited. Larger diamonds that are completely colorless or highly colored, such as the seven in this exhibit, are so unusual that even the majority of experienced diamond dealers and collectors will never have the chance to handle them. Large colored diamonds with colors like these described in this article are uncommon even for GIA to encounter. For most gemologists, as for members of the public, this is a once-in-a-lifetime opportunity to see and enjoy these "touchstones" of gemology.

ABOUT THE AUTHORS

Mr. King is laboratory projects officer in the GIA Gem Laboratory, New York. Dr. Shigley is director of Research at GIA in Carlsbad, California.

ACKNOWLEDGMENTS: The authors thank Thomas M. Moses, vice president of identification services and research, and Matthew Hall, analytical equipment supervisor at the GIA Gem Trade Laboratory in New York, for their comments. They also thank Nir Livnat of the Steinmetz Group of Companies, Sam Abram of SIBA Corp., Ronald Winston of Harry Winston Inc., Ara Arslanian of Cora Diamond Corp., and Aliza Moussaieff of the House of Moussaieff, for their willingness to share these diamonds with the general public through a museum display and to provide information for this article. William Goldberg of William Goldberg Diamond Corp., New York, kindly provided information on several of these diamonds. The authors also thank Dr. Jeffrey E. Post, curator of Gems and Minerals in the Department of Mineral Sciences of the National Museum of Natural History, Smithsonian Institution, as well as the Smithsonian's management and staff, for their efforts to make this special exhibit possible.

REFERENCES

Ashbaugh C.E. (1989) Gemstone irradiation and radioactivity. *Gems & Gemology*, Vol. 24, No. 4, pp. 196–213.

Auction Report (October Sales) (1997) *The Gemstone Forecaster*, Vol. 15, No. 4, http://www.preciousgemstones.com/gfwin97one.html.

Balfour I. (2000) *Famous Diamonds*. Christie, Manson and Woods, London.

Bari H., Sautter V., Eds. *Diamonds* (2001) Translated by M. Hing, Vilo International, Paris.

Branigan T. (2002) Gang in £200m dome diamond raid sent to jail. *Guardian Unlimited*, February 19, http://www.guardian.co.uk/dome/article/0,2763,652620,00.html.

Crowningshield R. (1963) Naturals prove color origin. *Gems & Gemology*, Vol. 11, No. 4, p. 104.

Crowningshield G.R. (1989) Grading the Hope diamond. *Gems & Gemology*, Vol. 25, No. 2, pp. 91–94.

Fritsch, E., Scarratt K. (1992) Natural-color nonconductive gray-to-blue diamonds. *Gems & Gemology*, Vol. 28, No. 1, pp. 35–42.

Fryer C.W., Koivula J.I. (1986) An examination of four important gems. *Gems & Gemology*, Vol. 22, No. 2, pp. 99–102.

Gang "planned robbery of the millennium" (2001) *Guardian Unlimited*, November 9, http://www.guardian.co.uk/dome/article/0,2763,590866,00.html.

GIA Diamond Dictionary (1993) Gemological Institute of America, Santa Monica, CA.

Harlow G., Ed. (1998) *The Nature of Diamonds*. Cambridge University Press, Cambridge, UK.

Harry Winston to unite Dresden Green diamond with historic Hope diamond for the first time ever (2000) Press release, June 20, http://harry-winston.com/greendiamond.html.

Hopkins N., Branigan T. (2000) The great dome robbery. *Guardian Unlimited*, November 7, http://www.guardian.co.uk/dome/article/0,2763,394291,00.html.

Kane R.E. (1987) Three notable fancy-color diamonds: Purplish red, purple-pink, and reddish purple. *Gems & Gemology*, Vol. 23, No. 2, pp. 90–95.

Kane R.E., McClure S.F., Menzhausen J. (1990) The legendary Dresden Green diamond. *Gems & Gemology*, Vol. 26, No. 4, pp. 248–266.

King J., Moses T. (1997) GTLN: Rare Fancy Vivid orange [diamond]. *Gems & Gemology*, Vol. 33. No. 3, p. 213.

King J.M., Moses T.M., Shigley J.E., Liu Y. (1994) Color grading of colored diamonds in the GIA Gem Trade Laboratory. *Gems & Gemology*, Vol. 30, No. 4, pp. 220–242.

King J.M., Moses T.M., Shigley J.S., Welbourn C.M., Lawson S.C., Cooper M. (1998) Characterizing natural-color type IIb blue diamonds. *Gems & Gemology*, Vol. 34, No. 4, pp. 246–268.

King J.M., Shigley J.E., Guhin S.S., Gelb T.H., Hall M. (2002) Characterization and grading of natural-color pink diamonds. *Gems & Gemology*, Vol. 38, No. 2, pp. 128–147.

Moody G. (2003) Mystery of the priceless pink diamond. *Sunday Times* (South Africa), June 15, http://www.sundaytimes.co.za/2003/06/15/news/news13.asp.

Moses T. (1997) GTLN: Two noteworthy stones from the Americas. *Gems & Gemology*, Vol. 33, No. 1, pp. 54–55.

Post J.E. (1997) *The National Gem Collection*. Harry N. Abrams, New York.

Shigley J.E., Chapman J., Ellison R.K. (2001) Discovery and mining of the Argyle diamond deposit, Australia. *Gems & Gemology*, Vol. 37, No. 1, pp. 26–41.

Smith C.P., Bosshart G., (2002) Star of the South: A historic 128 ct diamond. *Gems & Gemology*, Vol. 38, No. 1, pp. 54–64.

The Splendor of Diamonds (2003) Exhibit brochure. National Museum of Natural History, Smithsonian Institution, Washington, DC.

LAB NOTES 2003

EDITORS

Thomas M. Moses, Ilene Reinitz, Shane F. McClure, and Mary L. Johnson
GIA Gem Laboratory

CONTRIBUTING EDITORS

G. Robert Crowningshield
GIA Gem Laboratory, East Coast

Karin N. Hurwit, John I. Koivula, and Cheryl Y. Wentzell
GIA Gem Laboratory, West Coast

CHRYSOBERYL, Non-phenomenal Vanadium-Bearing

Recently, the East Coast laboratory received a 4.29 ct transparent highly saturated green oval mixed-cut stone for identification (figure 1). The client, Atlantic Gem Corp. of New York, believed the stone to be chrysoberyl. Synthetic non-phenomenal chrysoberyl of this color was referenced as early as 1994 (Fall 1994 Gem News, p. 200), and was known to be colored by vanadium by the authors of a Fall 1996 Gem News item (pp. 215–216) prior to their identifying a similarly colored natural material with the same chromophore. We have seen few examples of this natural material in the lab since then.

Standard gemological testing proved that the stone was chrysoberyl, with properties very similar to those of the natural non-phenomenal green chrysoberyls studied in 1996: R.I. = 1.740–1.749; birefringence = 0.009; S.G. (determined hydrostatically) = 3.69; inert to both long- and short-wave UV; strong blue-green/yellow pleochroism; and a 440 nm cutoff in a desk-model spectroscope. The stone's only inclusion was a small, very shallow fracture near the culet. While it did show some straight growth zoning, this was merely an indication of natural origin, not proof.

EDXRF spectroscopy revealed Al, V, Fe, Ga, and Sn, but no Ti or Cr. Previously studied Russian hydrothermal synthetic non-phenomenal chrysoberyl contained significant concentrations of V and Cr, but no appreciable Fe, Ga, or Sn (Fall 1996 Gem News, pp. 215–216); thus, the composition of the present sample is consistent with a natural origin. It is always a pleasure to see a large *natural* stone with such vivid color and high clarity.

Wendi M. Mayerson

Figure 1. This 4.29 ct chrysoberyl gets its highly saturated color from vanadium.

Brown-Yellow DIAMONDS with an "Amber Center" and Pink Lamellae

Color in diamond is caused by defects that have selective absorption within the visible range and/or a tail of an absorption band that extends into the visible range. The ~480 nm band (known as the amber center) commonly causes a pleasing yellow-orange coloration, while the ~550 nm band results in an attractive pink. These broad absorption bands are distinct from many other defects in diamond because of their coupling between electronic and vibrational transitions. This coupling is so strong that the zero-phonon line is too weak to be detected, with the result that the side band broadens into a single band. The East Coast laboratory recently examined two unusual diamonds that displayed not only a strong ~480 nm band, but also pink lamellae that are caused by a ~550 nm band (see E. Fritsch, "The nature of color in diamonds," in G.E. Harlow, Ed., *The Nature of Diamonds*, Cambridge University Press, 1998, pp. 23–47). The color of these stones appeared to be influenced primarily by the amber center, resulting in a less attractive, predominantly brown-yellow bodycolor.

The two diamonds (1.02 and 2.03 ct) were fashioned as marquise brilliants (figure 2). The smaller one (11.24 × 5.28 × 2.99 mm) was graded Fancy Deep brown-yellow, and the larger (14.98 × 6.16 × 3.75 mm) was graded Fancy Dark brown-yellow.

Editor's note: The initials at the end of each item identify the editor(s) or contributing editor(s) who provided that item. Full names are given for other GIA Gem Laboratory contributors.

Gems & Gemology, Vol. 39, No.2, pp. 144–151

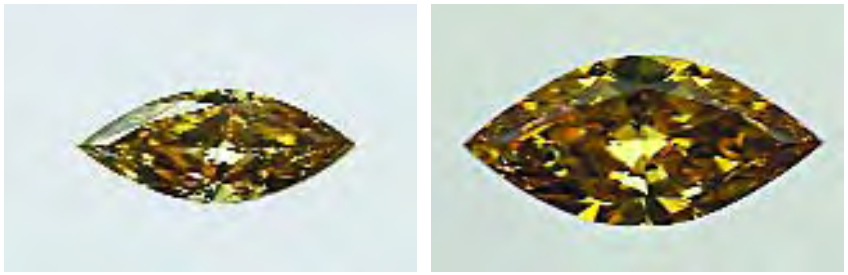

Figure 2. These two natural-color brown-yellow diamonds (1.02 and 2.03 ct) have an unusual combination of defects.

Both were type IaA, with relatively low concentrations of nitrogen and moderately high levels of hydrogen impurities. The smaller diamond showed a moderately chalky, strong orangy yellow fluorescence to long-wave ultraviolet radiation, and moderate yellow fluorescence and phosphorescence (lasting for more than 30 seconds) to short-wave UV. The same fluorescence and phosphorescence features were also observed in the larger diamond, except for small portions that showed a blue reaction to long-wave UV. We did not observe any mineral inclusions with the gemological microscope. An outstanding feature of the larger diamond was the presence of strong parallel pink lamellae in about half the stone (figure 3). Weak pink lamellae were seen at one tip of the smaller stone. Most of these gemological features are comparable to natural yellow-orange diamonds that have an amber center, and the blue fluorescence to long-wave UV is common in pink diamonds.

UV-Vis spectroscopy of both diamonds showed two strong, broad absorption bands at 370 and 480 nm (figure 4). In addition, relatively weak absorption bands at 415 (N3) and 426 nm were also detected. A ~550 nm band related to the pink lamellae is not evident in figure 4, due to overlap with the tail of the 480 nm band. The combination of these individual bands led to a gradual increase in absorption from ~600 nm to the higher energy side, resulting in the brown-yellow coloration.

The defects responsible for the 480 and 550 nm absorption bands are not known. The occurrence of pink lamellae in a yellow stone and also of two vibronic centers without a zero-phonon line within the same diamond is very unusual. There are no reported cases of these absorptions having been created by any sort of treatment in either natural or synthetic diamonds. Based on this and the other gemological and spectroscopic features, the evidence was compelling that the color in these two diamonds was natural.

Wuyi Wang and TMM

Figure 3. The 2.03 ct brown-yellow diamond contained parallel pink lamellae in about half the stone. Magnified 60×.

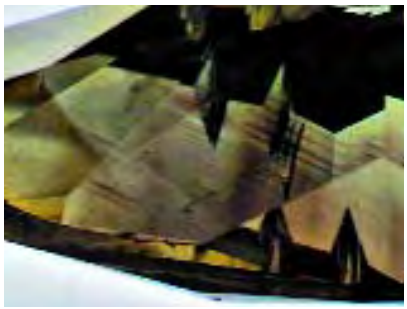

Figure 4. An unusual combination of absorption bands in the UV-Vis region produced the brown-yellow coloration in both the 1.02 and 2.03 ct diamonds. (Incident light passed through girdle of 5.28 mm in maximum dimension.)

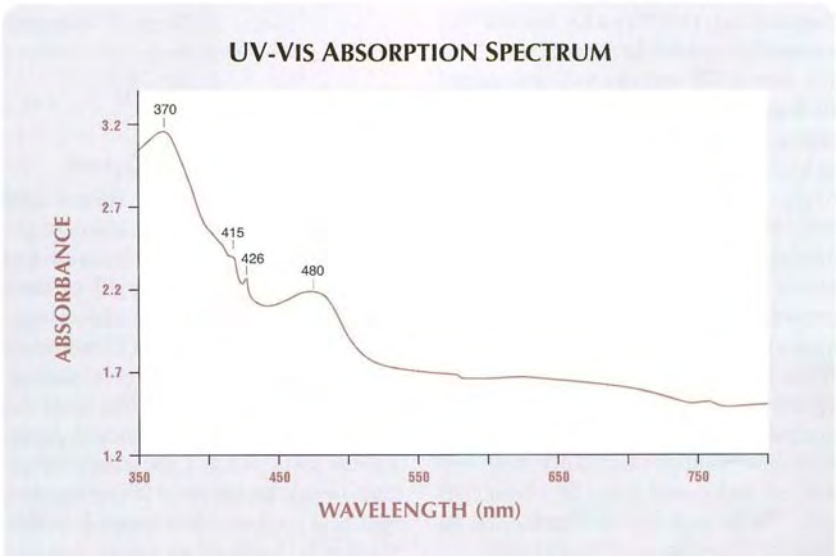

GARNET, Color-Change Grossular-Andradite from Mali

Grossular-andradite garnets from Mali have become a familiar addition to the gem market (see, e.g., M. L. Johnson et al., "Gem-quality grossular-andradite: A new garnet from Mali," Fall 1995 *Gems & Gemology*, pp. 152–166). Recently, the West Coast laboratory received a particularly unusual specimen, with an appearance and color change that mimicked alexandrite from Sri Lanka (described by R. Webster in *Gems*, 5th ed.,

Figure 5. This 1.79 ct grossular-andradite garnet from Mali showed a color change from grayish green in fluorescent light (left) to brown in incandescent light (right).

Butterworth-Heinemann, Oxford, 1994, pp. 137–138). The 1.79 ct (6.78 × 6.72 × 5.20 mm) stone was dark in tone, changing from grayish green in fluorescent light to brown in incandescent light (see figure 5). It was relatively free of inclusions except for three small partially healed fractures that reached the surface in one corner. One of these "fingerprints" had a coarse appearance typical of similar inclusions in alexandrite. Although one might easily confuse this unusual gemstone with its better-known lookalike, the gemological properties readily separated this material from alexandrite and other gems.

The stone was singly refractive, displaying the "snake bands" of anomalous double refraction. The R.I. was 1.770 and the S.G. (measured hydrostatically) was 3.66, both properties that are consistent with other grossular-andradite garnets from Mali. It exhibited yellowish green and brownish green color zones with associated straight, parallel growth zones that, when examined between crossed polarizers, had the layered appearance also typical of garnets from this locality. The absorption spectrum was similar to that of an andradite garnet, with total absorption below approximately 450 nm and an additional band at about 590 nm. There was no luminescence to long- or short-wave UV radiation.

Because this stone was the first of its kind seen in the laboratory, we performed Fourier-transform infrared (FTIR) and Raman spectroscopy to confirm its identity. FTIR revealed a spectrum consistent with other garnets on file. Although color-change garnets are usually of the pyrope-spessartine series (see Fall 1998 Gem News, pp. 222–223), the Raman spectrum was consistent with the spectra of grossular and demantoid (andradite) in our database rather than those of pyrope or spessartine. This, along with the absorption spectrum in the desk-model spectroscope, helped identify this stone as a grossular-andradite. We later learned that the stone was indeed sold to the client as a grossular-andradite garnet from Mali.

Cheryl Y. Wentzell

GLASS

Imitation of Tsavorite Garnet

A few months ago, the West Coast laboratory was asked to identify the attractive green oval mixed cut shown in figure 6. This 12 ct item was remarkably well cut and showed fairly high dispersion. At first glance, it reminded us of the intense yellowish green tsavorite garnets that are mined in East Africa. Standard gemological tests (R.I. = 1.74, singly refractive; weak anomalous birefringence; and S.G. = 3.66, determined hydrostatically) seemed to verify our initial assumption. In addition, the sample did not show any inclusions. All these properties strongly suggested that it was indeed the tsavorite variety of grossular garnet.

However, when viewed with a handheld spectroscope, the sample showed a general absorption around 500 nm, which is not usually seen in tsavorite garnet. It was inert to long-wave ultraviolet radiation, but it fluoresced strong chalky yellow to short-wave UV. This reaction proved that it was not a garnet (garnets are inert to both long- and short-wave UV). Indeed, strong chalky fluorescence to short-wave UV radiation is often a characteristic of manufactured products such as glass. Additional testing was needed.

Senior research associate Sam Muhlmeister performed Raman spectroscopy and EDXRF chemical analysis to further characterize this material. The peaks obtained on the Raman matched those for glass. EDXRF revealed silicon and zirconium as major elements and the following trace elements: zinc, strontium, and the rare-earth elements yttrium and lanthanum. The rare-earth elements were undoubtedly responsible for the green coloration. While we have seen many glass imitations of popular gemstones, such high-property glass is seldom encountered in the laboratory.

KNH

"Planetarium"

Figure 6. Although it appeared at first to be a tsavorite garnet, this 12 ct oval mixed cut proved to be an unusual glass imitation.

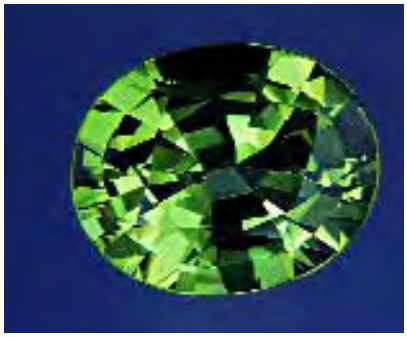

"Planetarium"

Manufactured glass is the oldest and most common of all gem substitutes. Because it has been used in so many decorative ways over the centuries, glass is frequently encountered by gemologists as a gem imitation. However, occasionally some particularly interesting glass items are submitted to the GIA Gem Laboratory, such as the partially devitrified "pupurine" glass cabochon described in the Summer 2000 Lab Notes (pp. 157–158).

Not all manufactured glass "gems" are intended to mimic natural stones; some are fashioned as interesting art objects. Martin Guptill, a Graduate Gemologist and lapidary from Canyon Country, California, recently sent one such piece of faceted glass to the West Coast laboratory for examination.

The item, which weighed 27.73 ct and measured 14.21 x 14.41 x 10.32 mm, was intense yellow and transparent (figure 7). Immediately apparent under the table facet were two spherical inclusions that measured approximately 2.8 and 1.5 mm in diameter.

Standard gemological testing quickly proved that it was glass. The material was over the limits of the refractometer, but its polariscope reaction proved that it was singly refractive. Examination with a desk-model spectroscope using transmitted light showed general absorption in the blue region from approximately 439 nm downward. No other absorption features were present. The specific gravity, determined hydrostatically, was 6.58. The sample was inert to UV radiation.

With magnification, we saw that the positioning of the opaque spherical inclusions resembled a planet with an orbiting moon, giving the overall look of a miniature planetarium. The inclusions had an interesting crenulated surface texture, and appeared to take on the bodycolor of their host, suggesting that they were probably white (figure 8). While the inclusions were too deep to analyze by Raman spectroscopy, Mr. Guptill had submitted some of the original rough glass with the faceted gem; in some areas, a white crystalline crust had formed on the edges as a result of devitrification. The Raman spectrum obtained from this white crust matched that of cristobalite, so it was extrapolated that the inclusions might also be cristobalite.

Figure 7. Two spherical inclusions, a "planet" and its "moon," highlight the interior of this 27.73 ct faceted piece of manufactured glass.

To complete the description of this material, EDXRF analysis was performed by senior research associate Sam Muhlmeister. This analysis showed the presence of silicon together with lead and a minor amount of calcium.

JIK and Maha Tannous

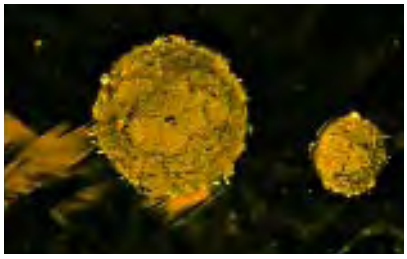

Figure 8. Products of devitrification, the two spherical inclusions in this manufactured glass are most likely cristobalite. Magnified 5x.

inclusions were exposed on the surface and well polished.

With magnification, the reddish brown transparent-to-translucent inclusions showed numerous cracks that appeared to be associated with cleavage planes. The inclusions were relatively large, and because they were not undercut during polishing, we were able to obtain a refractive index reading from them in the range of 1.66–1.68. The inclusions were also inert to both long- and short-wave UV radiation. A small fragment obtained from one of the inclusions yielded a specific gravity by the sink-float method (i.e., in heavy liquids) of approximately 3.1.

Raman analysis of the inclusions gave a strong pattern that could not

GUATEMALAN JADE with Lawsonite Inclusions

A slab of Guatemalan jade was provided to the West Coast laboratory for examination of its interesting "root beer"-colored inclusions, which had yet to be identified. The sample came from Ventana Mining Company in Los Altos, California, through Pala International in Fallbrook, California. To prepare it for examination, Leon Agee of Agee Lapidary in Deer Park, Washington, cut and polished the slab into an 87.84 ct disk that measured 33.19 x 33.80 x 7.24 mm (figure 9). During lapidary preparation, the

Figure 9. This 87.84 ct polished disk of Guatemalan jade contains reddish brown inclusions of lawsonite.

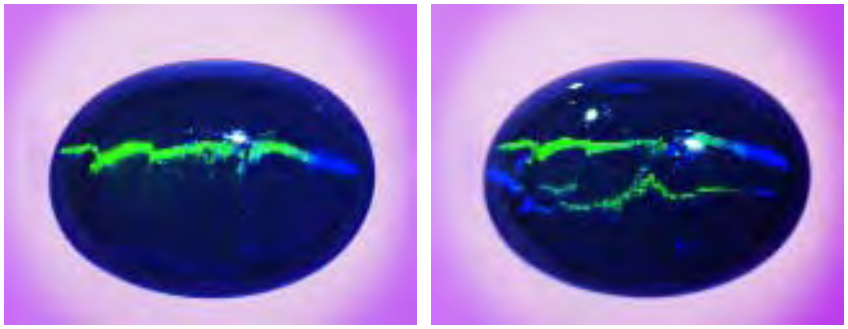

Figure 10. This 0.36 ct black opal cabochon from Virgin Valley, Nevada, shows a distinct play-of-color eye across its dome (left). When a second light source is brought near, two play-of-color bands are clearly visible (right). If the stone is rotated between the lights, the bands will merge together and then split again, so the eye appears to open and close.

diffraction analysis performed by Identification Services manager Dino DeGhionno produced a pattern that matched the mineral lawsonite, an orthorhombic calcium aluminum silicate hydroxide hydrate. The R.I. and S.G. previously obtained also supported this identification. Lawsonite is a metamorphic mineral that is common in low-temperature, high-pressure settings, in which it may be stable with jadeite. It is usually colorless, white to gray, or sometimes pale blue. The reddish brown "root beer" color is unusual. This is the first time we have encountered the mineral lawsonite in any form in the GIA Gem Laboratory.

JIK and Maha Tannous

Chatoyant OPAL with Eye that "Opens and Closes"

While most of the opals seen in the GIA Gem Laboratory show typical play-of-color patterns, on occasion we encounter some atypical examples. One such relatively rare pattern, as reported in the Spring 2003 Lab Notes (pp. 43–44), appeared as a spectral band of chatoyancy across the dome of an otherwise gray opal cabochon. More recently, gem dealer and gemologist Elaine Rohrbach of Pittstown, New Jersey, sent the West Coast laboratory a cat's-eye opal cabochon in which the play-of-color chatoyancy was even more unusual.

This 0.36 ct oval cabochon (6.09 mm long)—from Virgin Valley, Nevada—had an opaque black bodycolor with a bright vitreous luster. Its gemological properties were typical for natural opal. It showed a single, distinct, vibrant, and somewhat jagged thin band of color extending across the length of the dome (figure 10, left). Magnification showed that this band was due to the presence of a very finely layered or lamellar structure. The band was clearly visible in any form of white-light illumination, including fluorescent lighting.

Aside from the rarity of such a stone, its most interesting feature was that the play-of-color eye "opened and closed" when a second light source was brought near and the stone was slowly rotated. This resulted in two chatoyant bands positioned more-or-less parallel to each other (figure 10, right) that would merge into one band, and then split again into two separate bands as the stone was turned between the two light sources.

The opening and closing of the eye in chatoyant gems is a relatively well-known secondary phenomenon in stones where the chatoyancy is caused by parallel bundles of acicular inclusions. However, our literature search could find no prior reference to this phenomenon in other play-of-color cat's-eye opals. Therefore, this appears to be the first report of such an occurrence.

JIK and Maha Tannous

Imitation PEARLS, Variously Colored, with Iridescent Appearance

Recently a friend of the laboratory sent us some variously colored imitation pearls for examination. The dealer was told by his supplier that these imitation pearls were fashioned from crushed mother-of-pearl that had been reconstituted and shaped into large beads up to 15 mm in diameter. Since our client believed that these beads represented a new variety of imitation pearls, he wanted to share this information with us and other interested readers.

Figure 11 shows a uniform strand with 29 imitation pearls in all the colors that reportedly are available: pink, yellow, gray, and purplish brown. All these "pearls" had a high metallic-appearing luster and were approximately 14 mm in diameter. To the unaided eye, they were very similar in appearance to large Chinese freshwater cultured pearls. With magnification, however, they were easily identified as simulants.

Close examination with standard 10× magnification showed that the surface of these beads consisted of small opaque pink and green particles in an unidentified substance that had been applied in parallel layers. This distribution produced an almost iridescent effect. In addition, this material was fairly soft and could easily be indented with the tip of a metal probe. There were also some smaller areas where the surface material had been removed, exposing a dull layer that did not show any iridescent-like effect. With strong oblique fiber-optic illumination, the banded structure of the underlying material became visible. The surface layer on these "pearls" was quite unlike that found in natural or cultured pearls, which typically shows suture lines formed by the overlap-

Figure 11. Although similar in appearance to Chinese freshwater cultured pearls, these approximately 14 mm imitation pearls are easily identified with magnification.

ping aragonite crystals in the nacre layer. Raman analysis identified the cores of the imitation pearls as aragonite, which gave them the right "heft," unlike the lighter weight of some imitations with plastic or glass centers.

While these beads may indeed be a new variety of imitation pearls (we had not seen this material previously in the lab), they can be easily distinguished from either natural or cultured pearls by observation of the surface with magnification.

Thomas Gelb and KNH

SAPPHIRE/Synthetic Color-Change Sapphire Doublets

Assembled stones have been used to simulate valuable gems since at least the days of the Roman Empire (R. Webster, *Gems*, 5th ed., Butterworth-Heinemann, Oxford, 1994). Although their popularity dimmed with the advent of synthetic corundum and synthetic spinel in the early 20th century, they still turn up in jewelry today for several reasons. Some remain in circulation within estate jewelry pieces, while others are used as a less expensive alternative to newer synthetics (e.g., a synthetic spinel triplet imitating an emerald is much less costly than a flux-grown synthetic emerald). Fragile gems such as opal and Ammolite can be given added durability through combination with tougher materials, and, of course, many are created for the sole purpose of deception.

Such is the case with corundum doublets. Usually consisting of either a synthetic ruby or synthetic sapphire pavilion, they are almost always topped with a natural green sapphire crown. The material in the pavilion dominates the face-up color, so the green of the crown is not apparent. Unlike garnet-and-glass doublets, in which the harder garnet "cap" protects the softer glass, the natural sapphire crown is used solely for the deceptive value of its inclusions and other natural features. They are particularly deceiving if the doublet is bezel set to hide the separation plane at the girdle (see, e.g., Winter 1987 Lab Notes, p. 233).

The East Coast laboratory recently encountered two unusual corundum doublets weighing approximately 1.73 and 2.29 ct. Standard gemological testing proved that both doublets had the typical natural green sapphire crowns, but curiously both also had synthetic sapphire pavilions that showed a color change. When viewed in the face-up position, they appeared greenish blue in daylight-equivalent illumination and reddish purple in incandescent light (figure 12). In profile view with diffused transmitted light, their assembly was easy to see, as was

Figure 12. These sapphire/synthetic sapphire doublets (1.73 and 2.29 ct) showed a change-of-color from greenish blue in daylight-equivalent illumination (left) to reddish purple in incandescent light (right). The color change comes solely from the synthetic color-change sapphires that form the pavilions.

Figure 13. In profile, with diffused transmitted light, both parts of the doublet become evident, as do the curved color bands in the synthetic color-change sapphire pavilion.

curved color banding in the synthetic pavilions (figure 13). Face-up, however, this banding was obscured by the straight blue banding in the natural sapphire crowns. It should be noted that the curved color banding seen here is unusual, as synthetic color-change sapphires usually contain only curved striae (i.e., structure lines) without color banding. Proof of synthesis was provided both by the typical synthetic sapphire indicators seen with magnification (gas bubbles and curved growth features) and a spectrum taken on the pavilions with a desk-model spectroscope that revealed chrome lines and a 474 nm line. The pavilions also showed the UV fluorescence (medium strong orange to long-wave and medium orange to short-wave) typical of synthetic color-change sapphires, while the natural green sapphire crowns were inert to both long- and short-wave UV.

With the increasing popularity of color-change stones such as alexandrite and garnet, these doublets should serve as yet another reminder that no matter how old or simple, imitations are still very much a part of the 21st century gem market.

Wendi M. Mayerson

Unusual "Red" SPINEL

In the Spring 2003 Lab Notes (pp. 44–45), we reported on blue quartz that had gained its apparent color from the presence of numerous thin-to-thick, randomly oriented indicolite rods and fibers. We recently encountered another instance of inclusion-caused color when gemologist Kusum S. Naotunne of Ratnapura, Sri Lanka, sent a well-polished dark orangy red cabochon (figure 14) to the West Coast laboratory for examination.

The cabochon, which reportedly was from Okkampitiya, Sri Lanka, was easily identified as spinel by its 1.73 spot refractive index, 3.60 hydrostatic specific gravity, and isotropic nature. It weighed 1.68 ct, measured 6.78 × 5.98 × 4.44 mm, and showed a distinctive silvery red schiller, together with weak asterism in sunlight or overhead incident illumination.

Figure 14. The dark orangy red color of this 1.68 ct spinel cabochon is caused by crystallographically oriented sheets and plates of hematite. Notice the silvery schiller that highlights the dome of the cabochon.

Magnification revealed that the bodycolor of the spinel was actually a pale purplish pink; the orangy red color apparent to the unaided eye was due to the presence of numerous ultra-thin sheets and plates of what appeared to be an iron compound, possibly hematite (α-Fe_2O_3—trigonal) or its dimorph, maghemite (γ-Fe_2O_3—isometric). The inclusions showed a precise orientation along octahedral planes (figure 15), which suggested that these color-causing zones might be the result of exsolution in their spinel host after it formed.

Dichroism, from dark red to orangy red (depending on the thickness and orientation of the inclusion), was indicative of hematite and not maghemite, which is isometric and shows no dichroism. No magnetic attraction was detected when the cabochon was tested with a magnet, which also suggested hematite over maghemite.

Figure 15. Precise orientation along octahedral planes suggests that these color-causing sheets of hematite might be the result of exsolution in their Sri Lankan spinel host. Magnified 10×.

The visible absorption spectrum of the spinel cabochon matched the spectrum shown by ultra-thin deep red specular hematite flakes. There was complete general absorption in the deep blue and overall weak absorption through the yellow-orange, causing the upper blue through the orange region to appear dull, and clearly passing only the red region. Since this was the first spinel of this type that we had encountered, we used Raman analysis to confirm the optical and physical identification of the inclusions as hematite.

Other examples of orangy red color caused by inclusions of ultra-thin platelets and flakes of specular hematite are found in some rock crystal quartz gems, sunstone feldspars not colored by copper, and "bloodshot" iolite from India. Sri Lankan spinel can now be added to this list.

JIK and Maha Tannous

TANZANITE, Diffusion Treated?

Heat treatment is routinely used to enhance the color of vanadium-bearing zoisite [$Ca_2Al_3Si_3O_{12}(OH)$] to purplish blue or blue. However, the ongoing concern about the diffusion treatment of sapphire with beryllium (see article on pp. 84–135 of this issue) has raised concerns about diffusion treatment of other gem materials. In late 2002, InterColor Fine Stones, New York, submitted two tanzanites that were represented to them as being treated by a similar method of "heat with a coating to make it darker in color."

Both stones were deep purplish blue. One was a 4.19 ct oval mixed cut, and the other was a 2.51 ct triangular shape. No evidence of fractures or inclusions was seen with the gemological microscope. In contrast to

Figure 16. To investigate possible diffusion treatment, a 4.19 ct tanzanite was sawn through the center. The area close to the culet (marked by the dashed line) was lighter in color than the rest of the stone. The solid red line indicates the location of electron microprobe analyses.

many of the bulk/lattice-diffused sapphires that GIA has examined, they showed no clear surface-conformal color zonation while they were immersed in methylene iodide. With the client's permission, the oval stone was sliced through the center (figure 16) to facilitate chemical analysis by electron microprobe and LA-ICP-MS. Examination of the profile showed that the area near the culet was slightly lighter than the rest of the stone, and a straight and sharp color boundary was observed with immersion.

Although these observations did not suggest the presence of a diffusion treatment, electron microprobe analysis was performed to further characterize the oval sample. In total, 36 point analyses of the following elements were taken across the 5.8-mm-long profile shown in figure 16: Si, Ti, Al, Cr, Fe, Mn, Mg, Ca, Na, K, Ni, Co, and V. To increase the instrument detection limit, counting time for the minor/trace elements was extended to 200 seconds. The major elements (Ca, Al, and Si) were measured in the amounts expected for tanzanite. The only detectable trace element was V; all the others were below or near the instrument detection limit. The V_2O_3 content varied from 0.13 to 0.26 wt.%, which is typical for tanzanite. The lowest concentrations of V were measured in the lighter-colored area near the culet (figure 17). Contents of Cr, which may cause green coloration in zoisite, were very low (0.01–0.03 wt.% Cr_2O_3) and close to the instrument detection limit. Trace-element distribution was determined using LA-ICP-MS. It not only confirmed the V distribution found with the electron microprobe, but it also revealed similar distribution patterns for Ti, Cr, Mn, Fe, Ga, Pb, U, and rare-earth elements. The B and Be contents were below instrument detection limits.

It has been suggested that small amounts of V may cause the purplish blue color of tanzanite (C. S. Hurlbut Jr., "Gem zoisite from Tanzania," *American Mineralogist*, Vol. 54, 1969, pp. 702–709). This is consistent with the variations in V content measured in the color-zoned oval gemstone. However, a lattice-diffusion process involving V would lead to *higher* concentrations of this element at the rim, not lower as in the analyses performed near the culet. The color distribution in this sample, as well as the sharp and straight color boundary that did not follow the outline of the stone, indicate that the color zoning and vanadium heterogeneity are related to crystal growth rather than lattice diffusion.

It is also important to note that, as a hydroxyl-bearing mineral, tanzanite would not be stable at a very high temperature, which is essential for V or any other chemical impurities (except H) to diffuse at a reasonably fast rate. Although neither of the two stones described here showed evidence of chemical diffusion, the GIA Gem Laboratory will continue to monitor this situation.

Wuyi Wang

Figure 17. Some variation in V_2O_3 content was detected by the electron microprobe. Within about 1.0 mm of the stone's culet, the vanadium content was relatively lower than in the rest of the stone. This is contrary to the result expected for diffusion treatment.

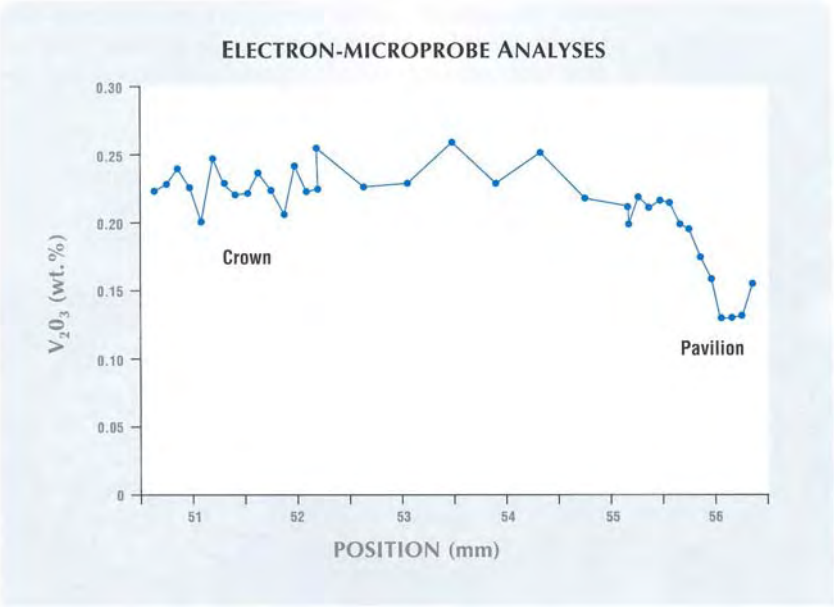

PHOTO CREDITS
Elizabeth Schrader—figures 1, 2, 12, 13, and 16; Wuyi Wang—figure 3; Maha Tannous—figures 5, 6, 7, 9, and 14; John I. Koivula—figures 8, 10, 15; Don Mengason—figure 11.

DIAMONDS

"Additional" facets and their effect on scintillation. The face-up appearance of diamonds is usually described by three key attributes—brightness, fire, and scintillation. However, what is not as well understood is the contribution of each of these characteristics to an overall pleasing face-up mosaic appearance.

While it is generally agreed that a diamond should be bright—that is, have a significant amount of white light return—to be considered desirable, the amount of fire and scintillation necessary for a diamond to qualify as "high performing" is less well defined. While fire consists of the single appearance aspect of colored light exiting the crown of a diamond, we are finding that scintillation is composed of several different appearance aspects. One of these consists of the flashes of light that change as the diamond, observer, or light source move in relation to one another. Another is related to the patterns of bright and dark areas seen in the diamond when it is observed face-up. In diffused light, one sees these contrasting patterns created by the facets breaking up the total light exiting the crown. Although these patterns can reduce the total amount of white light returned to the observer, we have found that they may, in some cases, *increase* the overall desirability of a diamond. This pattern effect is directly related to the number of facets, their size and shape, their interrelated angles, and the

Figure 1. This Cento-cut diamond (0.74 ct) is an example of a 100-facet design that shows a pleasing scintillation effect. Courtesy of Rosy Blue Inc.; photo by Elizabeth Schrader.

Figure 2. The Cento design incorporates additional facets on the pavilion which act to increase the observable scintillation of the diamond. Courtesy of Rosy Blue Inc.

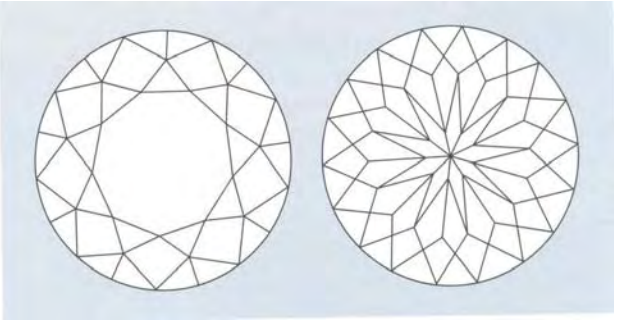

quality of their placement on the diamond (i.e., symmetry).

The 100-facet round modified brilliant shown in figure 1, known as the Cento cut and created by Rosy Blue Inc., exhibits some of these performance characteristics. The scintillation effect displays a pleasing symmetrical pattern with a good balance of contrasting bright and dark areas. This scintillation results from the faceting angles and facet arrangement used in this cut design (see figure 2).

In our extensive experience with computer modeling at GIA, we have found it challenging to compare the appearance aspects of brightness, fire, and scintillation of standard round brilliants to that of other modified faceting styles. Often these modified styles create unique face-up appearances that highlight different desirable aspects. In the case of the Cento cut, we observed increased scintillation due to the ability of the additional facets to "break up" the overall brightness pattern of the diamonds.

These observations reinforce our overall research findings that every facet matters when assessing the overall appearance of a diamond; therefore, no diamond should be judged solely by one attribute alone (see T. S. Hemphill et al., Fall 1998 *Gems & Gemology*, pp. 158–183; I. M. Reinitz et al., Fall 2001 *Gems & Gemology*, pp. 174–197). Our observations also indicate that modifications of the traditional round brilliant design can have a great impact on scintillation effects, specifically on the light and dark patterns and specular reflectance that are observed. In many cases, the additional facets result in more pronounced scintillation than is typically encountered with a standard round brilliant cut.

Tom Moses
GIA Gem Laboratory, New York
Ron Geurts
TT Consulting, Antwerp

COLORED STONES AND ORGANIC MATERIALS

"Alphabet" agates from Indonesia. At the 2003 Tucson gem show, New Era Gems of Grass Valley, California, had four complete sets of Indonesian agate cabochons with patterns resembling letters of the Roman alphabet. The agates are typically off-white with orange to orangy brown markings (figure 3). According to general manager Jim Steelman, New Era Gems received their first complete set in mid-2002, from an Indonesian friend who had been collecting the agates for 15–20 years. Some letters such as "Q" and "R" proved difficult to obtain, so it took the collector three years to complete the alphabets from his collection. One set of numerals was also assembled, with "8" and "5" being the most difficult to find. Most common are simple cross patterns.

Mr. Steelman indicated that the cabochons are cut from large pieces of agate that contain Fe-stained microfractures in a variety of patterns. To produce the various letters and numerals, the cutter creatively fashions the cabochons so they intersect the iron-stained patterns with the desired effect. Both ovals and rounds are shaped in sizes that typically range from 10 to 14 mm. The most attractive sets use cabochons that are well matched in size and markings. Although he did not know total production, Mr. Steelman estimated that it probably ranges from a few hundred cabochons per year of the letters or other figures, to a few thousand annually of the crosses.

Figure 3. Agate cabochons from Indonesia have been fashioned with patterns resembling every letter in the Roman alphabet, as well as numbers and other forms. The patterns are reportedly caused by iron staining along microfractures. Courtesy of New Era Gems; photo by Maha Tannous.

A collection of these agate cabochons was donated to GIA in June 1999 by Ben Hoo of Ben's International Gemological Center in Singapore. Included are several that mimic various letters and numbers, as well as patterns that resemble Asian characters, a turkey, and abstract forms. Mr. Hoo told this contributor that the agates are found on the island of Java, in three main areas: (1) Jampangkulon—approximately 50 km southwest of Sukabumi in western Java; (2) Garut—approximately 50 km southeast of Bandung, also in western Java; and (3) Prambanan—approximately 60 km northwest of Yogyakarta in central Java. Agates from the first two locations are mostly sold in Jakarta, and those from the third area go mainly to Surabaya. In addition, many of the big cities have agate centers where the polished agates are sold. In Indonesia, the agates are worn principally by men. Patterns that resemble the 12 zodiac signs are expensive, but the most highly prized are those that mimic a dragon.

BML

Editor's note: Interested contributors should send information to Brendan Laurs at blaurs@gia.edu (e-mail), 760-603-4595 (fax), or GIA, 5345 Armada Drive, Carlsbad, CA 92008. Any original photos will be returned after consideration or publication.

GEMS & GEMOLOGY, Vol. 39, No. 2, pp. 152–165

Figure 4. These cat's-eye beryl cabochons (24.78 and 23.67 ct) were purchased as quartz in Brazil. Photo by Jaroslav Hyrsl.

Figure 5. Oriented inclusions (probably hematite) were responsible for the chatoyancy shown by the beryls in figure 4. Photomicrograph by Jaroslav Hyrsl; magnified 9×.

Unusual cat's-eye beryl from Brazil. Cat's-eye beryl is not uncommon, but two cabochons (24.78 and 23.67 ct; figure 4) purchased by this contributor in Brazil in 2001 proved very unusual. Although sold as quartz, their identity as beryl was established by a spot R.I. of 1.57 and an S.G. of 2.80 (measured hydrostatically). The samples were inert to long- and short-wave UV radiation, and no features were visible with a hand spectroscope. Both showed strong aventurescence due to abundant reddish brown inclusions oriented along a hexagonal prism, parallel to the c-axis. These inclusions were also responsible for the chatoyancy oriented perpendicular to the c-axis. With magnification (figure 5), the shape of these inclusions varied from pseudohexagonal to elongate, and their appearance suggested they were hematite. In addition, the aventurescence caused weak asterism, with two rays present in addition to the two dominant rays that corresponded to the chatoyancy. These beryl samples were noteworthy not only for their aventurescence and asterism, but also for the fact that their chatoyancy was caused by mineral inclusions, rather than hollow tubes.

Jaroslav Hyrsl (hyrsl@kuryr.cz)
Kolin, Czech Republic

Magnetic corundum. These contributors recently were presented with a dark brownish red sample of star corundum, which had the amazing property of being strongly attracted to a common magnet (figure 6). The specimen weighed 17.9 grams and was polished on one end, where it exhibited weak asterism. According to the owner, it was found in India.

The sample had a very high S.G. of 4.2 (determined hydrostatically; corundum is typically 3.99–4.00), and a spot R.I. of ~1.77 was measured on the polished end. Microscopic observation revealed black surface-reaching inclusions; in reflected light, they exhibited a metallic luster that contrasted with the vitreous luster of the host corundum. Also present was an area surrounding the core of the sample that showed a slightly different luster. The magnetism was stronger on the rim, but also very noticeable on the polished part of the core.

To determine the cause of the magnetism and to identify these inclusions, we studied the stone with a scanning electron microscope (SEM). First we used magnification in backscattered electron (BSE) mode to observe differences in atomic weight. Figure 7 shows the polished face of the crystal, looking down the c-axis. The inclusions appear bright white against the host corundum, due to their relatively high atomic weight. The mottled light gray rim of the sample also contrasts with the corundum core. Closer examination of the rim showed that it consists of several phases (figure 8).

Using the EDX (energy-dispersive X-ray spectroscopy) capabilities of the SEM, we performed semi-quantitative chemical analysis on seven specific portions of the speci-

Figure 6. This unusual 17.9 gram corundum specimen was strongly magnetic; it is shown here with a magnet (the metallic sphere). Photo by T. Hainschwang.

men: (1) the host corundum, (2–3) two selected inclusions, (4) a large area of the rim, and (5–7) three areas of the rim that appeared light gray, medium gray, and dark gray in BSE mode. The host corundum was Al_2O_3, as expected, with minor amounts of Fe. The various areas of the rim showed different amounts of Fe, Cr, Ti, Mn, Mg, Zn, O, and some Al. Chemical analysis of the two inclusions identified them as members of the hematite-ilmenite series, with the formulas Fe_2O_3 and $FeTiO_3$. Since minerals of this series are usually rather weakly magnetic, we suspected that the sample might also contain minerals of the magnetite-ulvöspinel (Fe_3O_4–Fe_2TiO_4) series. Analysis of the rim area revealed that the lightest area was mainly hematite (Fe_2O_3), and the medium gray area consisted of a mixed form of spinel with a possible formula of $(Fe,Mg,Mn,Zn,)Al_2O_4$. The analyzed "spinel area" mainly contained Fe and Mg (in equal proportions), and thus can be called a pleonaste—a mix of spinel ($MgAl_2O_4$) and hercynite ($FeAl_2O_4$)—with minor galaxite ($MnAl_2O_4$) and gahnite ($ZnAl_2O_4$). The darkest phase of the rim was identified as corundum. Interestingly, the seven point analyses did not identify members of the magnetite-ulvöspinel series in this specimen. If indeed these strongly magnetic minerals are not present, then the strength of the magnetism in this sample is very surprising. None of the identified oxide minerals (hematite, ilmenite, and pleonaste) normally exhibits such strong magnetism.

The formation of the rim is rather unclear; one possibility might be that fluctuations in late-stage growth conditions led to the formation of iron-rich spinel in addition to corundum; the hematite could have been formed as a result of the exsolution of Fe from either the corundum or the pleonaste.

Reviewing the above findings, we propose the following possible explanations for this magnetism:

- Heating of hematite may strengthen the magnetism of this mineral.
- Ilmenite with rather strong magnetism has been described in the mineralogical literature.
- The Fe_2O_3 may exist in another state, called gamma-Fe_2O_3 or maghemite, and this iron oxide is magnetic. It can be formed by oxidation of magnetite and by other conversion processes from various iron-containing minerals (see http://www.geo.arizona.edu/Paleomag/book/chap02.pdf). Since hematite has the same chemical makeup, hematite and maghemite cannot be distinguished from one another by EDX.

The last possible explanation could be that we simply missed identifying the minerals of the magnetite-ulvöspinel series in our seven point analyses.

Thomas Hainschwang (gemlab@adon.li)
Gemlab Gemological Laboratory
Vaduz, Principality of Liechtenstein
Wolfgang Keutschegger
Ivoclar, SEM facility
Schaan, Principality of Liechtenstein

Figure 7. This backscattered electron image of the polished part of the specimen in figure 5 shows a core area of corundum (gray) with inclusions of much higher atomic weight (bright white); the mottled light gray rim is of intermediate atomic weight overall.

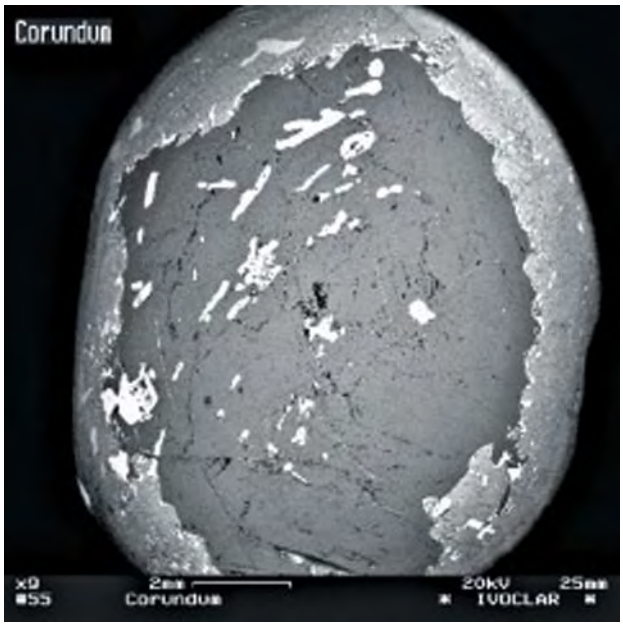

Figure 8. Close examination of the rim of the specimen in backscattered electron mode shows that several phases are present.

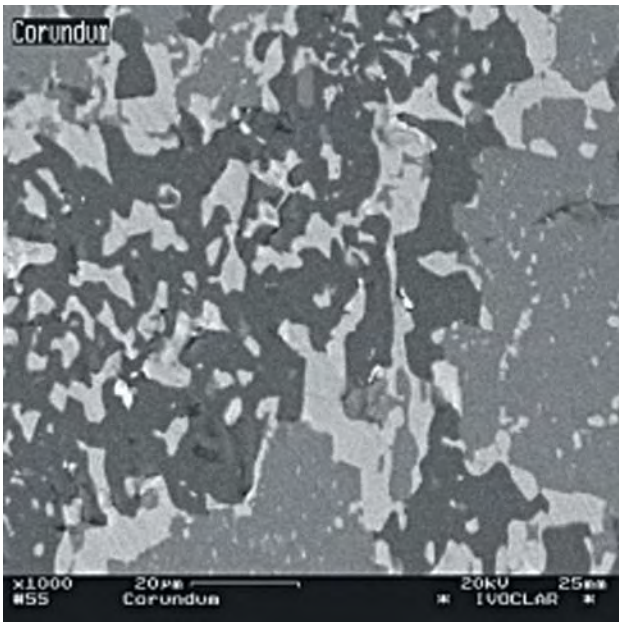

Figure 9. This 1,372.10 ct fluorite, faceted by Maria Atkinson, was mined in northern Pakistan. Photo by Jeff Scovil; © Terra 2003.

Large pink fluorite from Pakistan. At the 2003 Tucson gem show, David Atkinson of Terra in Sedona, Arizona, displayed a large and impressive deep pink fluorite from Nagar, Northern Areas, Pakistan (figure 9). The rough, which weighed approximately 7 kg, was found during the 2001 mining season. At 1,372.10 ct, this faceted stone was more than twice the weight of the 673.14 ct pink fluorite from Pakistan that appeared at the Tucson show in 1993 (see Spring 1993 Gem News, p. 56). It may represent the largest pink fluorite that has ever been faceted.

BML

Crystals of color-change garnet from Bekily, Madagascar. Rough pyrope-spessartine garnets from Bekily, southern Madagascar, normally are found only as irregularly shaped fragments without crystal faces. Therefore, when examining two parcels of rough that were purchased in Madagascar by a German dealer in 2002, this contributor was surprised to see several perfectly terminated, transparent color-change garnet crystals (see, e.g., figure 10). These crystals were blue-green or yellowish green in daylight, and purple, purplish pink, or pink in incandescent light (see K. Schmetzer and H.-J. Bernhardt, "Garnets from Madagascar with a color change of blue-green to purple," Winter 1999 *Gems & Gemology*, pp. 196–201). The samples showed the trapezohedron {211} as the dominant crystal form and subordinate dodecahedra {110}. This is precisely the crystal habit proposed by a previous study of the internal growth structures in pyrope-spessartine garnets from Bekily (see K. Schmetzer et al., "Pink to pinkish orange Malaya garnets from Bekily, Madagascar," Winter 2001 *Gems & Gemology*, pp. 296–308).

KS

The Lion Cut for colored stones and diamonds. Diamex Inc. of New York recently shared with these contributors several examples of Lion Cut gemstones. Developed by Paul C. A. de Maere in 1999, this design combines the traditional rose cut with the modern brilliant. In contrast to the flat table of a brilliant-cut stone, the table of the Lion Cut is composed of eight facets angled toward a low peak in the center of the crown, the "crown culet." The examples we saw included round, oval, and pear shapes made from diamond, ruby, and pink tourmaline. This cut has been applied to a wide variety of gems, including sapphire, emerald, aquamarine, quartz, peridot, and kunzite.

The Lion Cut has some noteworthy effects on face-up appearance. In colored gems, for example, it substantially strengthens the face-up color. This effect was put to excellent use in the pink tourmaline in figure 11, where the cut transformed a rather weak bodycolor into a saturated, evenly displayed face-up color. In the near-colorless diamonds we examined, it produced a pronounced and interesting scintillation pattern. This pattern was composed of triangles—which became lighter or darker as the stone, observer, or light source was moved—arranged around the crown culet.

There are two Lion Cut variations for a round shape, each named for particular elements of the scintillation pattern. The Lion Cut Brilliant Cross has the star facets oriented above the pavilion mains, and produces a "brilliant cross" in the center of the pattern. A treated-color blue diamond that we examined was cut in this style, but the color of the gem competed with the display of scintillation. The other variation is the Lion Cut Brilliant Star, in which the crown is rotated with respect to the pavilion, placing each star facet over the center of a lower-girdle facet. Display of these and other elements of the scintillation pattern requires that the multiple facets replacing the

Figure 10. These color-change garnet crystals from Bekily, Madagascar (about 4–5 mm in diameter), show dominant trapezohedra {211} and subordinate dodecahedra {110}. An idealized crystal drawing (clinographic projection) is provided for comparison. Photo by Maha Tannous; incandescent light.

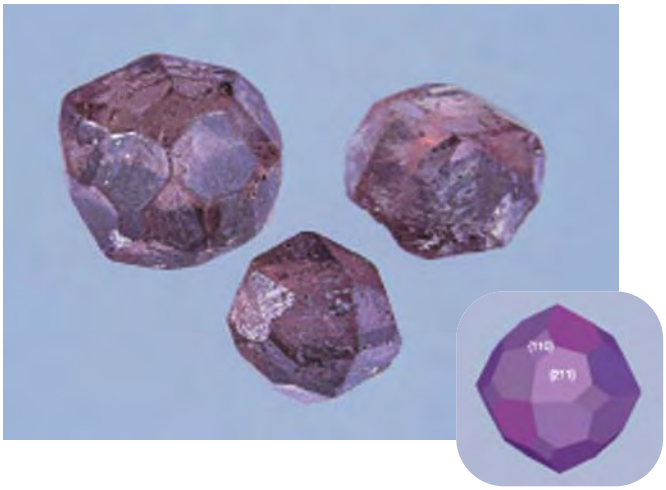

Figure 11. The gemstones in these three rings utilize the Lion Cut, developed and manufactured by Paul C. A. de Maere of Ghent. The diamond weighs 1.54 ct, the ruby 1.22 ct, and the tourmaline 1.50 ct. Courtesy of Diamex Inc.; photo by Maha Tannous.

table be well centered over the pavilion facets and culet.

Mr. de Maere is both producing and marketing Lion Cut gems from his office in Ghent, Belgium. So far, diamonds of this cut have ranged from 0.01 to 5.00 ct. Twelve fancy shapes have been cut from both diamonds and colored gemstones: rectangle, cut-corner rectangle and square, pear, marquise, heart, oval, cushion, kite, octagon, triangle, and shield. Lion Cut gems are being distributed by Handsetters & Verhaere BVBA of Antwerp (diamonds), and W. Constantin Wild & Co. of Idar-Oberstein (colored stones).

Ilene Reinitz (ireinitz@gia.edu)
and Tom Moses
GIA Gem Laboratory, New York

Tale of a swallowed Tahitian cultured pearl. In January 2003, Kay Kostelny of Coffin & Trout Jewelers, Chandler, Arizona, told *Gems & Gemology* about a customer whose Tahitian cultured pearl earring was swallowed by a dog. The earring was reportedly in the dog's digestive tract for two days before it passed on the third day. Although the earring was structurally undamaged, the cultured pearl underwent some noticeable changes (figure 12).

Ms. Kostelny kindly loaned both earrings to GIA, and reported that the cultured pearls were previously closely matched in terms of size, color, and luster. The most obvious difference after the incident was the size: The swallowed sample measured 7.90 mm, whereas the other one was 9.20 mm in diameter. The nacre appeared to be evenly dissolved from the swallowed sample. The color of that cultured pearl was noticeably darker and less green. However, it still retained a high luster. Nevertheless, because the cultured pearls were no longer well matched, the customer decided to have Ms. Kostelny replace the swallowed sample with another Tahitian cultured pearl.

An interesting comparison to this swallowed cultured pearl can be drawn with the ancient practice of "cleaning" pearls by feeding them to chickens (see K. Nassau and A.E. Hanson, "The pearl in the chicken: Pearl recipes in *Papyrus Holmiensis*," Winter 1985 *Gems & Gemology*, pp. 224–231). In that article, Dr. Nassau performed his own experiments by feeding soiled Japanese Akoya cultured pearls to chickens, and found that under certain conditions "this represents a valid way of cleaning a pearl by removing a thin layer from the surface while maintaining an excellent surface quality" (p. 227). Indeed, the swallowed Tahitian cultured pearl also retained an attractive luster. *BML*

Trapiche rubies displaying asterism. Trapiche rubies are composed of six translucent-to-transparent ruby sections that are delineated by "arms" of translucent-to-opaque material, resulting in a fixed six-rayed "star." Such rubies have been reported from both Mong Hsu, Myanmar (see K. Schmetzer et al., Winter 1996 *Gems & Gemology*, pp. 242–250; Summer 2000 Gem News, pp. 168–169; and V. Garnier et al., "Rubis trapiches de Mong Hsu, Myanmar," *Revue de Gemmologie*, No. 144, 2002, pp. 5–12) and Yen Bai Province, Vietnam (see Fall 1998 Gem News, p. 225). The arms in the Mong Hsu material reportedly consist of ruby and solid, liquid, and two-phase inclusions, with the solid inclusions composed of calcite and dolomite; micas reportedly form the "star" in the Vietnamese material.

At the Pueblo Inn during the February 2003 Tucson shows, David Burton of Burton's Gems & Opals, Anaheim, California, had five heat-treated cabochons of trapiche ruby that also showed asterism. According to Mr. Burton, such material has been found only in Mong Hsu. We

Figure 12. The Tahitian cultured pearl earring on the left was swallowed by a dog. Although the size and color no longer match the cultured pearl in the other earring, it still displays a high luster. Courtesy of Coffin & Trout Jewelers; photo by Don Mengason.

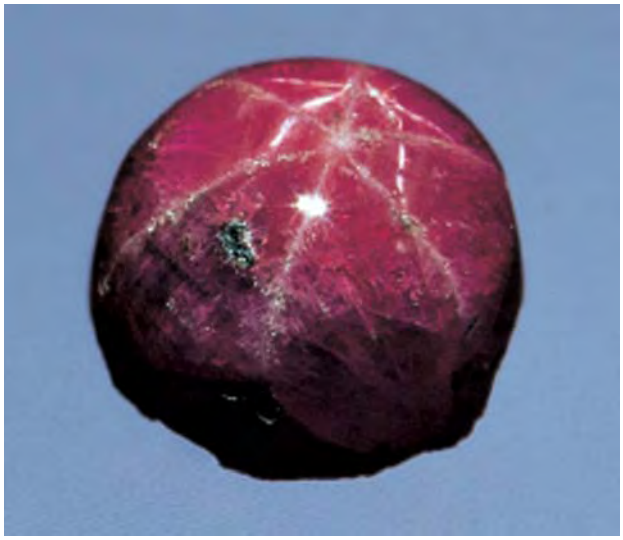

Figure 13. Asterism is displayed by this unusual 0.49 ct trapiche ruby, reportedly from Mong Hsu, Myanmar. Photo by Maha Tannous.

examined a 0.49 ct sample (figure 13) that was acquired by one of these contributors (EQ). It had a spot R.I. of 1.77 and a specific gravity (measured hydrostatically) of 3.86; the latter is slightly lower than the values previously reported for trapiche rubies. The sample displayed a typical ruby (chromium) absorption spectrum when viewed with a desk-model spectroscope. It fluoresced moderate to strong red to long-wave and weak chalky red to short-wave UV radiation. Viewing the sample with magnification and a UV lamp revealed that the fixed arms fluoresced a very weak chalky yellow to long-wave UV only. (However, this effect was nearly overpowered by the fluorescence of the surrounding ruby.) Magnification also revealed fine silk, hexagonal growth zoning, numerous fingerprints, growth tubes, and cavities.

EDXRF analysis of one of the ruby sections revealed traces of K, Ca, Ti, V, Cr, Fe, and Ga. Another analysis of the top of the dome where the arms of the fixed star came together showed significantly more Ca and Ti, and less K and Fe, than the ruby section. The bottom of the sample (the only part tested in this way) effervesced slowly to 10% HCl, mainly along the fixed arms, indicating the presence of a carbonate mineral. Unfortunately, it was not possible to confirm the identity of the mineral(s) in those arms by Raman spectroscopy, due to the strong fluorescence of the sample.

The two stars in this asteriated trapiche ruby were created independently by different types of inclusions. It has been suggested (in the above-referenced articles) that the fixed arms of the Mong Hsu trapiche rubies are primary inclusions. The asterism is created by fine silk, however, which is secondary and crystallizes as the corundum cools.

Sam Muhlmeister (smeister@gia.edu)
and Elizabeth Quinn
GIA Gem Laboratory, Carlsbad

Cat's-eye scapolite from Tanzania. At the 2003 Tucson AGTA GemFair, Gregory Krichel of Michael Couch and Associates, West Des Moines, Iowa, had some interesting cat's-eye scapolite. According to Mr. Krichel, the rough was purchased in Dar es Salaam, but was reportedly mined from a new primary deposit in central Tanzania—specifically in the Dodoma-Morogoro area. Unlike the yellow cat's-eye scapolite that previously came from this region (see D. M. Dirlam et al., "Gem wealth of Tanzania," Summer 1992 *Gems & Gemology*, pp. 80–102), or the better-known fibrous semi-transparent pink cat's-eye material from Myanmar, this new scapolite was brown to reddish brown. Mr. Krichel purchased about 200 kg of the rough and said that there was substantially more available. Most of the available cabochons measured approximately 10 × 12 mm (or ~5.5 ct).

Scapolite is actually a mineral group formed by a solid solution between marialite ($3NaAlSi_3O_8 \cdot NaCl$) and meionite ($3CaAl_2Si_2O_8 \cdot CaCO_3$). Although not well known in the gem trade, colorless and yellow cat's-eye scapolite from Tanzania was studied in detail in the early 1980s (see G. Graziani and E. Gübelin, "Observations on some scapolites of central Tanzania," *Journal of Gemmology*, Vol. 17, No. 6, 1981, pp. 395–405; G. Graziani et al., "Observations on some scapolites of central Tanzania: Further investigations," *Journal of Gemmology*, Vol. 18, No. 5, 1983, pp. 379–381). Similar material with a reddish brown bodycolor due to inclusions was reportedly found in Kenya in 1984 (Spring 1984 Lab Notes, pp. 49–50).

One of these contributors (WM) borrowed two cabochons (5.42 and 5.57 ct; figure 14) from Mr. Krichel, for comparison with the scapolite studied in the early 1980s. One sample had a reddish brown bodycolor of variable saturation and a slightly less sharp eye, due to its irregularly distributed inclusions. The other cabochon was brown and had a distinct, sharp eye. With a loupe and a penlight, black and orangy red fine needles could be seen as the cause of the chatoyancy. Magnification and darkfield illumination revealed that the area between the inclusions was actually colorless; the reddish brown cabochon contained more of the orangy red inclusions than the brown one. These findings indicated that the inclusions caused not only the chatoyancy, but the bodycolor as well. The spot R.I. measured on the dome of both cabochons was 1.57, while the flat polished bases each yielded 1.560–1.585 (birefringence = 0.025). This is very similar to the colorless scapolite tested by Graziani and Gübelin in 1981 (R.I. = 1.556–1.582, birefringence = 0.026). The S.G. of both cabochons was 2.75, measured hydrostatically. This too is similar to the previously studied stones (S.G. = 2.71 and 2.72). Since R.I. and S.G. increase with increasing Ca content, these results indicate that the stones were likely closer to the meionite end of the series (C. Klein and C. Hurlbut, *Manual of Mineralogy*, John Wiley & Sons, New York, 1993, p. 548).

Like the material studied in the early 1980s, the chatoyancy in this scapolite was caused by iron-rich minerals;

Figure 14. These chatoyant cabochons (5.42 and 5.57 ct) were identified as Na-rich meionite, an intermediate composition in the scapolite series. Photo by Elizabeth Schrader.

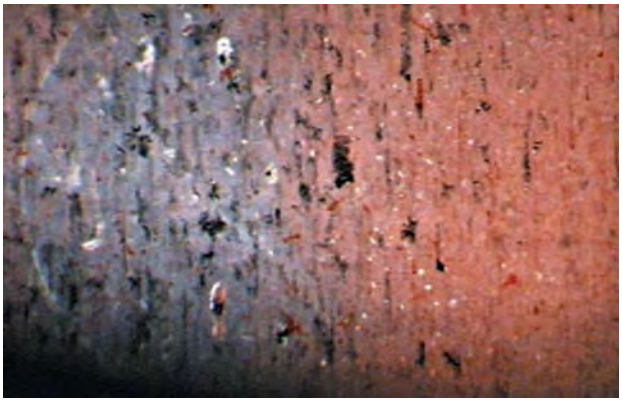

Figure 15. The color zoning in this cat's-eye scapolite is due to a greater abundance of hematite inclusions in the reddish brown part of the cabochon. The gray area contains mostly magnetite inclusions. Both minerals are present as needles, elongated platelets, and dendrites. Photomicrograph by Wendi Mayerson; magnified 50×.

however, the exact minerals were different. Graziani et al. (1983) found pyrrhotite, lepidocrocite, and maghemite, whereas (using Raman spectroscopy) we identified the reddish orange inclusions in our samples as hematite and the black inclusions as magnetite. Both of these minerals were present in three forms: as fine needles, elongated platelets, and small flat dendrites (see figure 15).

The Raman spectrum of each stone matched the reference spectrum for scapolite, and the powder X-ray diffraction patterns matched that of "mizzonite," an intermediate composition near the meionite end of the series (i.e., a Na-rich meionite). EDXRF chemical analysis also yielded results consistent with a Na-rich meionite.

With such large quantities available and the recent increase in demand for phenomenal gems, more of this material could be encountered in the market in the near future.

Wendi M. Mayerson (wmayerson@gia.edu)
GIA Gem Laboratory, New York
Shane Elen and Philip Owens
GIA Gem Laboratory, Carlsbad

Miscellany from Tucson. While large and expensive gems are always pleasing to see, some of the most fascinating items at the 2003 Tucson shows fell into one or more of three different categories: (1) notable materials, (2) unusual gems (often with special lapidary treatment to bring out their character), and (3) gems with interesting and/or educational inclusions.

Notable Materials. Kevin Lane Smith, a lapidary and jewelry designer in Tucson, had a form of rhyolitic matrix opal that had been fashioned into small drilled ovoid beads. Each rhyolite bead contained a single gas pocket filled with opal that showed intense play-of-color (figure 16). A limited quantity of this material was discovered in 2002 at a new locality in Magdalena, Mexico. Because they were pre-drilled, these beads could be easily used creatively for simple but interesting jewelry in a number of different ways, from single drops on a neck chain to pairs of unusual earrings.

Uwe Barfuss, managing director of Queensland Opal Mines Pty. Ltd., Cunnamulla, Queensland, informed one of us (JIK) that in late 2002 his company had purchased the Hart's Range ruby mine in Australia's Northern Territory, located northeast of Alice Springs (see R. Scambary, "Australia adds rubies to its mineral riches," Fall 1979 *Gems & Gemology*, pp. 220–221). The deposit has been worked intermittently since about 1978. Since mining resumed in late 2002, the production has consisted of translucent to semi-opaque tabular hexagonal crystals with a pleasing red color, and elongate crystals of pale

Figure 16. This rhyolite and opal bead (14.6 × 7.4 mm) is from a new find of opals in Magdalena, Mexico. Photo by Maha Tannous.

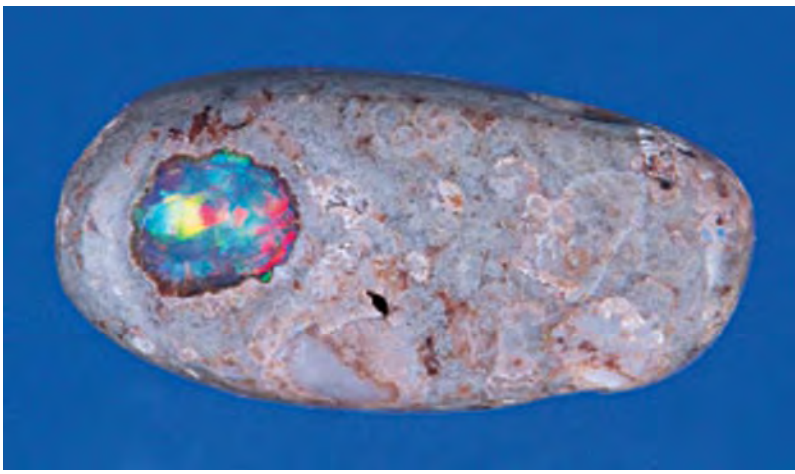

Figure 17. Recent mining at the Harts Range ruby mine in Australia is producing ruby crystals like those shown here. The largest crystal is 25 mm long, while the small tabular ruby in the right foreground, with the hexagonal growth hillock, weighs 1.44 ct. Photo by Maha Tannous.

color that are coated by the gneiss host rock (figure 17). The tabular crystals make excellent mineral specimens for collectors, while cabochons can be cut from the elongate crystals. Queensland Opal Mines is currently looking for a chemical and/or mechanical way to remove the micaceous gneiss matrix from the larger crystals without damaging the underlying ruby.

Another interesting find was an unusual 8.36 ct multiple spinel twin (figure 18) from Mogok, Myanmar, which belonged to Mark Smith of Thai Lanka Trading Ltd., Bangkok, Thailand. The transparent-to-translucent twinned crystal, which measured 13.28 mm on its longest dimension, was intense red and displayed relatively sharp crystal faces, which suggests that it was mined from a primary deposit or had not been transported far from its original source-rock. While Burmese red spinel is not rare, it usually occurs as single crystals of octahedral habit; twins normally consist of two individual octahedrons joined according to the spinel law. Goldschmidt (1923) shows only one drawing that depicts a somewhat similar cyclically twinned spinel crystal (see V. Goldschmidt, *Atlas der Krystallformen*, 1923, Vol. 8, table 48, figure 26). This is the first time that we have seen a multiple twin of this nature.

Figure 18. This 8.36 ct spinel crystal from Mogok, Myanmar, shows an unusual cyclic twinned habit. Photo by Maha Tannous.

Figure 19. Looking like a jagged iceberg, the cavernous etch pits in this 40.6 × 31.4 mm polished topaz add considerable interest to their host. Photo by Maha Tannous.

Unusual Gems. Falk Burger of Hard Works in Los Alamos, New Mexico, had two unique gems on display: a 139.08 ct deeply etched colorless topaz from Brazil that looked like it had captured an iceberg during crystallization (figure 19); and a 27.75 ct elongated cushion-shaped cabochon of hypersthene, thought to be from Sri Lanka, which showed remarkable lamellar twin–related optical effects. As this stone or the light source above it was moved, bold bands of "golden" brown color shifted dramatically across the surface (figure 20).

Kevin Lane Smith showed these contributors a large "anyolite" (ruby in zoisite) pendant from the Longido mine in Tanzania (figure 21). This cabochon measured 60.59 mm in its longest dimension, and contained a hexagonal crystal of ruby that was artistically framed by the

Figure 20. The lamellar twinning in this 33.35-mm-long cabochon of hypersthene is visible as bright reflective bands that change in reflectance as the light and/or stone are moved. Photos by Maha Tannous.

green zoisite and black hornblende matrix rock. While anyolite from Tanzania is not particularly unusual, this example was exceptional because of the size, perfection, placement, and reflective nature of the ruby crystal, which resulted from light bouncing off lamellar twin planes that were at or near the surface of the polished ruby.

In addition to the Harts Range ruby crystals discussed above, Uwe Barfuss also had a wide variety of Australian opals for sale. Some of these were of the type known as Yowah nuts, and one split pair showed a unique mirror-image pair of "mushroom" shapes in the opposing halves (figure 22).

Interesting Inclusions. Because it can take a relatively long time to identify some inclusions, this year's finds will probably stimulate and nurture our inclusion research for several years. A few of the inclusion surprises found so far are mentioned here. Stalks and fibers of astrophyllite in quartz from Kola, Russia (figure 23), and bright yellow crystals of helvite in quartz from Hunan Province, China (figure 24), were obtained from Dr. Jaroslav Hyrsl of the Czech Republic. Dr. Hyrsl identified the inclusions using Raman spectroscopy and powder X-ray diffraction analysis. Orange spessartine and opaque black ilmenite (both identified by Raman spectroscopy) were present in a faceted rose quartz from Rakwana, Sri Lanka (figure 25), that was obtained from gemologist Kusum S. Naotunne of Ratnapura. An incredible, complex, multiphase primary fluid inclusion in a colorless beryl crystal from Teófilo Otoni in Minas Gerais, Brazil, contained countless tiny spherical to subspherical "daughter crystals" of an unknown nature (figure 26). This sample was obtained from Luciana Barbosa, of the Gemological Center in Belo Horizonte, Minas Gerais, Brazil.

John I. Koivula (jkoivula@gia.edu) and Maha Tannous
GIA Gem Trade Laboratory, Carlsbad

Figure 21. Although "anyolite" from Tanzania is not particularly unusual, this example is exceptional because of the size (60.59 mm long), perfection, placement, and reflective nature of the ruby crystal. Photo by Maha Tannous.

SYNTHETICS AND SIMULANTS

Cubic zirconia briolettes. At the AGTA show in Tucson this year, Anil Dholakia of Anil B. Dholakia Inc., Franklin,

Figure 22. This matched pair of 16-mm-long Yowah opals displays a virtually identical pair of mushroom images on the opposing halves. Photo by Maha Tannous.

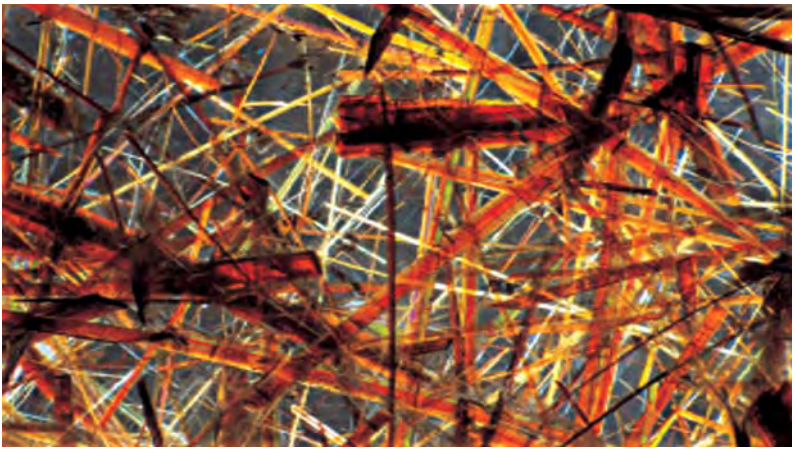

Figure 23. Stalks and fibers of astrophyllite decorate the interior of an 83.53 ct quartz cabochon from Kola, Russia. Photomicrograph by John I. Koivula, in cross-polarized light; magnified 10×.

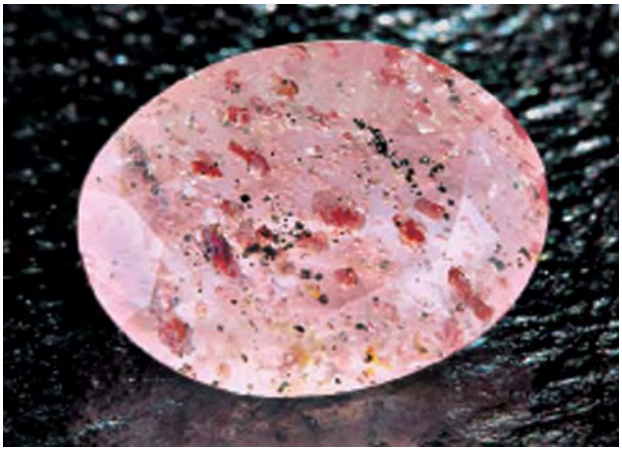

Figure 25. This 7.28 ct faceted rose quartz from Rakwana, Sri Lanka, hosts inclusions of spessartine and ilmenite. Photo by Maha Tannous.

North Carolina, had strands of cubic zirconia briolettes in seven colors: purple, blue, red, green, pink, lavender, and colorless (figure 27). This contributor had not previously heard of CZ cut in this fashion.

Figure 24. Bright yellow crystals of helvite are enclosed in quartz from Hunan Province, China. Photomicrograph by John I. Koivula; magnified 15×.

Cubic zirconia has been used to imitate diamond since its introduction in the early 1970s. It is available in nearly every shape and facet arrangement, and has even imitated diamond rough. It was therefore not surprising to see these briolettes, since this cut has become so popular recently. Mr. Dholakia told this contributor that he has also cut CZ into beads and rondelles, although they do not show the dispersion seen in the briolettes. The briolettes are cut to order in Trichinapalli, a city in southern India where sev-

Figure 26. A colorless beryl from Teófilo Otoni in Minas Gerais, Brazil, contains a complex multiphase primary fluid inclusion that holds numerous tiny spherical to subspherical "daughter crystals" of an unknown nature. Photomicrograph by John I. Koivula, in cross-polarized light; magnified 5×.

eral thousand people are employed in cutting synthetic and imitation gems.

Cubic zirconia is no threat to any natural gem market, as it can be identified by basic gemological examination. Since its specific gravity is almost twice that of diamond (5.80 vs. 3.52), heft alone can provide a strong indication; combined with differences in hardness and fluorescence, the identity is easily revealed (see, e.g., Lab Notes: Fall 1982, p. 169; Winter 1988, p. 241; and Fall 1996, p. 205; and Spring 1994 Gem News, p. 47).

With the price of diamond briolettes being out of reach for most people, CZ briolettes may offer an attractive alternative.

Wendi M. Mayerson (wmayerson@gia.edu)
GIA Gem Laboratory, New York

Figure 27. These seven strands of colored briolettes (approximately 10 × 5 cm and 12 × 6 cm) were reportedly fashioned from cubic zirconia. Courtesy of Anil B. Dholakia Inc.; photo by Maha Tannous.

A bicolored synthetic diamond. Blue coloration in synthetic diamond is created by adding boron to the growth cell; this boron doping frequently results in blue and near-colorless zones. However, the coloration of the synthetic diamond crystal reported here is quite unusual, and has not been seen before by these contributors: It was bicolored, with areas of blue and yellow (figure 28). Due to mixing of the colors, the stone appeared green when viewed in certain directions.

The 0.33 ct crystal was grown by a typical high pressure/high temperature process from an Fe-Co-C system at the Institute for Superhard Materials in Kiev, Ukraine, by Dr. S. A. Ivakhnenko; according to him, boron was introduced into the press accidentally. The synthetic diamond had a distorted cuboctahedral shape, and the blue color was distributed as cubic areas and rather irregular patches. Thus, some blue zones seemed to be confined to the cubic {100} sectors, while others did not appear to correspond to any crystallographic direction.

Microscopic examination revealed elongate metallic inclusions, due to which the synthetic diamond was rather strongly attracted by a common magnet; cubic growth features were seen on the surface. The synthetic diamond exhibited strong, irregularly distributed green luminescence to short-wave UV radiation, with a persistent phosphorescence lasting more than two minutes; the blue sectors appeared to luminesce more strongly than the yellow ones. The crystal was inert to long-wave UV.

As expected, testing for electrical conductivity revealed that the blue zones conducted electricity while the yellow zones did not.

To investigate the cause of color, we recorded infrared spectra on several different areas of the crystal, in the range of 7200–400 cm^{-1}, with a Perkin-Elmer Spectrum BXII FTIR-spectrometer. We then measured photoluminescence (PL) spectra from 533 to 794 nm with an SAS2000 Raman spectrometer at cryogenic temperature (77 K), and Vis/NIR spectra (400–1000 nm) with an SAS2000 spectrophotometer at room temperature.

We were unable to obtain IR spectra for each color separately, so the different areas showed only slight variations, and were mainly characterized by boron-induced absorptions at 4080, 3710, 2928, 2802, 2455, and 1290 cm^{-1} (figure 29). In addition, we recorded a weak sharp peak at 1344 cm^{-1}, a rather strong sharp feature at 1332 cm^{-1}, a shoulder at 1135 cm^{-1}, and peaks at 1046 and 950 cm^{-1}. The features at 1344 and 1135 cm^{-1} can be attributed to single-substitutional nitrogen (N^0), and the peaks at 1332, 1046, and 950 cm^{-1} are ascribed to N^+ (see S. C. Lawson et al., "On the existence of positively charged single-substitu-

Figure 28. This 0.33 ct bicolored synthetic diamond crystal exhibits both blue and yellow zones. Photo by T. Hainschwang.

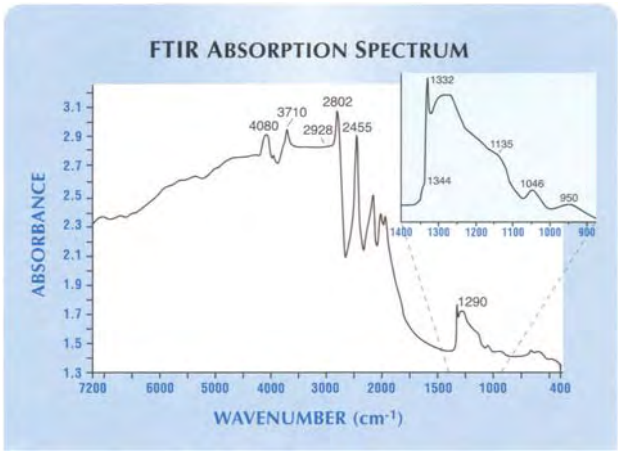

Figure 29. The IR spectrum of the synthetic diamond in figure 28 is mainly characterized by boron-induced absorptions. The inset shows the one-phonon area in more detail.

tional nitrogen in diamond," *Journal of Physics: Condensed Matter*, Vol. 10, No. 27, 1998, pp. 6171–6180).

The low-temperature PL spectrum showed a first-order Raman peak (at 573 nm) and a sharp, weaker peak at 694 nm (figure 30); this emission has recently been assigned to submicroscopic inclusions of synthetic ruby in synthetic diamonds (K. Iakoubovskii and G. J. Adriaenssens, "Comment on 'Evidence for a Fe-related defect centre in diamond,'" *Journal of Physics: Condensed Matter*, Vol. 14, No. 21, 2002, pp. 5459–5460) and relates to the Cr^{3+} emission of ruby.

The low-temperature Vis/NIR spectrum showed a rise in transmission up to about 540 nm and then a gradual decrease in transmission to 1000 nm; this spectrum is not indicative for the unusual coloration of this diamond.

Figure 30. The low-temperature PL spectrum of the bicolored synthetic diamond exhibits a first-order Raman peak (at 573 nm) and the 694 nm peak that is probably due to microinclusions of synthetic ruby.

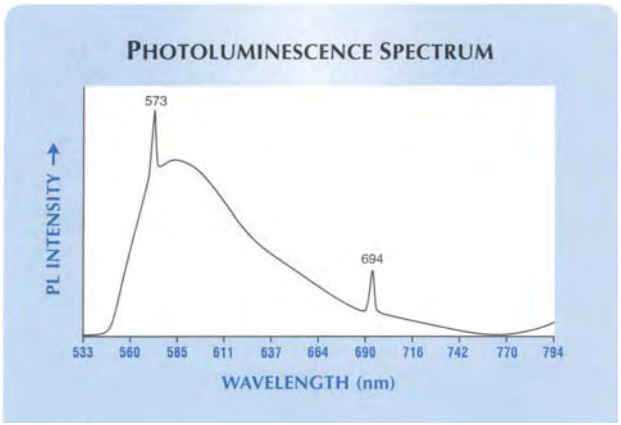

The blue and yellow coloration in this synthetic diamond is apparently due to a combination of boron and single-nitrogen defects. Although traces of nitrogen appear to be present in nearly all boron-containing diamonds, the presence of boron and relatively *high* amounts of nitrogen in the same stone is rather unusual. Normally, weak features due to N^+ and extremely weak absorptions due to N^0 can be found in natural diamonds. Synthetic blue diamonds sometimes show stronger N^0 peaks, but we have not yet seen them as defined as in this sample. Since nitrogen acts as an electron donor in diamond and boron as an electron acceptor, nitrogen will "neutralize" the effect of boron (H. Kanda and S. C. Lawson, "Growth temperature effects of impurities in HP/HT diamonds," *Industrial Diamond Review*, Vol. 2, 1995, pp. 56–61). Therefore, the dominant impurity will determine color and conductivity. The nitrogen:boron ratio is dependent on crystallographic orientation. Both prefer the octahedral {111} sectors, but nitrogen has a stronger affinity; boron is the major impurity in the cubic {100} and/or dodecahedral {110} sectors (R. C. Burns et al., "Growth-sector dependence of optical features in large synthetic diamonds," *Journal of Crystal Growth*, Vol. 104, 1990, pp. 257–279).

It has been shown that fluctuations in growth temperature can cause changes in the color of synthetic diamonds during growth (again, see Kanda and Lawson, 1995). This temperature-dependent variation of color from yellow to blue can only occur when a flux is used without a nitrogen getter (e.g., Ti, Zr, or Al). Under these conditions, both single nitrogen and boron can be incorporated into a synthetic diamond as substitutional atoms, and depending on the ratio of N and B, some areas are yellow, while others are blue. The bicolored crystal described here, which apparently was grown without a nitrogen getter, probably experienced these temperature fluctuations.

Thomas Hainschwang (gemlab@adon.li)
Gemlab Gemological Laboratory
Vaduz, Principality of Liechtenstein
Andrey Katrusha
Institute for Superhard Materials
Kiev, Ukraine

ANNOUNCEMENTS

Digital geologic map of Madagascar. In May 2003, Go Spatial Limited launched a detailed vector geological map of Madagascar for use with Geographic Information System (GIS) software. The map was digitized from the 1:1,000,000-scale geological map compiled in 1964 by Henri Besairie. The original French version has been translated into English, and re-projected to geographic (latitude/longitude) coordinates. The various data "layers" include general geology, mineral deposits, structure, and annotation; other layers such as roads, railroads, towns,

and hydrologic systems have been added to the data from the company's standard vector base map products. For more information, visit www.gospatial.com or e-mail info@gospatial.com.

Thailand gem adventure. The GIA Alumni Association is hosting a gem tour of Thailand from August 30 to September 12, 2003. The group will tour gem-cutting and manufacturing facilities in Bangkok as well as regional mines and gem centers. Also included are admission to the Bangkok Gems & Jewelry Fair and a visit to GIA Thailand. Call Sandy Kemp at 800-922-5027 or e-mail trafacil@aol.com.

AGTA Spectrum Awards competition. The AGTA Spectrum Awards, celebrating their 20th anniversary this year, recognize outstanding colored gemstone and cultured pearl jewelry designs from North America, as well as achievements in the lapidary arts. Winning entries will be displayed and award recipients honored at the 2004 AGTA GemFairs in Tucson and Las Vegas. The entry deadline is September 22; the competition will be held in New York City during October. For entry forms and more information, visit www.agta.org or call 800-972-1162.

Conferences

Jewellery World Expo 2003. Held in Toronto, Canada, on August 10–12, this show will feature several seminars on the current state of the diamond industry, jewelry illustration and rendering, and prevention of identification theft and diamond switching. Visit www.jewelleryexpo.ca or call 888-322-7333.

GIA GemFest USA. Held in conjunction with the Dallas Fine Jewelry Show in Dallas, Texas, on Saturday, September 20, 2003, GemFest USA will feature presentations on jewelry retailing and merchandising from the GIA School of Business, as well as the latest findings from the GIA Gem Laboratory. Also offered will be a Student Lab and alumni reception. Admission is free but pre-registration is required for the Student Lab; call 760-603-4001 or 800-421-7250, ext. 4001. For more information, visit www.gia.edu/alumni or www.midasshow.com.

IGC postponed. The International Gemmological Conference, which was planned for this September 24–30 in Wuhan, China, has been postponed until September 2004 due to concern over the SARS outbreak.

Training courses in heat treating corundum. In October 2003, a one-week class in Bangkok, Thailand, will be taught by Ted Themelis to give participants hands-on experience with heat treating ruby and sapphire. Both traditional and beryllium processes will be covered. Tuition is $1,200 per person, with a maximum of five students. Visit www.themelis.com/Products-6-Training.htm or e-mail gemlab@themelis.com.

Geophysical exploration for diamonds. The South African Geophysical Association is hosting its 8th Biennial Technical Meeting and Exhibition on October 7–10, 2003, at Pilanesberg National Park, South Africa. Diamonds are one of the conference themes, and a post-meeting field trip will visit the Premier mine on October 11. Visit www.sagaonline.co.za/2003conference, fax 27-12-362-5285, or e-mail ronelle.ce@up.ac.za.

Diamonds—From Source to Use. This colloquium will take place October 29–30, 2003, in Randburg (near Johannesburg), South Africa. Topics to be covered include the geology of diamond deposits, mining and recovery, the history of diamonds, applications in industry and technology, and global and South African perspectives on the jewelry industry. Visit www.saimm.co.za, fax 27-11-838-5923, or e-mail sam@saimm.co.za.

HRD diamond marketing conference. Following last year's conference on international diamond politics, the Antwerp Diamond High Council (HRD) will be holding a conference on diamond marketing and branding on November 3 and 4, 2003. Further information will be available as the dates approach; visit www.diamonds.be/hotnews.

SEG diamond and kimberlite course. The Society of Economic Geologists is holding a one-day course on diamond exploration and kimberlite geology at the University of Laval, Quebec, on November 24, 2003. The course will take place in conjunction with *Québec Exploration 2003*, and includes both lectures and hands-on sessions. Visit www.quebecexploration.qc.ca or e-mail chbochud@ggl.ulaval.ca.

Exhibits

Enamels at the Newark Museum. "Capturing the Sublime: The Enamels of Marilyn Druin" will be on display until December 31, 2003, at the Newark Museum in Newark, New Jersey. This memorial exhibition will feature over 30 pieces of her work, spanning three decades. Visit www.newarkmuseum.org/pages/exhibit/index.htm#Druin or call 973-596-6550.

Art Deco at the Royal Ontario Museum. "Art Deco 1910–1939," a traveling exhibit of more than 250 examples of early 20th century design, will be featured at the Royal Ontario Museum, Toronto, from September 20, 2003, through January 4, 2004. Visit www.rom.on.ca/explore/future.php or call 416-586-5549.

Tourmaline at Mineralientage München. This year's Munich gem show will take place from October 31 to November 2, and will feature an exhibit on multicolored tourmaline slices. A jewelry design competition also will be showcased. Visit www.mineralientage.com or e-mail info@mineralientage.de.

THANK YOU DONORS

GIA appreciates gifts to its permanent collection, as well as stones, library materials, and other non-cash assets to be used in GIA's educational and research activities. These contributions help GIA further its public service mission while offering donors significant philanthropic benefits. We extend sincere thanks to all 2002 contributors.

$100,000 OR HIGHER

Banks International Gemology, Inc.
Daniel & Bo Banks
KCB Natural Pearls
(K. C. Bell, G.G.)
Chatham Created Gems, Inc.
(Thomas H. Chatham)
J.O. Crystal Company, Inc.
(Judith Osmer)
William & Jeanne Larson
Kurt Nassau, Ph.D.
Art Sexauer
Ambaji Shinde
D. Swarovski & Co.
(Helmut Swarovski)

$50,000 TO $99,999

Robert & Marlene Anderson
Roben & Vergie Hagobian
Michael J. Kazanjian
R. Schwager

$10,000 TO $49,999

Anonymous
Aaland Diamond Company
American Gem Trade Association
German Ayubi
Rick Canino
Dust Devil Mining Co.
Susan G. Goldstein, G.G.
Korite International
Mayfield's Inc.
Stephen M. Neely, M.D.
Mona Lee Nesseth, G.G.
Pala International, Inc.
Fred & Carol Seeman
Star Ring, Inc.

$5,000 TO $9,999

Anonymous
Bear Essentials Co.
Jerry Bearman
Capalion Enterprises
Charles H. Fox
Harpaz Gem & Pearl, Inc.
Ben Jen Hoo, G.G.
Gerald Stockton
USAA Alliance Services Co.
Mary E. Wurst, Gemologist, A.J.P.
Helen Zara

$2,500 TO $4,999

Anonymous (3)
David M. Baker, G.G., C.G.A
Dudley Blauwet
China Pearl
Lance Davidson
Estate of James R. McShane
Robert J. Flude, III
Laura Hastings
Jewelmer International Corporation
Linda Koenig, G.G.
Rudolph W. Kopf
Oliver & Mo Martindale
Bromley Mayer
Moriarty's Gem Art
Elaine C. Rohrbach, Gemologist
Sean L. Trickett
Herb Walters

$1000 TO $2,499

Anonymous
Cosmo Altobelli, G.G., C.G.A
The Altobelli Jewelers, Inc.
Kirk & Brad Bandy
Barker & Co.
Robert Bell
Gordon Bleck
Mark Castagnoli
George R. Kaplan
Paul A. Krause
Gail Brett Levine, G.G.
Gerald L. Manning
McCormack & Puryear Jewelers
Martin Rapaport
Ramiro M. Rivero
Muriel Roston
Sterling Turquoise

$500 TO $999

Richard Ashley
Irmgard Blum, G.G.
Edgar Cambыre, G.G.
Edward Chase
Gems By Ivan, Inc.
Jeff Gurecky
Farooq Hashmi
Mary L. Johnson, Ph.D.
Johnston-Namibia C.C.
Herbert Mair
Fernando Cйsar Onofri
Bill Pinch
Douglas Rountree
Scheherazade Jewelers
Lewis & Alice Silverberg
Doris Wright

UNDER $500

Anonymous (5)
Gerald A. Alvarado, G.G.
Arthur L. Anderson
Auction Market Resource
Patrick B. Ball, G.G.
Boutique Art Designs
Kenneth S. Brown
Patricia A. Doolittle
Catherine B. Enomoto
Charlene Fischman, G.G.
Jesse Fisher
Si & Ann Frazier
Barry Friedman
Hershel M. Graubart, G.G.
Richard Heckle
Syed Iftikhar Hussain
Dr. Jaroslav Hyrsl
Stephen E. Ingraham
A. J. A. Janse, Ph.D.
Robert W. Jones
Joseph's Jewelers
Samir-Pierre Kanaan
Robert E. Kane, G.G.
Alice S. Keller
Haleem Khan
Kathryn Kimmel
Koblenz & Co. Estate Jewelry
Brendan M. Laurs, G.G.
Manfred Lehrl
Jack Lowell (Colorado Gem)
Peter Lyckberg
Joe Meyer
David Olson
Renato & Adriana Pagano
William L. Pankey
Charlotte Preston
Nicholas Rochester
Ralph Shapiro
Russell B. Shor
Marjorie J. Sinkankas
Rolf Tatje
Treasures of the Earth, Inc.
Ventana Mining Co. L.L.C.
Eva L. Weber, M.D.
Albert Zakin
Chen Zhonghui

GIA needs donations that vary in nature. Examples are signed pieces of historical jewelry, natural untreated and treated stones, synthetics and simulants, rare gemological books, and equipment and instruments for ongoing research support. If you are interested in making a donation and receiving tax deduction information, please call Patricia Syvrud at (800) 421-7250, ext. 4432. From outside the U.S., call (760) 603-4432, fax (760) 603-4199.

Book REVIEWS

2003

Krystallos—Brazil: Gem-Crystals in Design

By Sonia Fonseca and Norman M. Rodi, Eds., 178 pp., illus., publ. by Terra das Artes Editora, São Paolo, Brazil, 2002. US$120.00

Krystallos is an imaginative production that lovers of gem tomes may treasure as much for the experience as for its visuals and editorial content. The book's 16 1/2 x 12 inch (42 x 30.5 cm) size is the first clue its creators were thinking big and were emboldened to go over-the-top.

From the very first page, the book demands participation from the reader. Wrapping text is used to recapitulate a jeweler's design, a cutter's form, or the magic of nature's crystal shapes. Thereafter, artists' drawings trace design elements from creative spark to inspired experimentation, culminating in the finished pieces captured in superb photographs. Next, page cutouts invite the curious as readers uncover and discover for themselves the Brazilian gem bounty that exalted explorers and continues to enthrall the world. This book is distinguished from other works featuring extraordinary photography by its elevation of visual photographic images into the experiential. Treated papers shaped to evoke crystals and mineral specimens unfold to invite touch and inspire wonder. Smooth surfaces commingle with rough to create an interactive encounter beyond two dimensions. The heavy paper stock, rich color, and sewn binding contribute added quality to a richly sensual experience.

The featured pieces are no less inventive. Soaring crystals and vivid cut stones exemplify the spectacular trail of more familiar—but no less extraordinary—Brazilian gems. An aquamarine specimen suggests a horse's head and torso struggling to emerge from its stony confines while simultaneously appearing to melt off the page. Regal portrayals of Imperial topaz crystals validate the ancient Greek designation of *krystallos*, their word for transparent ice thought to have hardened into what we recognize today as a crystal.

The inventive layout uses English translations to mirror the Portuguese text in a bilingual format arranged to inform and underscore a design's essence. Speaking through their designs (and, sometimes, in their own words), the 16 artists herald an emerging Brazilian presence unconstrained by European traditions. Some designers incorporate native elements such as seeds and straw into their work. The German and Scandinavian design influences are like the book's few translucent pages, which allow light to pass through yet cast a distinctive beauty all their own. As one example, Ruth Grieco's tourmaline crystal cross is a stunning interpretation of a familiar motif taken to another level.

Editorial collaborators Fonseca and Rodi, the latter a graduate gemologist, have combined their talents with those of gifted photographers, lapidaries, jewelry artists, and book designers to celebrate Brazil's gem landscape and proclaim pride in their cultural heritage. Though the book requires more head-turning, effort, and reading space than most, jewelry designers, gemologists, gem and mineral collectors, and all who seek the unique and extraordinary will find ample reward in the realm of *Krystallos*.

MATILDE PARENTE
Rancho Mirage, California

The Fabergé Menagerie

*Organized by the Walters Art Museum, Baltimore, MD, in cooperation with the Fabergé Arts Foundation, Washington, DC, 192 pp., illus., publ. by Philip Wilson Publishers, London, 2003. US$25.00**

In 1900, railroad magnate Henry Walters cruised the Baltic Sea on his yacht. In St. Petersburg, he was taken to visit the House of Fabergé, where he made the first of many purchases. In so doing, he became one of Fabergé's first American clients. Walters's collection of Fabergé animal carvings lies at the heart of an exhibition that was on display at the Walters Art Museum from February 13 through July 27, 2003.

Created to accompany the exhibition, this book contains a wealth of information on the House of Fabergé and the amazing objects produced in its workshops. Starting with a historical overview of the firm, the book then moves into a chapter devoted to Fabergé's clients and some of the magnificent items made especially for them. Notable in these chapters are the amazing Easter eggs created for the Russian czars. Also included is a discussion of gem and jewelry arts in Russia during the 17th through the 19th centuries. The catalog of the exhibition follows, with each item beautifully photographed. Interestingly, the exhibition begins with pieces that can be viewed as precursors to Fabergé's

work as well as a collection of Japanese netsuke, the tiny animal carvings once used as belt toggles. The influence of these items can be seen in many of the Fabergé pieces. Well written and beautifully presented, this book can be enjoyed by anyone, even those who did not have the good fortune to visit the exhibition.

JANA E. MIYAHIRA-SMITH
Gemological Institute of America
Carlsbad, California

The Great Book of Amber

By Elżbieta Mierzwińska, photos by Marek Żak, 160 pp., distrib. in the U.S., Canada, and Australia by Amber#1, San Francisco, CA, 2002. US$45.00

From the moment you see the cover, with its gallant hippocampi (horses with serpent-like tails), you'll know this is no ordinary book about amber. While amber's scientific value as a window into the past is well known, its value as a material of fine art is often overlooked, and few museum collections have exhibits devoted entirely to amber. Malbork Castle in Poland, once home to the Teutonic Knights and now a renowned museum, features a huge assemblage of rare amber ornaments known as the Malbork Amber Collection. The 2,000+ items, which started out as lumps of ancient tree resin, have been artistically transformed into caskets, altars, sculpted figures, folk art, and other objects in shades of off-white, yellow, brown, and orange. These items, along with unusual specimens in their natural state, are featured in the more than 150 beautiful color images accompanied by a historical timeline. Written by the senior custodian of the exhibit, this book explains the creation of ancient amber forests, details the development of amber artistry in the Baltic region, and displays amber objects dating from Neolithic to contemporary times.

Unfortunately, the book suffers somewhat from Polish-to-English translation problems. The organization is also odd (it lacks both a table of contents and an index), and the text layout makes the book difficult to read in spots. Explanatory details are sometimes lacking in discussions of the featured pieces. Nevertheless, my overall impression of this book is positive. It is of a good size, and the materials are high quality. The information is very interesting, and some of the scenic and scientific illustrations dating from as early as the 1500s are quite impressive. My personal favorite was of men in boats "fishing" for amber in the sea.

The writer's stated purpose is to further the knowledge and love of amber in Poland and throughout the world; in this she has succeeded. Amber collectors, historians, and European travelers will find this book of great interest. Much like the ancient resin that protected the trees from invaders and preserved the insects for later study, this book serves well to preserve and protect the works of master amber craftsmen throughout time.

MARY MATHEWS
Gemological Institute of America
Carlsbad, California

The Rings Book

*By Jinks McGrath, 128 pp., illus., publ. by Krause Publications, Iola, WI, 2003. US$24.95**

This book describes the basics of ring making, although it is most appropriate for the intermediate jeweler. Ms. McGrath assumes that the reader has a practical knowledge of the essential techniques of jewelry making, as she does not cover the specifics of soldering, filing, sanding, and the like. Project based, the book is divided into four major sections: building shanks, mounting, setting, and finishing. In addition, there is a gallery of contemporary rings, a glossary of terms, and a list of suppliers.

In the first section, on the building of shanks, the projects proceed logically from the simple to the complex. The first project is the simple band, which is followed by a half-round ring, a double-banded ring, hollow rings, tension-set rings, and so on—a dozen rings in all. Carving wax, enameling, anticlastic raising, fusing, and texturing are covered. The discussion of each ring is preceded by a list of requisite supplies and contains various tips. There are numerous clear photographs, and the text is understandable and concise. The second section describes the construction of mounts and contains effective diagrams and useful formulas. Various styles and shapes of bezels are discussed, as well as how to fabricate a claw mount. Each mount is made to be soldered to the rings fabricated in section one. The third section deals with the actual setting of stones into the mounts; bezel, gypsy, and bead setting are covered. The final section deals very briefly with finishing issues: polishing, matte finishes, sizing, and the like.

While there is useful information in this book, at 128 pages (including the photo gallery) it is far too brief to adequately cover all of the subjects addressed. In general, the sections on shanks and mounts are useful, but those on setting and finishing could be much expanded.

STEVE WORKMAN
Gemological Institute of America
Carlsbad, California

OTHER BOOKS RECEIVED

The Ultimate Orient: Philippine South Sea Pearls. *Photography by Scott Tuason, 175 pp., publ. by Jewelmer International Corp., Makati City, Philippines, 2001, US$65.00. E-mail: sales@jewelmer.com.* This book is a striking collection of images captured by award-winning underwater photographer Scott Tuason. More than 160 photos follow the journey of the Philippine South Sea cultured pearl from the *Pinctada maxima* oyster to finished jewelry. Also shown are Philippine pearl farm seascapes and colorful images of marine life.

STUART D. OVERLIN
Gemological Institute of America
Carlsbad, California

Gemological **ABSTRACTS**

2003

COLORED STONES AND ORGANIC MATERIALS

Agate: A study of ageing. T. Moxon, *European Journal of Mineralogy*, Vol. 14, No. 6, 2002, pp. 1109–1118.

The degree of crystallinity (i.e., crystallite size) of agates from 11 locations on five continents was determined by powder X-ray diffraction analysis. These agates formed within vesicles (gas cavities) in volcanic rocks; the ages of these rocks were obtained from the literature. The author found a strong correlation between agate crystallinity and age of the host rocks. Over geologic time, ageing allows the crystallite size to increase. Accordingly, the determination of agate crystallite size should allow an estimation of the approximate age of the host rock, which can be used to differentiate known agate deposits (since each has a unique age). The same correlation was deduced between agate density and age of the host rock.

These conclusions have several potential applications. For example, an agate "artifact" purchased in Idar-Oberstein was shown most likely to have originated from Brazil rather than Germany on the basis of its degree of crystallinity and density. However, for this technique to become an accepted gemological tool, a large database with crystallinity and age data for volcanic agates and their associated host rocks, from many localities worldwide, must be developed. This method is not currently applicable to agates occurring in sedimentary rocks. *KAM*

Bright prospects for pearl culture in India! A. K. Sonkar, *Infofish International*, January 2003, pp. 13–16.

In southern India, two species of freshwater mollusk (*Lamellidens marginalis* and *L. corrianus*) that commonly occur together in lakes and ponds are suitable for the production of spherical cultured pearls. In the Indian Ocean, the Andaman

This section is designed to provide as complete a record as practical of the recent literature on gems and gemology. Articles are selected for abstracting solely at the discretion of the section editor and his reviewers, and space limitations may require that we include only those articles that we feel will be of greatest interest to our readership.

Requests for reprints of articles abstracted must be addressed to the author or publisher of the original material.

The reviewer of each article is identified by his or her initials at the end of each abstract. Guest reviewers are identified by their full names. Opinions expressed in an abstract belong to the abstracter and in no way reflect the position of Gems & Gemology *or GIA.*

and Nicobar Islands are a source of the black-lipped pearl oyster *P. margaritifera*. Although no sites with a dense oyster population have been identified in these waters, hatchery techniques have been successfully developed. A project to produce high-quality cultured pearls is awaiting environmental approval from the Andaman Islands administration. India also has produced bead nuclei 8–22 mm in diameter from several indigenous mollusk species (e.g., the green turbo shell and the helmet shell). *CT*

Chinese Akoya—A tough road to a bright future. M. Wong, *Jewellery News Asia*, No. 217, September 2002, pp. 104–115 passim.

The main production and processing centers for Akoya cultured pearls in southern China are in Guangdong Province (~60%) and Guangxi Province (~40%). Both production and price have declined in recent years. The decline in production is due, in part, to an increase in the mortality rate of seeded oysters (from 30% to 50–70%), with an additional 10–20% mortality if typhoons occur. Mortality is attributed to: (1) ocean pollution from pesticides and high-density farming; (2) weak oyster species because those from hatcheries are repeatedly inbred, which increases the occurrence of genetic disease; (3) insertion of large (7 mm or larger) nuclei that are frequently expelled and cause weaker oysters to die; and (4) heavy rains, which can cause intolerable decreases in salinity. Decline in production is also related, in part, to continually falling prices and a sluggish global market that has forced farmers to operate below cost; 90% of the producers suffered losses in the past two years.

The prediction for 2003 is that the price for Chinese Akoya cultured pearls will rise to approximately US$1,100/kg, primarily because of a decline in Akoya production in both China and Japan. Increased education about improved farming techniques and proactive government support regarding ocean planning, density control, and species research (e.g., crossbreeding of oysters) will be needed for industry growth. Japanese companies are being encouraged to cultivate and process Akoya cultured pearls in southern China; their investment could revitalize the Chinese industry. Both price and production of Chinese Akoya cultured pearls are expected to rise in 2004. *CT*

Colour in quartz: From atomic substitutions to nanoinclusions. P. Vasconcelos, B. Cohen, and N. Calos, *Australian Gemmologist*, Vol. 21, No. 8, 2002, p. 278.

This brief review of the causes of color in quartz maintains that color intensity is directly proportional to Fe content. Furthermore, analytical results indicate that the untwinned *z*-sectors in amethyst have higher Fe contents than the twinned *r*-sectors, which is opposite to the distribution posed by other researchers.

In chrysoprase from Marlborough, Queensland, the color may be due not to nanoinclusions of willemseite (a Ni-talc), as previously suggested in the literature, but to "pimelite," a poorly ordered talc mineral. *RAH*

Experimental production of half pearls from tropical abalone *Haliotis varia* (Linn.) at Mandapam. A. C. C. Victor, B. Ignatius, and I. Jagadis, *Marine Fisheries Information Service, Technical & Extension Series*, No. 170, 2001, pp. 9–10.

In 1897, Louis Boutan pioneered the experimental growth of blister and semi-spherical cultured pearls in abalone. Others refined this technology, and in the 1950s Dr. Kan Uno produced "hemispherical" cultured pearls from several abalone species. Currently, there is no commercial production of spherical cultured abalone pearls, but cultured blister pearls are grown in many countries.

In the late 1990s, the Central Marine Fisheries Research Institute's regional center in Mandapam, India, developed a method for the production of cultured blister pearls from the tropical abalone *Haliotis varia*. Extreme care is taken to avoid trauma, shock, or injury to the abalones during nucleation, after which they are suspended in box-type cages in the ocean, fed seaweed (Ulva sp.) bi-weekly, and observed monthly for nacre coating. The cultured blister pearls are harvested after four months; about 40% have a good nacre coating. *CT*

Is the pearl's rarity under threat? M. Wong, *Jewellery News Asia*, No. 224, April 2003, pp. 32–33.

The world cultured pearl production in 2002 totaled about 558 tonnes, composed of Chinese freshwater (500 tonnes), Akoya (42.5 tonnes), black (11 tonnes), and South Sea (4.5 tonnes). Their combined value was $535 million. These figures show declines of 21% in tonnage and 30% in value from the "boom year" of 2000. The biggest decline (23% in tonnage and 60% in value) came in the Chinese freshwater product. Akoya production increased an estimated 10%, while black and South Sea cultured pearl production remained relatively constant in tonnage but declined significantly in value. In the case of Chinese freshwater cultured pearls, top-quality goods—perfectly round with good color—represent only a tiny fraction of the production, much less than 1%. Other categories have higher proportions of good-quality pearls—half are medium or high quality in shape and color.

Although prices have fallen, cultured pearls will retain their preciousness because such declines make it uneconomical for many producers to continue operating, thus better matching supply to demand. The article concludes that there will always be demand for cultured pearls, based on a long tradition of preciousness, and that in good economic times demand often exceeds supply. *RS*

Pioneer on hatchery technology shares views on pearling. J. Henricus, *Jewellery News Asia*, No. 218, October 2002, pp. 34–38.

Australia-based Pearl Oyster Propagators Pty. Ltd. (POP) has pioneered hatchery and cultivation technology since 1989. Innovations include stock enhancement or selective breeding to produce mantle tissue that influences the color and surface of South Sea cultured pearls. The company considers its greatest achievement to be the reliable and routine cultivation of large numbers of *Pinctada maxima* oysters for the commercial production of South Sea cultured pearls. POP typically achieves 97% or more saleable product from a harvest of hatchery-produced oysters, with the cultured pearls averaging about 0.78 momme (2.93 grams) each.

POP is involved in pearling in Australia, Indonesia, and Thailand, where it has designed and built hatcheries and farm-based camps, generally working with companies that are expanding or moving to hatchery production. Preliminary research in mantle-tissue selection with respect to factors affecting cultured pearl color indicates: (1) the graft may be more important than the host in determining the white/"silver" coloration; (2) some yellow and "golden" colors are not determined solely by the graft tissue, but instead they appear to be influenced by a combination of the donor tissue, host oyster, and marine environment; and (3) careful selection of mantle tissue from oysters with strong gold-lipped characteristics helps ensure the production of "golden" cultured pearls.

CT

Zuchtperlen vom Golf von Kalifornien, Mexiko (Cultured pearls from the Gulf of California, Mexico). L. Kiefert, *Gemmologie: Zeitschrift der Deutschen Gemmologischen Gesellschaft*, Vol. 51, No. 2–3, 2002, pp. 121–132 [in German with English abstract].

Historically, the Gulf of California was famous for its splendid natural black pearls, but these became scarce at the beginning of the 20th century. Since then, several attempts have been made—with varying degrees of success—to culture pearls in this area. Today cultured black spherical and mabe pearls are produced in a number of farms. One such farm at Guaymas, which first started as a university research project, is described along with an account of the current status of pearl culture in the Gulf of California. Typical properties of these cultured pearls are presented. *RT*

DIAMONDS

Conflict of interests or interests in conflict? Diamonds and war in the DRC. I. Samset, *Review of African Political Economy*, No. 93/94, 2002, pp. 463–480.

War has been raging within the Democratic Republic of the Congo (DRC) since August 1998. From 1998 to 1999, official diamond exports declined 40%; this decline was even sharper in 2000. During the latter part of 1998, the armies of Rwanda and Uganda, aided by insurgent Congolese, occupied vast sections of the country's eastern provinces. These countries have no indigenous diamond production, yet rough diamond exports from Uganda were $1.44 million in 1998, $1.81 million in 1999, and $1.26 million from January to October 2000. Exports from Rwanda rose from nearly nil in 1998 to $1.79 million in January-October 2000.

Both countries have drawn important economic benefits from diamonds taken from the DRC areas, through re-exportation fees, barter, and taxes. They have thus developed vital stakes in the continuation of conflict in the eastern portion of the DRC. Elsewhere in the country, former DRC president Laurent Kabila granted lucrative diamond mining concessions to Zimbabwe in exchange for that country's help in fending off the Ugandan-Rwandan backed rebels. The Zimbabwean venture, Operation Sovereign Legitimacy, won the right to two of the DRC's richest diamond deposits, Tshibwe and Senga Senga. These revenues have helped shore up Zimbabwean ruler Robert Mugabe's Zanu-PF party.

Within the DRC, the diamond-trading industry acquired more economic power than (then) President Kabila. This article cites an incident in which the head of the Congolese Diamond Federation (FCD), Ngoyi Kasanji, was arrested by Kabila's security forces as he brought a 266 ct diamond to the city of Kinshasa. The guards seized the stone, but Kabila was unable to sell it because the FCD and others instructed buyers not to buy it from him. Kabila eventually returned the stone to Kasanji who sold it to an Israeli dealer.

The article concludes that Uganda, Rwanda, and Zimbabwe, having gained control over part of the DRC's resources, have an economic interest in perpetuating their exploitation by prolonging the conflict. *RS*

Diamond genesis, seismic structure, and evolution of the Kaapvaal-Zimbabwe craton. S. B. Shirey, J. W. Harris, S. H. Richardson, M. J. Fouch, D. E. James, P. Cartigny, P. Deines, and F. Viljoen, *Science*, Vol. 297, No. 5587, 2002, pp. 1683–1686.

The Kaapvaal-Zimbabwe craton (mainly underlying South Africa and Botswana-Zimbabwe) of southern Africa has been the world's major source of diamonds since the 1870s. However, diamonds from various parts of the craton differ in many respects, such as age, origin, nitrogen contents, carbon isotope ratios, and types of inclusions. This article reports the results of two decades of geologic and mineralogic studies on more than 4,000 diamonds from the major diamond deposits in this craton, as well as geophysical studies (i.e., seismic imaging) of the lithospheric mantle. It then relates diamond formation and characteristics to the creation, assembly, and subsequent modification of the craton.

The lithospheric mantle beneath the Kaapvaal-

Zimbabwe craton shows variations in the seismic P-wave velocity at depths within the diamond stability field that correlate to differences in the composition of diamonds and their inclusions. Middle Archean (~3.2 By [billion years] ago) mantle depletion events initiated craton keel formation and early harzburgite-type diamond formation. Late Archean (2.9 By) accretionary events involving an oceanic lithospheric component (i.e., subduction) stabilized the craton and contributed to a younger generation of eclogitic diamonds. Subsequent Proterozoic tectonic and magmatic events (2 By) altered the composition of the continental lithosphere and added new lherzolitic and eclogitic diamonds. Thus, diamond formation in the Kaapvaal-Zimbabwe craton is episodic rather than continuous, with a time gap of ~300 million years (My) between the two Archean diamond formation events and a further gap of 900 My for the formation of the Proterozoic diamonds. These multiple generations of diamonds have characteristic properties. The diamonds were carried by kimberlites to the surface significantly later, between 1,600 and 65 My ago. *AAL*

Diavik diamond mine: Gems spill forth from Lac de Gras. H. Ednie, *CIM Bulletin*, Vol. 96, No. 1068, 2003, pp. 13–26.

Canada's second diamond mine, Diavik, consists of four kimberlite pipes that are about 55 million years old. Diamond production began in late 2002, and the mine is currently ramping-up to full production that is expected by 2004 to reach ~7 million carats annually for perhaps 20 years. The mine is a joint venture between Diavik Diamond Mines Inc. [Rio Tinto] (60%) and Aber Diamond Mines Ltd. (40%). The operation, ~300 km northeast of Yellowknife in the Lac de Gras region of the Northwest Territories, is in an extremely remote and inhospitable location, which made mine construction extremely difficult. This was further complicated by the fact that all of the pipes are under the shallow waters of a large lake.

This article presents a summary of all aspects of the Diavik project (except the initial exploration and economic evaluation of the pipes). Particular emphasis is on: the engineering aspects of constructing the water-retention dikes that isolate the kimberlites from the lake, thus enabling the pipes to be mined by open-pit methods; mining techniques that are challenged by the very abrasive host rock (i.e., granite) of the kimberlites; extracting the diamonds from the ore (i.e., crushing the kimberlite and then extracting the diamonds with a dense medium [ferrosilicon]); commitment to responsible operation (i.e., attention to the environment in matters such as wildlife habitat and water quality); and serving the surrounding community (e.g., a commitment to employ northerners and to ongoing employee training). An advisory board of aboriginal, company, and government representatives meets periodically to review environmental and other issues. Diavik is a true success story when it comes to cooperation, partnerships, and involvement with local communities. *CT*

I Diamanti a Roma. L. Oggioni and R. Appiani, *Rivista Mineralogia Italiana*, Vol. 27, No. 1, 2003, pp. 6–15.

An account is given of an exceptional diamond exhibition held in Rome in 2002. It is illustrated by 20 color photographs, including those of the 616 ct rough diamond from the Dutoitspan mine at Kimberley, and the following faceted stones: the 101.27 ct "Dawn of the Millennium," the light blue "Idol's Eye" (70 ct) from Golconda, a 10.57 ct "rose" diamond, the "amber"-colored 61.50 ct "Tiger Eye" from the Vaal River near Kimberley (recently remounted by Cartier in an aigrette), and the 60.19 ct Mouawad-Mondera diamond. *RAH*

The Kimberley Process: Conflict diamonds, WTO obligations and the universality debate. T. M. Price, *Minnesota Journal of Global Trade*, Vol. 12. No. 1, 2003, pp. 1–69.

This article traces the background of the wars in Angola, Sierra Leone, and the Democratic Republic of the Congo, and the legal framework for the rough-diamond certification scheme designed to end traffic in diamonds that sustained these conflicts—that is, the Kimberley Process (KP).

The KP mandates that each participating diamond-producing nation provide certification for all diamonds it exports from legitimate sources. Importing nations must require the certificates before allowing the shipments to enter the country. All certificates must carry the same information, including the total carat weight of the parcel, quality characteristics of the diamonds, value, and identification of both exporter and importer. Importing diamonds without such certification could result in legal sanctions. Enactment of KP initiatives, especially in the U.S., is essential, as the U.S. imported $800 million in rough diamonds in 2000, much of which was re-exported elsewhere.

One potential obstacle to implementing the requirements of the Kimberley Process was the World Trade Organization (WTO), which bans discriminatory trade practices. However, the author argues that the WTO is not the proper overseer for such a regulatory enforcement scheme and that it would be a mistake to allow a narrow interpretation of its rules to prevent action against security threats, environmental concerns, and humanitarian crises. [*Abstracter's note:* The WTO recently ruled that the KP was not a violation.]

The author believes that the KP certification scheme is not a fail-safe guarantee against the trade of conflict diamonds. Monitors will have to keep track of statistics from each participating country and be alert to anomalies. Ultimately, the KP can work only to the extent that each country vigorously enforces the ban on conflict dia-

monds at its own borders; it does not have the force of international law.

However, the KP regulations could help promote economic stability within diamond producing nations, thus allowing legitimate governments to establish adequate control over their diamond resources. This will enable them to reap benefits from tax revenues and remove the incentive for rebels to wage war to control diamond areas.

RS

Les Diamants. Du cœur de la terre au cœur du pouvoir (Diamonds. From the heart of the earth into the heart of power). *Pour la Science—Dossier*, April–June 2002, 120 pp. [in French].

This entire issue of the French edition of *Scientific American* was inspired by, and closely reflects, the diamond exhibition of (almost) the same name in Paris in 2001. It is divided into a foreword (A Diamond World) and four main sections of approximately equal size: Natural Diamonds, Diamonds as a Material, Gem Diamonds, and The Symbolism and Political Importance of Diamonds. Thirty-three authors have contributed 24 articles to this volume.

In the Natural Diamonds section, two articles give a clear and concise description of the formation of diamonds in the (upper) mantle and their transport to the surface, answering such questions as: What can diamonds and their inclusions tell us about the structure of the Earth or the growth conditions and age of diamonds? This is followed by articles on: a new (non-kimberlite or lamproite) type of diamond occurrence in French Guyana; the history of diamond exploration and mining in Canada; and the role of inclusions and crystal forms/surfaces in divulging the growth history of diamonds, including the puzzling characteristics that distinguish microdiamonds (<0.5 mm) from "normal" diamonds. Perhaps the most fascinating article in the volume is one on the discoveries made by astronomers. Not only are there xenon-containing nanodiamonds in meteorites that are older than the solar system, which probably came from supernovae, but nanodiamonds may also be major constituents of interstellar dust, possibly as clouds around giant stars grown by processes similar to chemical vapor deposition (CVD).

The Diamonds as a Material section reflects the diverse applications of diamonds in modern technology—they are no longer for just cutting and drilling. Two articles describe the history and modern synthesis of diamonds by "traditional" high pressure/high temperature procedures, as well as diamond films produced by CVD. Another investigates the surface of type II diamonds using tunnel microscopy. The remaining articles in this section describe a wide range of applications of diamonds in an equally wide range of fields, including their uses as semiconductors, UV laser diodes, detectors for specific molecules, storage devices for DNA strings, optical windows for lasers, laser lancets in eye surgery, and even in cell phones and flat screens.

The Gem Diamonds section gives a comprehensive survey of the all-important gemological aspects. These include the present and future role of synthetic diamonds in jewelry, the numerous diamond imitations (from glass to synthetic moissanite), treatments (laser drilling, fracture filling, HPHT), the colors of diamonds and their origins, and the criteria used for the classification of colorless diamonds. While these articles do not offer much new insight for the professional, they may well serve as an introduction for beginners in gemology.

The final section (The Symbolism and Political Importance of Diamonds) contains three articles. One analyzes how in recent years the diamond syndicate faced new competitors (e.g., the Argyle mine and Russia) yet managed to maintain control over much of the market. The second tells the well-known stories of the Hope and Koh-I-Noor diamonds (the photo on page 111 definitely does not show the old Koh-I-Noor cut, as stated in the caption) but missed the opportunity to relate the story of some of the newer large diamonds (e.g., the Centenary and the Incomparable). The final article discusses the role of diamonds in religion, philosophy, politics, and medicine, and is adapted from H. Bari and V. Sautter, Eds. (2001) *Diamants. Au Cœur de la Terre, au Cœur des Etoiles, au Cœur du Pouvoir*, Jeddah, Paris.

The volume is beautifully illustrated and contains much updated and well-organized information.

RT

A note on diamond incidence in Wairagarh area, Garhchiroli District, Maharashtra. K. Sashidharan, A. K. Mohanty, and A. Gupta, *Journal of the Geological Society of India*, Vol. 59, No. 3, 2002, pp. 265–268.

A single octahedral crystal (0.15 ct) of gem-quality diamond with a light green tint was found in a highly deformed conglomerate in the Wairagarh area of central India. The mining of this Early Proterozoic conglomerate for diamonds dates back to the 1400s, but this is the first diamond to be reported from the area in over a century. This discovery adds encouragement to the current search for diamond deposits in the Wairagarh area.

RAH

Optical characterization of natural Argyle diamonds. K. Iakoubovskii and G. J. Adriaenssens, *Diamond and Related Materials*, Vol. 11, No. 1, 2002, pp. 125–131.

This article details results of optical absorption and photoluminescence (PL) studies of the defect centers in diamonds from Australia's Argyle mine, including the rare pinks, greens, and blue-grays. These investigations indicate that: (1) a common feature of Argyle diamonds is the presence of optically active hydrogen and nickel atoms; (2) there is a direct correlation between the intensity of the 3107 cm^{-1} hydrogen-related peak and nitrogen concentra-

tion; (3) the correlation between the 3107 cm^{-1} peak and nitrogen concentration is not sensitive to the form of the nitrogen (i.e., NH_3, NH_4, and N_2 gases may have been sources of nitrogen during diamond growth); (4) many Argyle diamonds were naturally irradiated (with alpha particles) below 600°C, resulting in the green to green-gray crystals; and (5) the uniqueness of Argyle's blue diamonds results from the high hydrogen content, a low concentration of tri-nitrogen complexes, and a high concentration of the two- and four-nitrogen defects. *SW*

GEM LOCALITIES

Australian sedimentary opal—Why is Australia unique? D. Horton, *Australian Gemmologist*, Vol. 21, No. 8, 2002, pp. 287–294.

The sedimentary opal deposits of central Australia, which currently produce about 95% of the world's play-of-color opal, occur along flat-lying layers within 30 m of the Earth's surface and are a product of a unique set of geologic events. Between about 122 and 91 million years (My) ago, the area was covered by an epicontinental sea and the sediments being deposited there were derived from volcanic rocks and were organic-rich; these form the host rocks for the opal deposits.

Following their exposure at the surface due to the lowered sea level, the host rocks were subjected to prolonged subtropical weathering until about 40 My. During this period, the water table was close to the surface and was acidic, releasing Si and Fe from weathering of the host rocks. The climate then became more arid, the water table lowered, and the groundwater became alkaline. Mild folding of the rocks at 24 My gave rise to subtle long-wavelength surface folds that facilitated both lateral and vertical migration of the Si released earlier. Opal was preserved in the weathered profiles beneath the crests of developing surface folds as the water table lowered; siliceous cap rocks discouraged erosion. Geologists believe that the volume of opal produced in the past 150 years in Australia is only a minute fraction of the amount yet to be discovered. *RAH*

Edelsteinbergbau im Festgestein: Zwei Beispiele aus Pakistan (Gemstone mining in solid rocks: Two examples from Pakistan). H. C. Einfalt, *Gemmologie: Zeitschrift der Deutschen Gemmologischen Gesellschaft*, Vol. 51, No. 4, 2002, pp. 153–170 [in German with English abstract].

A comparative description is given of the Katlang/Shomzo topaz mine and the Gujar Killi emerald mine, both in northern Pakistan. They are believed to be geologically linked, and their origins are related to the collision of the Indian and Asian plates. After an overview of their geology and mineralogy, and especially of the formation of the topaz and emerald, there is a summary of the mining history and activities, production processes, and future prospects for these gem deposits. The former government-owned Gemstone Corporation of Pakistan has ceased mining these deposits, and the new private owners have encountered problems that have resulted in production delays. Nevertheless, there seems to be good potential at least for the Gujar Killi deposit. *RT*

Gem-quality spessartine-grossular garnet of intermediate composition from Madagascar. K. Schmetzer and H-J. Bernhardt, *Journal of Gemmology*, Vol. 28, No. 4, 2002, pp. 235–239.

In the course of conducting a study comparing the chemical and spectroscopic properties of pyrope-spessartine (Malaya) garnets from Bekily, Madagascar, with those of spessartines from various parts of Madagascar, the authors discovered an unusual spessartine-grossular garnet. This light yellowish orange gemstone weighed 0.42 ct and was found to consist of 49 mol.% spessartine, 41 mol.% grossular, 5 mol.% almandine, and 5 mol.% pyrope. Although the color and absorption spectrum were similar to that of low iron-bearing spessartine, this garnet can be separated from spessartine, as well as from the orange variety of grossular (hessonite), by its S.G. (3.97) and R.I. (1.770). Separating it from intermediate members of the pyrope-almandine and pyrope-spessartine series is accomplished on the basis of color and spectroscopic features. In the future, if other intermediate garnets in the spessartine-grossular series are found, particularly if they contain different trace-element contents, an overlap of gemological features could occur. *WMM*

Londonit aus Madagaskar—Eine neue Mineralart (Londonite from Madagascar—A new mineral species). F. Pezzotta, V. Diella, and F. Demartin, *Lapis*, Vol. 28, No. 2, 2003, pp. 35–38, 50 [in German].

This article offers some additional information to supplement the article on londonite published by B. M. Laurs et al. in the Winter 2002 issue of *Gems & Gemology* (pp. 326–339). While the *G&G* article focuses on the description of the gemological properties, this article mainly presents chemical analyses obtained to establish the properties of the rhodizite-londonite solid-solution series. *RT*

Mineralogical and geochemical studies on the different types of turquoise from Maanshan area, east China. X.-Y. Yang, Y.-F. Zheng, X.-M. Yang, X. Liu, and K. Wang, *Neues Jahrbuch für Mineralogie, Monatshefte*, No. 3, 2003, pp. 97–112.

Turquoise is found in veins and clefts within altered volcanic rocks of the Maanshan area in Anhui Province, China. It varies from "sky" blue to bluish green, and usually forms massive or botryoidal aggregates. Chemical analyses show that it belongs to the turquoise-chalcosiderite series, with some substitution of Al by Fe^{3+}. IR

spectra are presented. The Mohs hardness was calculated at 3.23–3.56, which is low for turquoise (perhaps due to its small grain size or alteration); the hardness of turquoise is generally 5–6. Normalized rare-earth-element patterns of three different types of turquoise from the area show a small negative europium (Eu) anomaly, which suggests that they all have the same genetic source. *RAH*

Mintabie opal drilling program. J. Gum, *MESA Journal*, Vol. 26, July 2002, pp. 26–27.

A concerted effort is being made, using the most modern exploration methods, to find additional opal reserves in and around Mintabie, South Australia. In 2001, a drilling program was conducted in which 135 rotary auger holes were drilled within the Mintabie Sandstone; the majority reached the target depth of 18.29 m (the nominal maximum depth of mining in the Mintabie area). This and previous drilling indicate two parallel zones of potentially opal-bearing sandstone lying northwest-southeast. Further drilling indicated significant areas of opal-hosting sandstone along the southern border of the area, a direction which could be expanded. Geophysical techniques employed include downhole logging tools from which useful gamma and neutron porosity logs have been obtained, as well as airborne surveys from which digital terrain models and total magnetic intensity images have been generated, which correlate well with the drilling results. Exploration is ongoing and encouraging. *CT*

Seltenheiten aus Mogok, Myanmar (Rarities from Mogok, Myanmar). R. Schlüessel, C. C. Milisenda, and F. Bärlocher, *Gemmologie: Zeitschrift der Deutschen Gemmologischen Gesellschaft*, Vol. 51, No. 4, 2002, pp. 185–190 [in German with English abstract].

Gemological and other properties are given for three rare gems recently discovered in Mogok: poudretteite ($KNa_2B_3Si_{12}O_{30}$), periclase (MgO), and thorite ($ThSiO_4$). A 3 ct faceted violet poudretteite had a density of 2.53 g/cm^3 and refractive indices of n_o = 1.511 and n_e = 1.532, with a maximum birefringence of 0.021. The rough was mined from marble. [*Editor's note:* See Spring 2003 *Gems & Gemology*, pp. 24–31, for a full report on this stone.] A periclase cabochon weighed 27.81 ct; it has a refractive index of 1.738 and density of 3.61 g/cm^3. Its numerous liquid inclusions gave the stone adularescence. A 14.69 ct thorite cabochon had a refractive index of 1.79 and a density of 6.59 g/cm^3. However, these readings were not sufficient to identify the stone. Because this mineral is metamict, it could not be identified by Raman spectroscopy (or other techniques that require the stone to be crystalline), and a chemical analysis was necessary to determine that it was a thorium silicate. *CD*

Update of Australia's gemstone and pearl resources. G. Brown, *Australian Gemmologist*, Vol. 21, No. 8, 2002, pp. 273–277.

Australia is the world's largest producer, by volume, of diamond, play-of-color opal, white South Sea cultured pearls, and chrysoprase. Its sapphire production is declining, and the large resources of nephrite are under-utilized. A status report is given on these products, with comments on changes affecting the economics of these industries. The limited exploration for further additional gem resources needs encouragement (e.g., from all levels of government), but is overshadowed by the search for such commodities as gold, iron ore, coal, and oil. *RAH*

JEWELRY HISTORY

Bergkristalle als funkelnde Meisterwerke der Kunst (Rock crystals as glittering masterpieces of art). G. Kandutsch, *Lapis*, Vol. 28, No. 3, 2003, pp. 31–38 [in German].

This article traces the art of cutting bowls, vases, and other artistic objects from rock crystal, from early Oriental cultures to the courts of Europe in the 16th century. The focus is on the masterpieces of the Miseroni and Saracchi families of Milan. The source of the rock crystal raw material is also addressed; recent research (e.g., analysis of fluid inclusions) has made it possible to infer the geographic origin of the rock crystal quartz used for some objects. Photographs of several outstanding pieces from the Vienna Museum of Art History accompany the text. *RT*

Forward to the past. E. Blauer, *New York Diamonds*, Vol. 75, March 2003, pp. 54–58.

Antique diamonds were in little demand until three-to-four years ago. Previously, the two primary reasons for acquiring antique diamonds was as replacement stones for antique jewelry and for recutting to a more contemporary look. With the weight loss and the risk of color change involved in recutting, and the rarity of stones of good color, diamond dealers showed little interest. However, the demand for antique stones began to grow as more retail jewelers began to handle estate jewelry. Then designers of modern jewelry began using older stones. Eventually, changing tastes and the individuality of the stones themselves caused the surge in popularity seen today. Demand began to outpace supply, and manufacturers were soon reproducing antique cuts. As such reproductions have become more common, profitability for retail jewelers has increased due to the new and distinctive market that has developed.

Distinguishing between original and modern "antique" diamonds can be achieved without great difficulty. Most originals are of a lower color (those of H color or better are rare) and clarity (e.g., chipped girdles) than modern stones. Genuine antique diamonds with fancy colors are especially rare and expensive. However, the originality and individuality of the antique cuts, even

those that are modern reproductions, has opened a new market for both clients and jewelers.

Ronald Stumman

Roman wheel-cut engraving, dyeing and painting microquartz gemstones. A. Rosenfeld and M. Dvorachek, *Journal of Archaeological Science*, Vol. 30, No. 2, 2003, pp. 227–238.

Eight samples of engraved carnelian and banded agate from the eastern Roman Empire were studied to determine the engraving techniques used by early Roman lapidaries. Detailed descriptions and photos are presented, together with the results of scanning electron microscopy (SEM) and energy-dispersive spectrometry (EDS). The samples, which range in maximum dimension from 12 to 20 mm, show a typical variety of Roman iconographic motifs (deities, animals, and equestrians) and shapes (mainly oval and cabochon). They were randomly chosen from a private collection and were most probably produced for mass consumption in Israel from the 1st to the 4th centuries AD.

The engraving techniques were typical of the period, as the gems were fashioned with iron, bronze, and brass drill wheel rotational lathes using abrasive polishing agents (corundum, emery, and possibly diamond) and lubricant materials (tin, lead, barite) in conjunction with water, oil, or waxy pastes. Some of these techniques are still in use today. Many of the samples were decorated with calcium carbonate and barite (as white pigments), as well as gold and silver, to emphasize pictorial elements. One sample was representative of a heat-treatment technique whereby carnelian was burned with calcium carbonate (limestone) to create a hard white material that was much desired by the Romans. Another was a hematite imitation created by painting the stone's surface with an iron oxide mixed with what was probably a bone glue of calcium, phosphorus, and carbon. *CT*

JEWELRY MANUFACTURING

Development of concave faceting of gemstones. A. D. Morgan, *Journal of Gemmology*, Vol. 28, No. 4, 2002, pp. 193–209.

Early work in the concave faceting of both diamond and colored stones dates back over a century. This faceting style may enhance the overall brilliance and beauty of a stone, due to the cylindrically concave lenslets and convex mirror surfaces. Incident ray paths diverge and produce elongated streaks of light instead of plane reflections of the light source. A resurgence of interest in this cutting style has resulted in a high demand for the work of American concave faceters for custom jewelry.

Commercial equipment for cutting concave facets is now available. Cutting machines discussed in detail include the OMF Faceter, Facetron Special Cut, Algar, and Morgan. Equipment should be rigidly constructed with facilities for microadjustment of related components. It is considered an advantage for the cutting cylinders to oscillate along the cylindrical axis to avoid formation of wear grooves on the cylinders. *CT*

SYNTHETICS AND SIMULANTS

Eine neue Opalsynthese aus Russland (A new type of synthetic opal from Russia). C. C. Milisenda, *Gemmologie: Zeitschrift der Deutschen Gemmologischen Gesellschaft*, Vol. 51, No. 2–3, 2002, pp. 115–120 [in German with English abstract].

Four new types of synthetic opals from the Scientific Centre for Applied Research, Russia, are described. They basically represent different stages of development. Types 1 and 2 are comparable to Gilson synthetic opals. Type 3 resembles natural white opal, but is virtually free of water and organic compounds. Type 4 shows almost all the features characteristic of natural opal, including H_2O spectral bands around 7000 and 5200 cm^{-1}, and absorption related to SiOH groups at 4500 cm^{-1}. This synthetic not only looks realistic, but even behaves like natural opal during cutting. However, it can be separated from natural opal by the "lizard skin" structure that is also seen in other synthetic opals. *RT*

50th Anniversary of first successful diamond synthesis. R. Caveney, *Industrial Diamond Review*, Vol. 2003, No. 1, pp. 13–15.

After a brief review of earlier unsuccessful attempts to synthesize diamond, an account is given of the successful experiment by the Swedish company ASEA on February 15, 1953. Iron carbide and graphite were used with thermite (a source of intense heat). The latter was activated by an electric pulse sent through a wire between the anvils in a spherical pressure intensifier (the Quintus press). The crystals were confirmed as diamond by X-ray diffraction. The yields in the successful runs were 20–50 crystals, from 0.1 to 0.5 mm in size; they had irregular faces and most were transparent and colorless, but a few were green, yellow, or gray. *RAH*

Hydrothermal growth of emerald laser crystals. Z. Chen, G. Zhang, C. Huang, and H. Shen, *Journal of Inorganic Materials*, Vol. 17, No. 6, 2002, pp. 1129–1134 [in Chinese with English abstract].

This article gives details of a technique used in China for growing hydrothermal synthetic emerald crystals that have applications to laser technology, as well as being a source of synthetic gems.

The autoclaves are 700 mm long and 38 mm in diameter; they are divided into a lower nutrient zone and an upper crystal growth zone, separated by a thermal insulation layer. The nutrient zone contains Al_2O_3 (16–19%), SiO_2 (pure quartz, 65–67%), Cr_2O_3 (1–3%), BeO

(13–15%), and sulfuric acid. "Quartz-seed stack-up structure" technology is employed, where three gold wire baskets filled with 2–5 mm colorless synthetic quartz grains and two seed plates of synthetic beryl (held at the bottom of each basket with metal wires) are stacked within the growth zone. The growth temperature is in the range of 500–600°C, and pressure is about 150–200 MPa.

After 10–15 days, six high-quality synthetic emerald crystals are obtained. Plates (25–35 × 20–25 × 7–16 mm) are then cut from these crystals. Infrared spectra of the crystals, which are similar to those obtained from hydrothermal synthetic emeralds grown in other countries, show three characteristic absorption peaks (at 5448 5274, and 5109 cm^{-1}) that distinguish them from natural emeralds. *TL*

Influence of silicates upon the growth of synthetic diamond crystals. A. A. Chepurov, V. M. Sonin, and A. I. Chepurov, *Proceedings of the Russian Mineralogical Society*, Vol. 131, No. 1, 2002, pp. 107–110 [in Russian with English abstract].

The growth of synthetic diamond crystals at 5.5 GPa and 1500°C in the system Fe–Ni–C was performed with the aid of silicate components (natural olivine and basalt) up to 20 wt.%. The introduction of >5% silicates leads to changes in the morphology of the synthetic diamond crystals, manifested in the loss of morphological stability by the {111} faces, with triangular hillocks with step-like lateral surfaces becoming transformed into sub-individuals. In doing so, the initial single crystal is eventually transformed into a parallel aggregate. In the growth process, the synthetic diamond crystals accept the inclusion of silicate phases, with local concentrations screening off growth and stopping it entirely at ≥20% silicate content. *RAH*

Research and development of high-quality gemstone crystals grown by hydrothermal method. W. Zhou, C. Zhang, Z. Chen, G. Zhang, and H. Shen, *Journal of Synthetic Crystals*, Vol. 31, No. 5, 2002, pp. 509–515 [in Chinese with English abstract].

More than 20 synthetic gem materials have been successfully produced using hydrothermal techniques, mainly in Russia and China. In China, the National Engineering Techniques Center of Research on the Special Mineral Material, in Guilin, is a leader in this area. It is currently focusing on producing high-quality crystals of hydrothermal synthetic corundum (ruby and sapphire) and synthetic beryl, both in many colors. This article compares the similarities and differences of gem-quality hydrothermal synthetic corundum and synthetic beryl produced in Guilin with those produced elsewhere, mainly in Russia by Tairus.

Tairus hydrothermal synthetic corundum crystals are grown at a higher temperature (620°C) and pressure (2 kbar) than those grown in Guilin (450–570°C, 1.5–1.8 kbar). At Tairus the seed plate is cut either parallel to the $(10\bar{1}0)$ face (and the c-axis), or parallel to the $(10\bar{1}1)$ face (inclined to the c-axis by 32°). At Guilin, the seed plate is always parallel to the hexagonal dipyramid $(11\bar{2}3)$ face. The dopants Cr^{3+}, Ni^{2+}, Ni^{3+}, and Cu^{2+}, either individually or in various combinations, are used to impart the various colors (14 are listed in this article) in the Guilin-grown synthetic corundum.

For growing synthetic beryl crystals, the orientation of the seed plate and the composition of the hydrothermal solution are critical. Compared to its natural counterpart, hydrothermal synthetic red beryl contains a higher concentration of CoO (~0.30 wt.% vs. not detected) and a lower concentration of combined Ti, Mn, and Fe. Other chromophores used to obtain the various colors in hydrothermal synthetic beryl are Cr^{3+}, Mn^{2+}, Mn^{3+}, Mn^{4+}, Fe^{2+}, Fe^{3+}, Cu^{2+}, and V^{3+}. A comparison of the gemological properties of hydrothermal synthetic colored beryl crystals from four producers (in Japan, Australia, and two in Russia) are presented.

In 2002, about 15 kg of hydrothermal synthetic colored corundum and 1.5 kg of hydrothermal synthetic colored beryl were produced in China. *TL*

Spectroscopic features due to Ni-related defects in HPHT synthetic diamonds. A. Yelisseyev, V. Nadolinny, B. Feigelson, and Yu. Babich, *International Journal of Modern Physics B*, Vol. 16, No. 6/7, 2002, pp. 900–905.

Nickel atoms in high-pressure/high-temperature (HPHT) diamonds occur not only as substitutional (Ni_s) and interstitial (Ni_i) forms but also as nickel-nitrogen (Ni-N) complexes or defects (designated as NE1, NE2, etc.). These defects contain various numbers of nitrogen atoms—for example, there are two in NE1, three in NE2 and NE3, and four in NE8. To study the photoluminescence (PL) characteristics of the Ni-N defects as related to the annealing temperature, the authors grew synthetic diamonds up to 1.00 ct at 1550 K and 5.5 GPa in Ni-Fe-C and Fe-C systems with a split-sphere apparatus. About 100 natural diamonds with yellow-green PL from Yakutian deposits were also studied. Electron spin resonance spectroscopy was used to establish the sequence of Ni-defect transformations as temperature increases.

Nickel is present mainly as Ni_s before annealing. After annealing at 1950 K, Ni_s, NE4, NE1, and NE2+NE3 occur in approximately the following amounts: 10, 15, 60, and 15%, respectively. After annealing at 2350 K, the proportions change to 2–3, 0, 20, and 60%, respectively. The remaining Ni occurs in more complicated NE8 and NE9 defects. The ultraviolet-excited PL shows no signal before annealing. After annealing at high temperatures, it shows a strong yellow-green emission that is most intense at 2350 K. *KSM*

Verneuil synthetic sapphire showing an iron absorption spectrum. J. M. Duroc-Danner, *Journal of Gemmology*, Vol. 28, No. 4, 2002, pp. 227–230.

A 7.02 ct blue oval brilliant-cut synthetic sapphire was found in a parcel of heat-treated natural sapphires. Although the stone shows some classic signs of its synthetic origin (e.g., curved color banding, minute gas bubbles, and Plato lines), it also contains some features normally associated with heat-treated natural sapphires (e.g., an iron line seen at 450 nm with a hand-held spectroscope, internal diffusion of color around pinpoints, glass filling in two small surface-reaching fractures near the girdle, and chalky green fluorescence to short-wave UV radiation).

The author surmises that the pinpoint inclusions originally contained unhomogenized trace element (Fe and Ti)-containing powder, which, due to the high-temperature formation of Verneuil synthetic sapphires, interacted and created the intervalence charge transfer ($Fe^{2+} \rightarrow Ti^{4+}$) responsible for the 450 nm line normally seen in natural sapphire. Because of its absorption spectrum, the stone was mistaken as natural and placed in a parcel of sapphires that were subjected to heat treatment (and glass filling). *WMM*

TREATMENTS

Eine neue Diffusionsbehandlung liefert orangefarbene und gelbe Saphire (A new diffusion treatment supplies orange and yellow sapphires). H. A. Hänni and T. Pettke, *Gemmologie: Zeitschrift der Deutschen Gemmologischen Gesellschaft*, Vol. 51, No. 4, 2002, pp. 137–152 [in German with English abstract].

Since 2001, large amounts of treated orange to yellow and "padparadscha"-like sapphires have appeared in the gem trade. The rough material mainly came from Songea (Tanzania) and Ilakaka (Madagascar). About 150 of these stones were examined with several methods. The results showed that the stones were not only heat treated, but also diffusion-treated with beryllium (Be). The diffusion-induced color may extend as much as several millimeters into the stone (which, when small, means the entire stone). Unlike traditional diffusion treatment, the Be diffusion may not be undetectable by viewing the color distribution in immersion.

The Be content in corundum is normally less than ~1 ppm. However, this new Be diffused corundum typically contains 10–15 ppm beryllium. The original trace-element contents of the natural material strongly influence the outcome of the diffusion treatment. This new type of diffusion-treated sapphire has raised concerns about the identification of such stones and the terminology used to describe them. *RT*

Falsche 'Sternsteine': Manipulationen an Edelsteinen zur Erzeugung oder Intensivierung von Asterismus (Fake östar stones': Manipulations of gemstones to create or enhance asterism). K. Schmetzer and M. Glas, *Lapis*, Vol. 28, No. 1, 2003, pp. 22–24, 37–41, 58 [in German].

This article offers a comprehensive overview of the methods that have been used to imitate or enhance asterism. These comprise: the creation of doublets and triplets with parts of natural stones showing asterism; the use of metal plates or foils engraved with patterns of parallel and intersecting striations; the engraving of striations into the back of cabochon layers of doublets and triplets; surface diffusion of natural and synthetic corundum; and the use of light-conducting fibers. While all of these possibilities may be applied occasionally to gems such as corundum, spinel, or garnet, artificial asterism recently has been found in stones in which this phenomenon is not known to occur naturally (e.g., tourmaline and amethyst). Sometimes the artificial asterism consists of "impossible" stars (e.g., with five or eleven arms). *RT*

A note on two star stones. R. R. Harding, *Journal of Gemmology*, Vol. 28, No. 4, 2002, pp. 231–234.

Two unrelated star stones are described. The first was a 16.57 ct opaque cabochon that displayed a strong 13-rayed star when lit with a single light source. The asymmetrical nature of the rays, as well as the fact that their odd number varied with the angle of illumination, indicated the star was not natural. Close examination revealed that it was caused by minute, closely spaced parallel grooves on the cabochon surface. The cabochon was found to consist of two rutile-group minerals, one occurring as the host and the other as oriented inclusions (or exsolution lamellae). Chemically, the host and its oriented inclusions were nearly identical except that the inclusions contained up to 8% tungsten.

The second star stone was an unusual, large (51.4 × 43 × 13.8 mm) colorless beryl crystal from Brazil; asterism in beryls is very rare. The stone had numerous crystal faces (basal pinacoids and first-order prisms dominate), which were sufficiently smooth to allow a clear view of the internal features. In this case, the six-rayed star was created by three bands of minute inclusions, crossing mutually at angles of 60°, that were aligned in the basal plane perpendicular to the first-order prism faces. *WMM*

The processing and heat treatment of Subera (Queensland) sapphire rough. M. Maxwell, *Australian Gemmologist*, Vol. 21, No. 8, 2002, pp. 279–286.

Heat-treatment experiments were undertaken on lower-quality rough sapphires from the Subera deposit (one of Australia's largest sapphire mines). The sapphires were heated at lower temperatures and for a shorter period of time than normally done for corundum, but these experiments failed to enhance their color, quality, and value. Almost as many stones lost value after the treatment as gained value. It is concluded that an efficient, money-saving bulk heat treatment of Subera rough is not feasible. *RAH*